CHARACTERIZATION OF COMMONLY ENCOUNTERED EXPLOSIVES USING HIGH-FIELD ASYMMETRIC WAVEFORM ION MOBILITY SPECTROMETRY COUPLED WITH MASS SPECTROMETRY

BY

JARED J. BOOCK

A THESIS PRESENTED TO THE GRADUATE SCHOOL
OF THE UNIVERSITY OF FLORIDA IN PARTIAL FULFILLMENT
OF THE REQUIREMENTS FOR THE DEGREE OF
MASTER OF SCIENCE

UNIVERSITY OF FLORIDA

2007

To my family and friends.

ACKNOWLEDGMENTS

I wish to thank my research director, Dr. Richard A. Yost, for teaching me a great deal about the fundamentals of mass spectrometry and providing guidance throughout my research. I would also like to thank Dr. Matthew Pollard at the Dr. Herbert H. Hill laboratory at Washington State University for providing two opportunities for me to conduct research on their instruments, and for providing invaluable assistance and conferring with me on the science. I thank Ion Metrics, Inc., of San Diego, CA, for funding these trips. I would like to recognize the members of my committee: Dr. David H. Powell and Dr. John R. Eyler. I would like to thank the US Air Force Institute of Technology Civilian Institutions program for giving me this opportunity. Thanks also go to my colleagues in the Yost group for their support.

Lastly, I would like to thank my parents and my friends, without whom I would have gone insane several times during this year and a half.

TABLE OF CONTENTS

page

ACKNOWLEDGMENTS 4

LIST OF TABLES 7

LIST OF FIGURES 8

LIST OF ABBREVIATIONS 11

ABSTRACT 12

CHAPTER

1 INTRODUCTION AND INSTRUMENTATION 13

1.1 Introduction 13
1.2 Atmospheric Pressure Chemical Ionization 15
1.3 High-field Asymmetric-Waveform Ion Mobility Spectrometry 16
1.4 Ion Optics 21
1.5 Quadrupole Ion Trap Mass Spectrometry 22
1.6 Multidimensional Mass Spectrometry 26
1.7 Thesis Overview 26

2 PROPERTIES AND CHARACTERIZATION OF EXPLOSIVES 27

2.1 Explosives that were Characterized 27
2.2 Classification of Explosives 27
2.3 Chemical Properties of Explosives 28
2.4 Instrument Settings 29
2.5 Compensation Voltage (CV) Scans 30
2.6 Characterized Compounds 31
2.6.1 Nitroaromatics 31
2.6.1.1 (2,4,6 –) Trinitrotoluene (TNT) 31
2.6.2 Nitramines 43
2.6.2.1 Cyclotrimethylene trinitramine (RDX) 43
2.6.2.2 Cyclotetramethylene tetranitramine (HMX) 46
2.6.3 Nitrate Esters 50
2.6.3.1 Nitroglycerin (NG) 50
2.6.3.2 Pentaerythritol tetranitrate (PETN) 51
2.6.3.3 Ammonium Nitrate Fuel Oil (ANFO) 53

3 FAIMS/MS AND IMS/FAIMS/MS OF EXPLOSIVES 57

3.1 Instrumentation 57
3.1.1 Electrospray Ionization (ESI) Source 57

3.1.2 Ion Mobility Spectrometer (IMS) 59
3.1.3 Orthogonal Dome FAIMS Cell 59
3.2 FAIMS Limitations 62
3.3 Effects of Addition of Helium to the Carrier Gas 63
3.4 High-resolution FAIMS (HRFAIMS) 63
3.4.1 Separation of Mixtures of Explosives 64
3.4.2 Resolving Isomers 68
3.5 Dispersion Voltage 69
3.6 Effects of Adjustment of Plate Gap 70
3.7 Relationship of DV to CV 80
3.8 Sensitivity 81
3.9 IMS/FAIMS of Explosives 81

4 CONCLUSIONS AND FUTURE WORK 83

4.1 Conclusions 83
4.1.1 Characterization of Explosive Compounds 84
4.1.2 FAIMS Characteristics 85
4.1.3 IMS/FAIMS/MS 85
4.1.4 High-resolution FAIMS 86
4.1.5 Mixture Separations with FAIMS/MS 86
4.1.6 Disadvantages of FAIMS 86
4.2 Recommendations 87
4.2.1 Further HRFAIMS Improvements 87
4.2.2 FAIMS Carrier Gas Experiments 87
4.2.3 Practical Separations and Analysis 88
4.2.4 IMS Gating 88
4.2.5 CV Scanning 88
4.2.6 Instrument Maintenance 89
4.3 Future Work 89
4.3.1 Ionization Sources 89
4.3.2 Development of Field Instruments 91

REFERENCES 92

BIOGRAPHICAL SKETCH 96

LIST OF TABLES

Table		page
2-1	Explosives to be Characterized.	27
3-1	Relative Ion Intensities.	79
3-2	Relative CV Values	79

LIST OF FIGURES

Figure		page
1-1	Finnigan LCQ APCI source.	15
1-2	FAIMS waveform and ion mobility behavior.	17
1-3	APCI source and FAIMS cell mounted on a Finnigan LCQ.	19
1-4	Ionalytics line-of-sight FAIMS cell geometry.	20
1-5	LCQ quadrupole ion trap showing ion trajectory.	23
1-6	Example of oscillating ion motion according to the Mathieu equation (let a=1 and q=1/5).	24
1-7	Mathieu stability diagram.	25
2-1	Compensation voltage (CV) scanning.	31
2-3	Negative ion APCI mass spectrum of TNT.	33
2-4	TNT total ion count over four 2 min CV scans.	34
2-5	FAIMS/APCI mass spectrum of TNT.	35
2-6	FAIMS/APCI mass spectrum of TNT: measured for 2 min at CV = 6.6V	36
2-7	FAIMS/MS/MS of TNT m/z 197.1 peak at 35% collision energy.	37
2-8	CV spectrum of 2,4-DNT.	38
2-9	FAIMS/MS mass spectrum of 2,4-DNT.	39
2-10	2,4-DNT: 2 min at CV = 11.5V.	40
2-11	CV spectrum of 2,6-DNT.	41
2-12	FAIMS/MS mass spectrum of 2,6-DNT.	42
2-13	Mass spectra of 2,6-DNT: 2 min at CV = 11.6V and 15.3V.	43
2-14	CV spectrum of RDX.	44
2-15	FAIMS/MS mass spectrum of RDX.	45
2-16	RDX: 2 min at CV = 5.1V.	46

2-17 CV spectrum of HMX. 47
2-18 FAIMS/MS mass spectrum of HMX. 48
2-19 HMX: 2 min at CV = 1.2V. 49
2-20 NG (MW 227) 50
2-21 FAIMS/MS mass spectrum of NG. 51
2-22 PETN (MW 316) 52
2-23 FAIMS/MS mass spectrum of PETN. 52
2-24 FAIMS/MS mass spectrum of ANFO made with hexane. 55
2-25 FAIMS/MS mass spectrum of ANFO made with nitromethane. 56
3-1 WSU electrospray ionization source. 58
3-2 WSU electrospray ionization source photograph. 58
3-3 Drawing of Ionalytics orthogonal dome FAIMS cell. 60
3-4 Photograph of Ionalytics orthogonal dome FAIMS cell. 61
3-5 WSU apparatus. 62
3-6 CV spectrum of HMX/RDX mixture. 65
3-7 Mass spectrum of HMX/RDX mixture. 66
3-8 CV spectrum of TNT/RDX mixture.. 67
3-9 Mass spectrum of TNT/RDX mixture. 68
3-10 CV spectrum of both isomers of DNT.. 69
3-11 RDX CV spectrum at 0.5 mm.. 71
3-12 RDX mass spectra at 0.5 mm.. 72
3-13 RDX CV spectrum at 0.75 mm. 73
3-14 RDX mass spectra at 0.5 mm. 74
3-15 RDX CV spectrum at 1.0 mm. 75
3-16 RDX mass spectra at 1.0 mm. 76

3-17 RDX CV spectrum at 2.0 mm. 77
3-18 RDX mass spectra at 2.0 mm. 78
3-19 Relationship between CV and DV. 80
4-1 Distributed plasma ionization source. 90

LIST OF ABBREVIATIONS

AFRL	Air Force Research Laboratory
AGC	automatic gain control
APCI	atmospheric pressure chemical ionization
DARPA	Defense Advanced Research Products Research Agency
CV	compensation voltage
DC	direct current
DV	dispersion voltage
FAIMS	high-field asymmetric-waveform ion mobility spectrometry
IED	improvised explosive device
IMS	ion mobility spectrometry
LOD	limit of detection
MS	mass spectrometry
QITMS	quadrupole ion trap mass spectrometer
RDECOM	Research, Development, and Engineering Command
RF	radio-frequency
SNL	Sandia National Laboratory
TOF	time-of-flight
UXO	unexploded ordnance
VOC	volatile organic compounds

Abstract of Thesis Presented to the Graduate School
of the University of Florida in Partial Fulfillment of the
Requirements for the Degree of Master of Science

CHARACTERIZATION OF COMMONLY ENCOUNTERED EXPLOSIVES USING HIGH-FIELD ASYMMETRIC WAVEFORM ION MOBILITY SPECTROMETRY COUPLED WITH MASS SPECTROMETRY

By

Jared J. Boock

May 2007

Chair: Richard A. Yost
Major: Chemistry

The goal of this research was to characterize explosive compounds using high-field asymmetric waveform ion mobility spectrometry (FAIMS) as an ion separation device interface to a mass spectrometer (MS). FAIMS is a relatively recently developed technology that is promising, adding a dimension of separation. This method was employed in such a way as to be conducive to possible future development of field instruments (e.g., use of atmospheric pressure chemical ionization (APCI)). In addition, several experiments were conducted with the application of this method, mainly dealing with optimization of the instrument parameters. These experiments led to the development of a new method: high-resolution FAIMS. An ion mobility spectrometer was used as a desolvation and ion-focusing device to drastically improve FAIMS resolution. This allowed for the separation of mixtures that otherwise could not have been separated. The resolution was high enough that isomers of the same explosive were successfully resolved. This can be beneficial to forensics studies.

CHAPTER 1
INTRODUCTION AND INSTRUMENTATION

1.1 Introduction

A major threat to the national security of the United States is the continued use of explosives abroad and possible use by terrorists on the domestic front.[1] As a result, there is a great need for improved separation and detection technologies for trace amounts of explosive compounds. There are many possible applications for such technologies, such as prevention of terrorist events, military weapons/cache detection, interception of explosives trafficking, improvised explosive device (IED)/landmine detection and identification, post-event forensics analysis, and unexploded ordnance (UXO) detection. A significant challenge to the detection of minute amounts of explosives is that oftentimes these analytes will be overwhelmed by complicated background matrices.[2] Another is that benchtop-size instruments are inadequate to provide timely analyses to meet the needs of the user. For instance, a military unit searching for landmines or IEDs in a combat zone cannot easily deploy a large and cumbersome instrument. To meet these needs, an instrument is required that can both provide separation of analyte from atmospheric background containing large amounts of volatile organic compounds (VOCs). The required limit of detection (LOD) for such an instrument has been determined by many field trials conducted by government and commercial agencies (US Air Force Research Laboratory (AFRL), US Army Research, Development, and Engineering Command (RDECOM) , Sandia National Laboratories (SNL), and Defense Advanced Research Products Agency (DARPA) are a few of these) to be in the parts-per-billion (ppb) range.[3]

One of the primary technologies in use for explosives detection today (as of 2006) is the ion mobility spectrometer (IMS).[4] An IMS consists of an ionization source, an atmospheric pressure drift tube, and a detector. A sample is ionized and the ions are introduced to the drift

tube and are passed through a series of ring electrodes held at increasing voltages of polarity opposite to that of the ions, which creates a strong electric field. Separation is based on mobility of each ion in the field, which depends on size, shape, and mass of the ion. The IMS has limitations, however. First and foremost is that it is easily susceptible to contamination from background matrix. The IMS as an explosives detector is primarily used in indoor facilities such as airports or railroad stations, and samples are usually introduced as a swipe rather than sampling vapor from air.[5]

Mass spectrometry could address many of the limitations of ion mobility. Research is currently being conducted by many different organizations to design and construct a field-portable time-of-flight (TOF) mass spectrometer (MS) to meet these needs.[6,7] Ions are accelerated through a vacuum drift tube by an electric field. The mass-to-charge (m/z) ratio is determined by the amount of time each ion takes to pass through the drift tube. In most cases, a TOF/MS is coupled with a gas chromatograph, which provides initial separation.[8] Current commercially available field-portable TOF/MS designs do not have a high enough resolving power to meet the above needs, and they are not sensitive enough to detect levels of explosive vapor that are practical to operational needs.[9]

A relatively recent (theorized in the late 1980s and developed in the 1990s and 2000s) and promising technology is high-field asymmetric-waveform ion mobility spectrometry (FAIMS),[10] which will be discussed in detail. FAIMS is a novel, continuous chemical separation method that has already proven successful in clinical, proteomics, and environmental analytical applications.[11] FAIMS does not have a high enough resolving power to function as a stand-alone device;[12] however, it is ideally suited to function as an ion separation device (in lieu of a chromatography instrument) that can be coupled to a mass spectrometer.

1.2 Atmospheric Pressure Chemical Ionization

Atmospheric pressure chemical ionization (APCI) is a gas-phase ionization technique that uses either a radioactive β-emitting source or a corona discharge at a pressure of 1 atm to produce reagent ions and ultimately analyte ions. This method was chosen for this series of experimentation because it most closely resembles an ionization source that is amenable to be used for field instruments. Most other ionization techniques either require vacuum or are large, complex systems containing lasers or high-voltage; these techniques are less suitable for a man-portable field instrument. The APCI method is not identical to the ionization method to be employed projected field instruments, as a difference arises from sample introduction. The APCI ionization source used for this series of experiments (see figure 1-1) is designed for

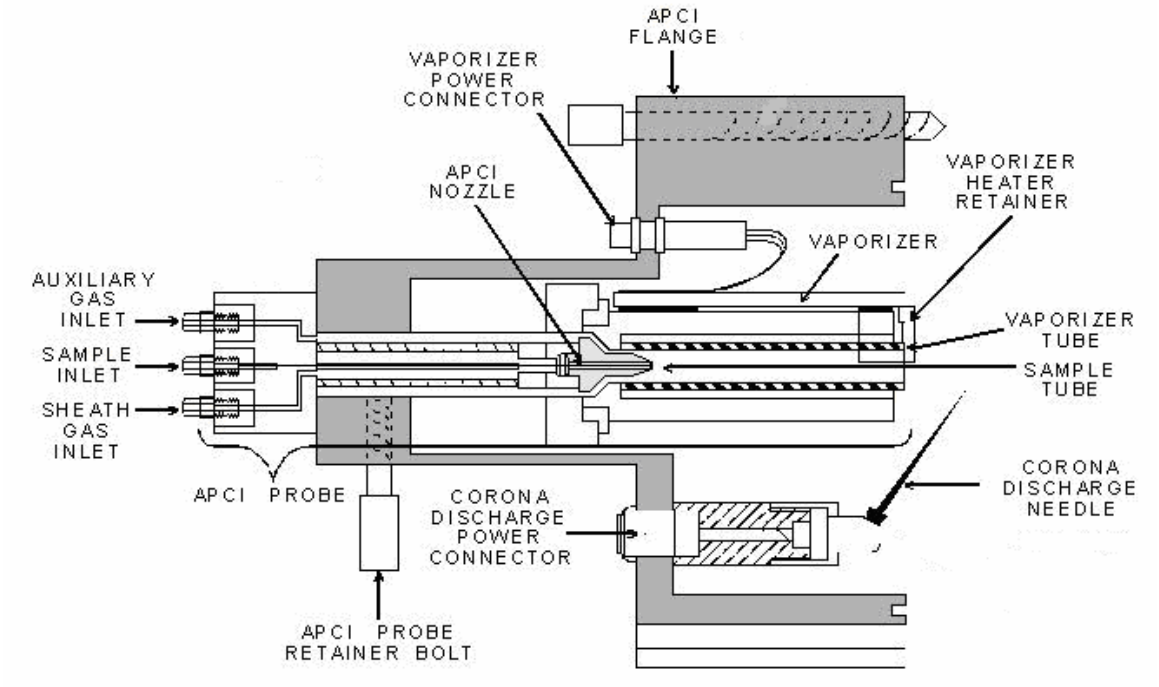

Figure 1-1. Finnigan LCQ APCI source. [Reprinted from Thermo-Electron Corp. 2004. *Finnigan LCQ Series APPI/APCI Combination Probe Operator's Manual*, Rev. A, Thermo-Electron Corp.]

interfacing to liquid chromatography, and, therefore, introduces analyte samples as liquid. The liquid sample is nebulized into droplets, which are passed pneumatically via nitrogen sheath gas into a heated region where they are vaporized. The nitrogen and vaporized solvent then serve as reagent gas as the vapor is passed over a corona discharge which produces reagent ions that ionize the analyte via ion-molecular reactions.[13] There are different mechanisms depending on the type of analyte and whether or not ionization is positive or negative. Explosive compounds tend to favor negative ionization (this behavior and ionization mechanisms will be discussed further in a later section).

1.3 High-field Asymmetric-Waveform Ion Mobility Spectrometry

As stated in the introduction, high-field asymmetric waveform ion mobility spectrometry (FAIMS) is a relatively recently developed technology that in this series of experiments serves as an ion separation device. FAIMS cells have many different configurations, though all basically consist of two electrodes separated by a gap; the simplest configuration is two parallel metal plates, which, consequently, was the first iteration of this design (Figure 1-2).[15] An asymmetric waveform is applied between these plates, which can either be the sum of two sine waves,[12] or a square wave; in this case, a sum of sines was used with a high negative potential of -4000 V for a short time, and a low positive potential for a slightly longer time. This peak voltage is known as the dispersion voltage (DV), and creates a strong electric field. The rapid change in polarity of the applied alternating potentials causes the ion to oscillate due to attraction/repulsion forces. For this reason, a high negative potential is typically used for negative ions.

The basis for separation for a FAIMS device is a change in the mobility of an ion as this field varies, unlike IMS which measures the mobility itself.[16] Ions exhibit a variety of mobility behaviors under high field, thus making FAIMS an ideal separation device. The changes in

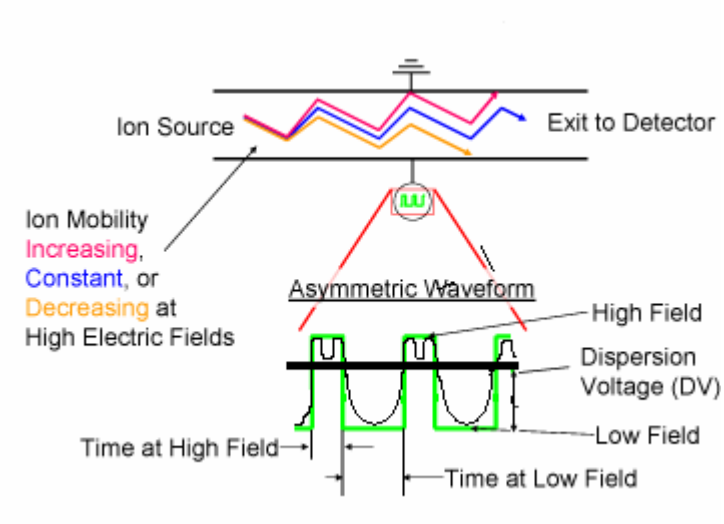

Figure 1-2. FAIMS waveform and ion mobility behavior. [Adapted from Guevremont, Roger. 2004. High-Field Asymmetric Waveform Ion Mobility Spectrometry (FAIMS). (p. 2, fig. 1-1). Ionalytics Corp., Ottawa, Canada.]

mobility are classified into three different categories: "A-type" behavior, or exponential increase in mobility proportional to change in field strength, "B-type" behavior, or exponential increase in mobility followed by exponential decay as field strength increases, or "C-type," which is exponential decay in mobility as field strength increases. The change in mobility affects the direction the ion travels toward or away from the plates (Figure 1-2).

If these conditions are maintained, then all ions will drift toward the plates according to each separate mobility. However, the drift of a particular ion can be halted by the application of a small DC voltage to one of the plates. This compensation voltage (CV) allows a single type of ion to pass through the plates. As mobility changes are greater, an increased compensation voltage is needed to balance the drift and allow transmission of the ion.

The mobility of an ion influenced by an electric field is described by

$$K_h(E) = K[1 + f(E)]$$

where $f(E)$ is the dependence of ion mobility (K_h) as a function of electric field.[12]

Field strength is described by units known as Townsend (Td), for which 1 Td = $10^{17} \times (E/N)$ where N is the number density of the carrier gas (expressed in atoms/m^3) and E is the field strength (in V/cm). Change in mobility is described by

$$K_h/K = 1 + \alpha(E/N)^2 + \beta(E/N)^4$$

where K_h is the ion mobility at high field and K is the mobility at low field.

The two constants α and β are dependent on the dimensions of the FAIMS cell. The estimated field strength for this series of experiments was calculated to be about 80 Td (20,000 V/cm) at 1 atm.

To analyze a mixture of analytes, with differing CVs, it is necessary to scan CVs over a range. Therefore, each analyte in the mixture is transmitted through the cell separately and a CV spectrum consisting of ion signal vs. CV can be acquired.

A simple FAIMS cell geometry of two parallel plates is not necessarily ideal. It is understood that when FAIMS is interfaced between an ionization source and mass spectrometer, there will be a degree of ion loss, though it should be noted that there is no loss of sensitivity. This may not make much of a difference; however, for even though signal is reduced, noise may be reduced even further. It has been proven that different types of cells such as the cylindrical cell used in this study have an additional ion focusing capability.[12]

An Ionalytics (Thermo) Selectra beta II prototype was used for the FAIMS work described in this thesis, though there were two different types of cell geometries used. The line-of-sight FAIMS cell was used for the characterization, and it consists of two concentric cylinders that are separated by a 1 mm gap. In order to assemble the cell, a solid stainless steel inner electrode fits into a hollow stainless steel outer electrode, and a PEEK endcap maintains uniform distance between these electrodes. The ends of the inner and outer cylinders are machined to have

hemispherical dimensions toward the exit aperture. Unlike a flat-plate design, the electric field in a cylindrical cell is not uniform; this configuration, along with the hemispherical exit area, allows for the focusing of ions toward the exit aperture. A PEEK sleeve prevents arcing and other types of electrical interference between the FAIMS cell and the environment. Figure 1-3 shows a photograph of the APCI source and FAIMS cell.

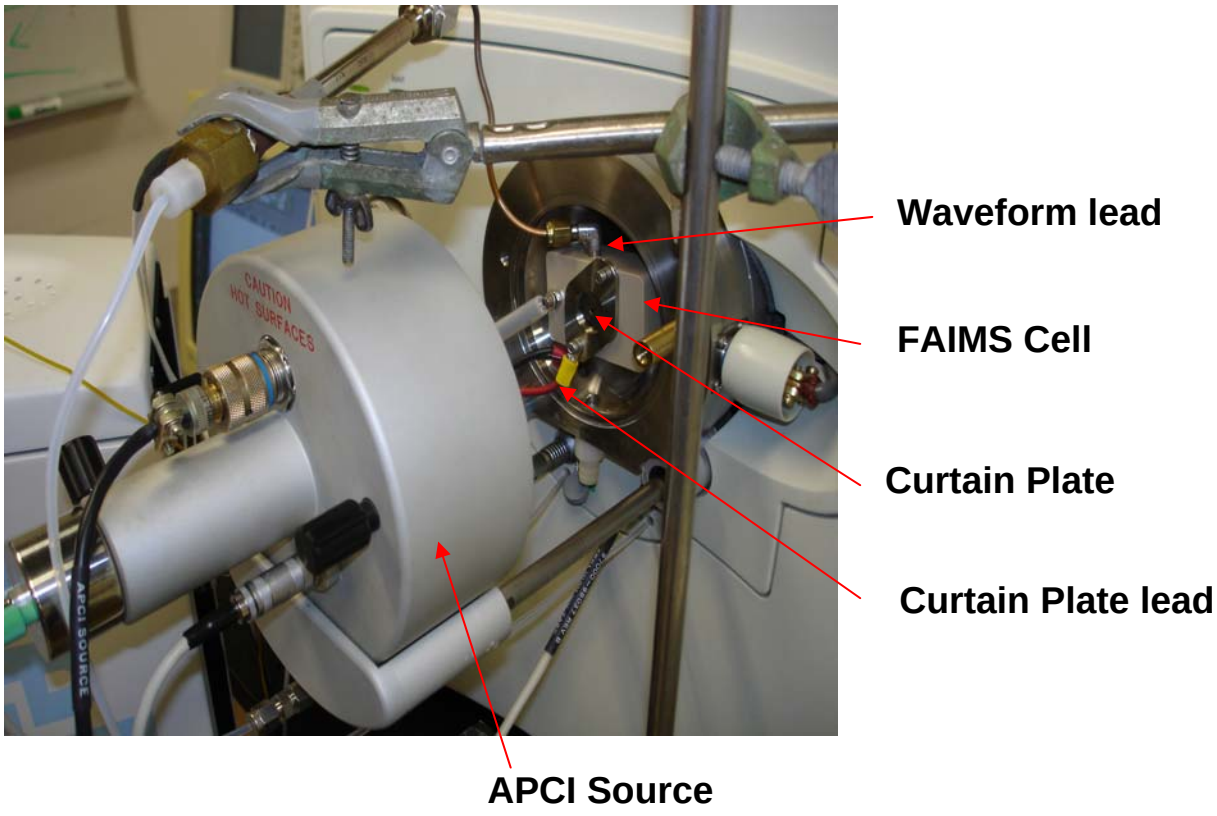

Figure 1-3. APCI source and FAIMS cell mounted on a Finnigan LCQ.

Prior to entering the FAIMS cell, ions pass through a hole in a curtain plate, which has a potential of the same polarity as the ion mode of the source, in order to ensure that ions are

repelled into the FAIMS cell. For positive ion mode, the curtain plate voltage is kept constant at +1000V, while negative ion mode curtain plate voltage is set to –1000V.

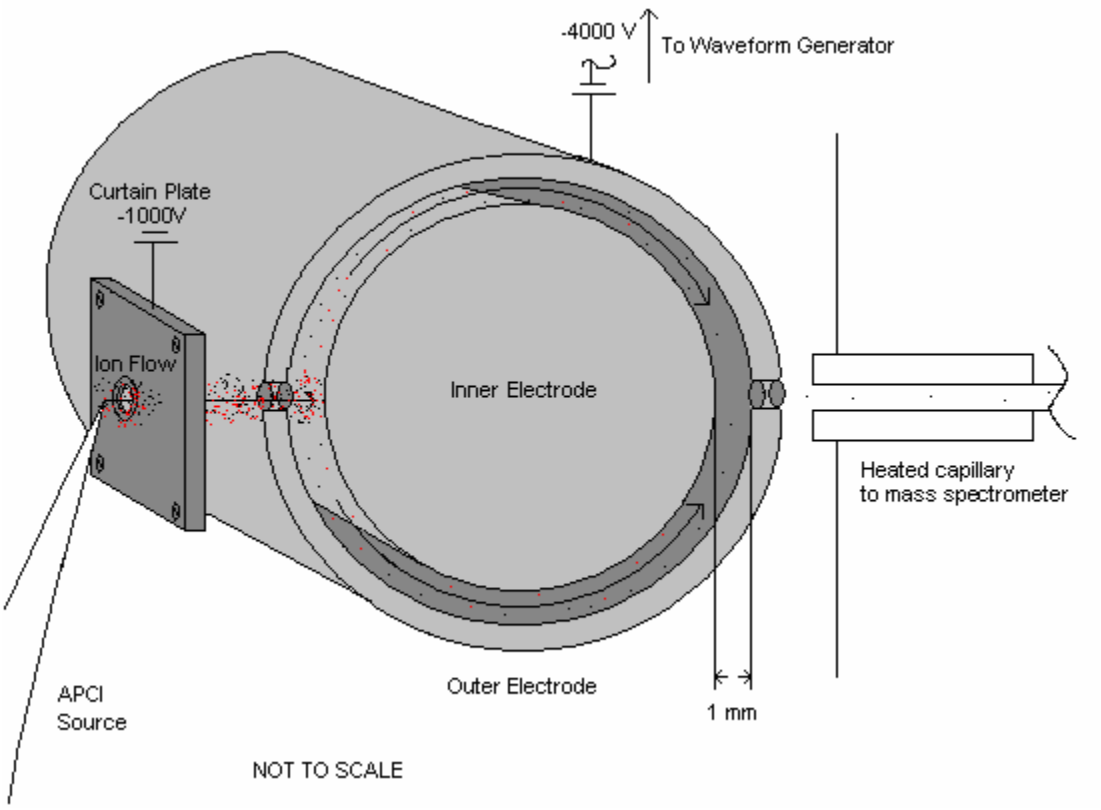

Figure 1-4. Ionalytics line-of-sight FAIMS cell geometry.

A clean, dry curtain gas is added to the FAIMS cell via a side port at a rate of 3 L/min. This curtain gas serves two purposes. First, a portion exits through the orifice in the curtain plate, which assists with desolvation of the ions and droplets from the ionization source and minimizes the accumulation of solvent neutrals from the APCI source into the FAIMS cell. The remaining gas propels the ions through the FAIMS cell and into the heated capillary of the mass spectrometer. This gas can consist of a pure gas or a gas mixture, typically nitrogen, helium or carbon dioxide; however, nitrogen was chosen for these experiments due to its predominance in

the atmosphere. Any moisture or trace hydrocarbons introduced to the carrier gas will affect the performance of the FAIMS device by reacting with the ions, so charcoal and/or molecular sieves are used, to purify the gas.

A waveform generator serves as the power source for the asymmetric waveform. A cable connects the generator directly to the FAIMS cell. There is also a connector on the waveform generator that allows the operator to observe the waveform on an oscilloscope and ensure that the waveform DV and shape are constant. The Selectra prototype FAIMS unit is extremely sensitive, and any slight interferences with the waveform cable can affect the waveform.

There are four different FAIMS "modes" depending on the polarity of the CV and DV polarity required to transmit a particular ion.[12] The determination as to which mode an ion falls under at this juncture is made experimentally, as a library has not yet been fully constructed, which justifies a portion of this thesis. An ion in the "N1" quadrant (including many explosives) passes through the FAIMS cell with a negative DV and positive CV; an ion in "N2" requires positive DV and positive CV; an ion in "P1" requires positive DV and negative CV; and "P2" ions are transmitted with negative DV and CV. This rule applies only for "A" and "C" type ions; for "B" type ion mobility behavior it is not well defined. The mobility behavior of an ion is affected by many factors, including: size, rigidity, and interaction with carrier gas (according to Stokes and Einstein).[17]

Although use of FAIMS as a separation device decreases total ion transmission, when the CV is set for a particular ion of interest, the relative signal to noise ratio of that ion increases greatly.

1.4 Ion Optics

The instrument used for this experimentation was a Finnigan (Thermo-Electron) LCQ, which is a commercial, benchtop quadrupole ion trap mass spectrometer (QITMS). After the

analyte is vaporized, ionized by APCI, and separated via FAIMS, ions pass through the heated capillary into a lower-pressure area, where the tube gate is located. The tube gate carries two potentials of a polarity opposite to the analyte ions, one which focuses the ions into the skimmer, which acts as a restriction between the higher pressure area (1 torr) of the tube gate and the lower pressure (10^{-3} torr) of the ion optics. The second potential is used to deform ions and prevent them from traveling further. The ion optics consist of a series of an octopole, lens, and a second octopole. An octopole is a set of eight metal rods that carry an RF voltage (400 V) and DC offset voltage (+10 V for negative ions) that induces an electric field that directs and focuses ions into the mass analyzer. The lens between the octopoles serves both as a focusing medium and as a pressure restriction, for the pressure once again decreases to $2x10^{-5}$ torr in the second octopole and mass analyzer. As pressure is continually decreased, the mean free path (mfp) is increased, and there are fewer neutral molecules and other ions present to interfere with the passage of the focused analyte ion beam.[18,19]

1.5 Quadrupole Ion Trap Mass Spectrometry

A quadrupole ion trap (Figure 1-5) consists of a hyperbolic ring electrode to which an RF potential is applied, as well as two end caps with a DC potential.[20] A DC offset voltage (-10 V for negative ions) is applied to the end caps so ions will enter the trap. An RF waveform of a particular drive frequency (Ω) is applied to the ring electrode which creates the quadrupolar electric field, causing the ions to oscillate on a controlled trajectory. He gas at approximately 10^{-3} torr removes excess kinetic energy from the ions so that they can be trapped. The ion trajectory in the center of the trap is not to scale.

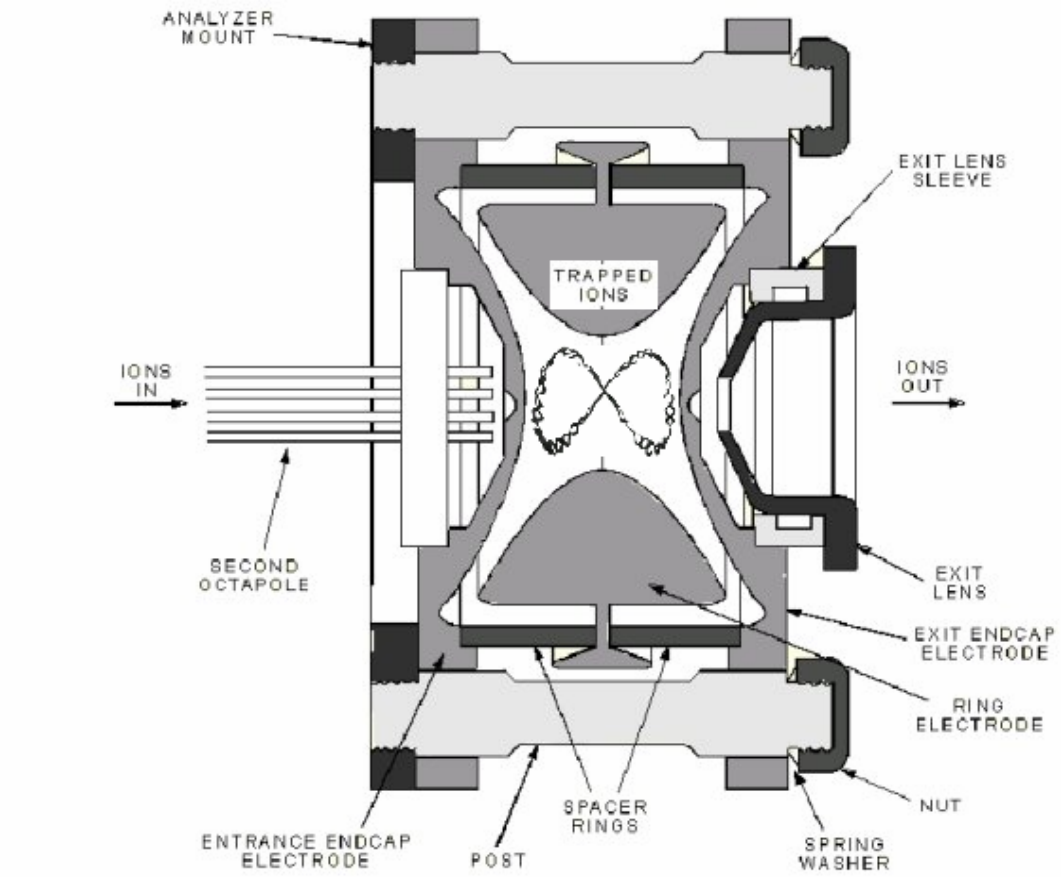

Figure 1-5. LCQ quadrupole ion trap showing ion trajectory. [Adapted from Thermo-Electron Corp. 2003. *Finnigan LCQ Series Hardware Manual*, Rev. A.]

The oscillating ion motion is described by the Mathieu equation:[22]

$$a_z = -2a_r = \frac{-16eU}{m\left(r_o^2 + 2z_o^2\right)\Omega^2} \qquad q_z = -2q_r = \frac{-8eV}{m\left(r_o^2 + 2z_o^2\right)\Omega^2}$$

The variables a_z and q_z are functions of the dimensions of the trap and the potentials applied, while z and r represent the axial and radial directions (between and perpendicular to the endcaps, respectively); U is the DC amplitude applied to the ring electrode (if any), V is the RF potential applied to the ring electrode, e is the charge on an ion, m is the mass of an ion, r_o is the inner radius of the ring electrode, z_o is the axial distance from the center of the device to the nearest point on one of the endcap electrodes, and Ω is the angular drive frequency. The angular drive frequency is equal to $2\pi f_{RF}$ where f_{RF} is the frequency of the main RF voltage in Hertz.[23] A

graphical example of the motion in arbitrary directions is shown in figure 1-6. The actual motion is similar to this example.

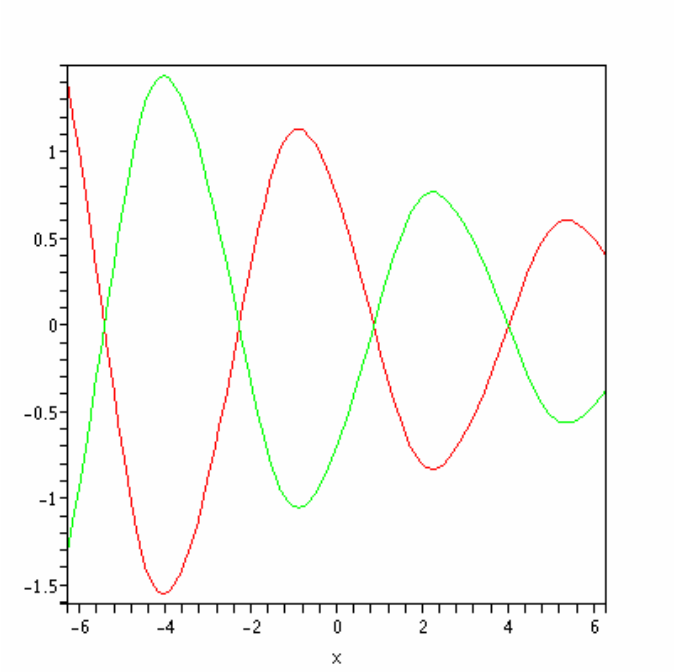

Figure 1-6. Example of oscillating ion motion according to the Mathieu equation (let a=1 and q=1/5). [Adapted from McLachlan, N. W. 1947. Theory and Application of Mathieu Functions, Dover].

For an LCQ, q_z = 0.1963 * [RF frequency (number of charges)/ion mass].[19] Solutions of the Mathieu equation describe a stability diagram (figure 1-7) from which it can be determined whether or not an ion will remain in the ion trap under a given set of conditions. If the q_z of an ion with known mass/charge falls within the boundaries of the stability diagram (is stable in both axial and radial directions), then it can be trapped. If the q_z falls outside the boundary, then the ion will collide with the end cap electrodes and be lost. The factor β is based on the secular frequency of the oscillation of an ion. When β equals one, the secular frequency equals half the frequency of the RF field, and the magnitude of its oscillation increases such that the ion is lost. Essentially, the β lines on the graph are voltage scans; in a quadrupole ion trap the amplitude of the DC and RF voltages are ramped (while keeping a constant RF/DC ratio), to obtain the mass

spectrum over the required mass range. The sensitivity is a function of the scanned mass range, san speed, and resolution.[24]

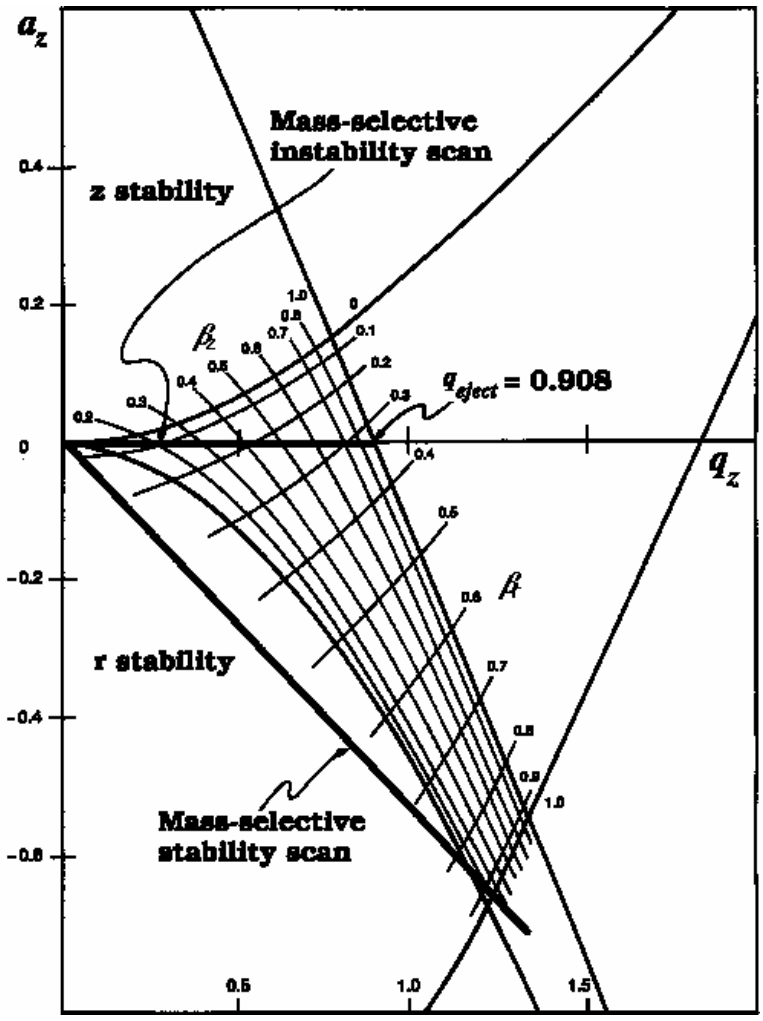

Figure 1-7. Mathieu stability diagram. [Reprinted from McLachlan, N. W. 1947. Theory and Application of Mathieu Functions, Dover].

The ion trap can only hold a certain number of ions at a time before repulsion forces (space charge) cause ion displacement, resulting in a loss of resolving power and band broadening. To counter this phenomenon, the LCQ employs a function known as automatic gain control (AGC) where a prescan is conducted that monitors the generation of ions in the trap.[25] The AGC scan and the full MS scan form a microscan. In these experiments, three microscans were used for each ion injection period.

1.6 Multidimensional Mass Spectrometry

Another capability of the LCQ is multidimensional MS or MS/MS. This function can be selected to determine the fragmentation patterns of an ion of a particular m/z in order to identify the ion creating the peak or to examine the chemistry of that ion. A ion is selected, known as the parent ion, and all other ions are ejected from the trap. An excitation RF voltage is applied across the end cap electrodes, causing the parent ion as kinetic energy to increase; collisions with the He gas in the trap result in parent ion dissociation into fragment (daughter) ions. The fragmentation pattern can be changed by altering the amplitude of the excitation RF voltage.[19,26]

1.7 Thesis Overview

This thesis is organized into four chapters. Chapter 1 is the introduction to the research and an overview of the equipment used for the characterization portion. Chapter 2 presents data relating to the characterization of explosives via FAIMS/MS. Chapter 3 introduces the second instrument and compares it to the instrument used for characterization. There were several experiments relating to FAIMS/MS and IMS/FAIMS/MS that were conducted throughout this research; these are discussed in chapter 3. Chapter 4 discusses the conclusions of this research and recommendations of other related efforts, as well as possible long-term future work.

CHAPTER 2
PROPERTIES AND CHARACTERIZATION OF EXPLOSIVES

2.1 Explosives that were Characterized

A list of explosives was selected for characterization by FAIMS/MS based on threat assessments by various government agencies (including the Department of Homeland Security (DHS) and Federal Bureau of Investigation (FBI)). This list is contained in the table 2.1. Each of these compounds will be discussed in great detail below.

Table 2-1. Explosives to be Characterized.

Compound	Formula	Molecular Weight
TNT (2,4,6-trinitrotoluene)	$C_7H_5N_3O_6$	227
HMX (cyclotetramethylene tetranitramine)	$C_4H_8N_8O_8$	296
RDX (cyclotrimethylene trinitramine)	$C_3H_6N_6O_6$	222
2,4-DNT (dinitrotoluene)	$C_7H_6N_2O_4$	182
2,6-DNT (dinitrotoluene)	$C_7H_6N_2O_4$	182
NG (nitroglycerin)	$C_3H_5N_3O_9$	227
PETN (pentaerythritol tetranitrate)	$C_5H_8N_4O_{12}$	316
ANFO (ammonium nitrate fuel oil)	*	*

*dependent on type of fuel used

2.2 Classification of Explosives

An explosive material is chemically unstable or becomes unstable under certain conditions, and as a result of rapid exothermic decomposition, can be destructive. There are many types of explosives; however, government threat assessments[1,27] have determined that only a certain number of them are significant threats to life and property, primarily due to factors such as supply and cost. As a result of this determination, the compounds of the highest threat levels were examined closely in these experiments, as well as their precursors and degradation products, if possible, as the presence of these can also be used to detect manufacture or storage of the respective explosive materials.

There are two forms of explosive decomposition. The more powerful of these, detonation, is characterized by an extremely fast supersonic shock wave released by the energy produced in the favorable chemical reaction. The sudden high pressure of the shock wave is the major cause of destruction resulting from a detonation. The other form of decomposition, deflagration, is the subsonic portion of an explosion, usually propogated by thermal conductivity of the substance in contact with the outer edge of the plume. Explosives are classified as either "low" or "high" depending on whether or not they detonate.[28] Low explosives include gunpowder and pyrotechnics. High explosives are those used for military applications, mining, or demolitions. All of the explosive compounds included in this study are considered high explosives.

There are also subcategories of high explosives: primary, secondary, or tertiary. Primary high explosives are extremely sensitive to shock, friction, and heat, and are difficult to store. Secondary high explosives are stable enough to be stored for a period of time, yet can be detonated due to a sudden shock or heat. Most of the compounds in these experiments are secondary high explosives. Tertiary explosives (blasting agents) will not easily detonate without the aid of a primary or secondary "booster." This list includes ammonium nitrate fuel oil (ANFO), which was a subject in this study.

2.3 Chemical Properties of Explosives

The majority of secondary high explosives characterized in this study are nitroaromatics, nitramines, or nitrate esters. In the nitroaromatics and nitramines, one or more nitro (NO_2) groups are attached to an aromatic ring structure. Nitrate esters also contain nitro groups. These nitro groups are bulky and electron-withdrawing, causing the nitrogen in the nitro groups to be partially positive. Under APCI, primarily negative ions ($[M]^-$ or $[M-H]^-$) are formed. Non-halogen groups with atoms that are more electronegative than carbon draw substantial electron density from the aromatic system. If enough internal energy is applied, one or more of the nitro

groups may detach from the ring or central structure, producing fragments. In either case, the ions produced are negative, and negative mode must be used in order to separate and detect explosives.

Nitroaromatics and nitramines are generally stable, but can be reactive; this property is especially apparent in functional groups attached to the ring at a position *meta* to a nitro group.[29] These compounds are thermally labile, so ionization techniques such as electron ionization (EI) and chemical ionization (CI) will result in significant fragmentation of the molecule, which makes detection difficult in a complicated background matrix. A "softer" ionization technique, such as atmospheric pressure chemical ionization (APCI) or electrospray ionization (ESI) is needed.[13] Due to their low volatility under standard conditions, only a small amount of these explosives will vaporize for detection in air, so a sensitive separation and detection techniques are required. Because these compounds can condense on dust or other particles present in the immediate environment, instruments designed to detect explosives in air should often sample for explosives present on particles[30,31] as well as the small amounts of vapor. Nitrate esters are much less stable, and require lower instrument operating temperatures for analysis.

Explosive compounds are also highly toxic,[28] creating an environmental hazard for areas around disposal sites. Vapors can be introduced to the lungs, and liquids can be absorbed through the skin, causing a variety symptoms depending on the relative concentration, even leading to death.[32]

2.4 Instrument Settings

Both positive and negative ions can be formed in the APCI source, and the LCQ can analyze ions of either polarity. As most of the explosives have large electronegative leaving groups, they favor the formation of negative ions.[33] It has also been shown that there is less

background noise in negative mode than positive mode. All of the mass spectra shown consist of 50 analytical scans, each consisting of three microscans.

The explosive solutions were diluted in a solvent containing 64.9% methanol and 35% deionized water, as earlier studies[13] have yielded excellent results using this ratio. Solvents that evaporate easily are best used for APCI, so that lower vaporizer temperatures can be used to prevent thermal degradation of the analytes of interest. An extremely small amount, approximately 0.1%, of carbon tetrachloride was added to the solutions as some of the explosive compounds favored the formation of a chloride adduct. This behavior will be discussed in turn. All solutions were diluted to a concentration of about 10 ppm, as this is fairly realistic based on calculated explosive detection applications.[34]

Solutions containing explosives were injected directly via the syringe pump of the LCQ into the vaporizer at a flow rate of 20 μL/min with a maximum ion injection time of 50 ms for AGC. The vaporizer was kept at a temperature of 300°C, while the heated capillary was set to 150°C. The LCQ software was used to tune the instrument as needed throughout the study in order to maximize signal strength.

2.5 Compensation Voltage (CV) Scans

For all of the characterization in this section, CV was scanned from 0-20V four times over 2 min, for a total period of 8 min. The transition at the end of the scan from 20V back to 0V is extremely fast, covering a period of milliseconds. The ion of interest will only pass through the FAIMS at its relative CV, therefore there will be a peak of ion flow at this voltage (ideally 100% transmission); at other voltages the ion collides with the wall of the cell and is not transmitted. (see Figure 2-1) This results in a peak at a particular time (and thus CV) in each of the four scans.

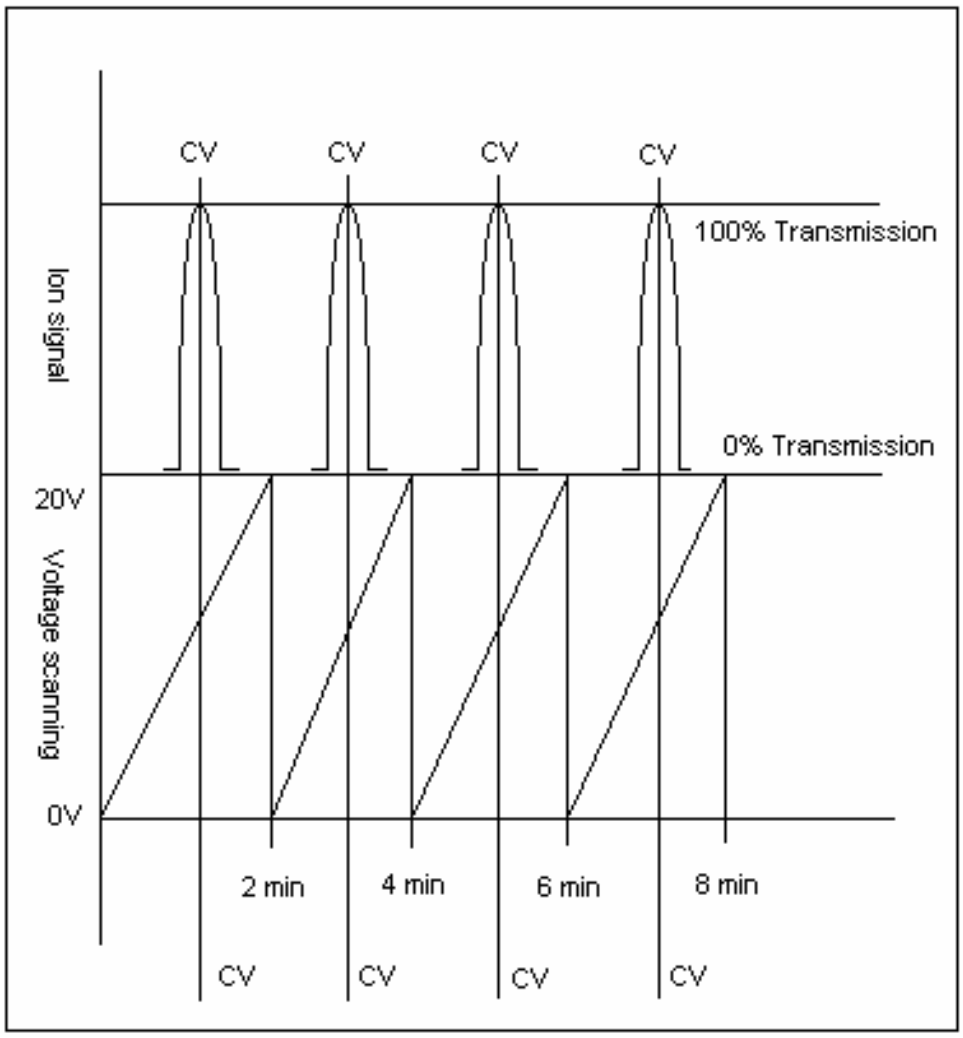

Figure 2-1. Compensation voltage (CV) scanning.

2.6 Characterized Compounds

2.6.1 Nitroaromatics

2.6.1.1 (2,4,6 –) Trinitrotoluene (TNT)

TNT is one of the most commonly encountered explosives due to its continued use for over a century in both military and commercial applications. It is deemed a significant threat for use by terrorists and other enemies of the United States. Like other nitroaromatics, it is stable until ignition, other than slow decomposition over a period of years.[28] Thus, there is the possibility of low amounts of degradation products present in samples of TNT. Therefore, the most common

of these should therefore be characterized, as well as precursors used in the manufacture of TNT. These compounds include the six dinitrotoluene isomers and trinitrobenzene (TNB). For the structures of the nitroaromatics characterized in this study, refer to Figure 2-2. TNT has been used on its own or as a component in mixtures, such as with ammonium nitrate (amatol), aluminum powder, or other explosives.

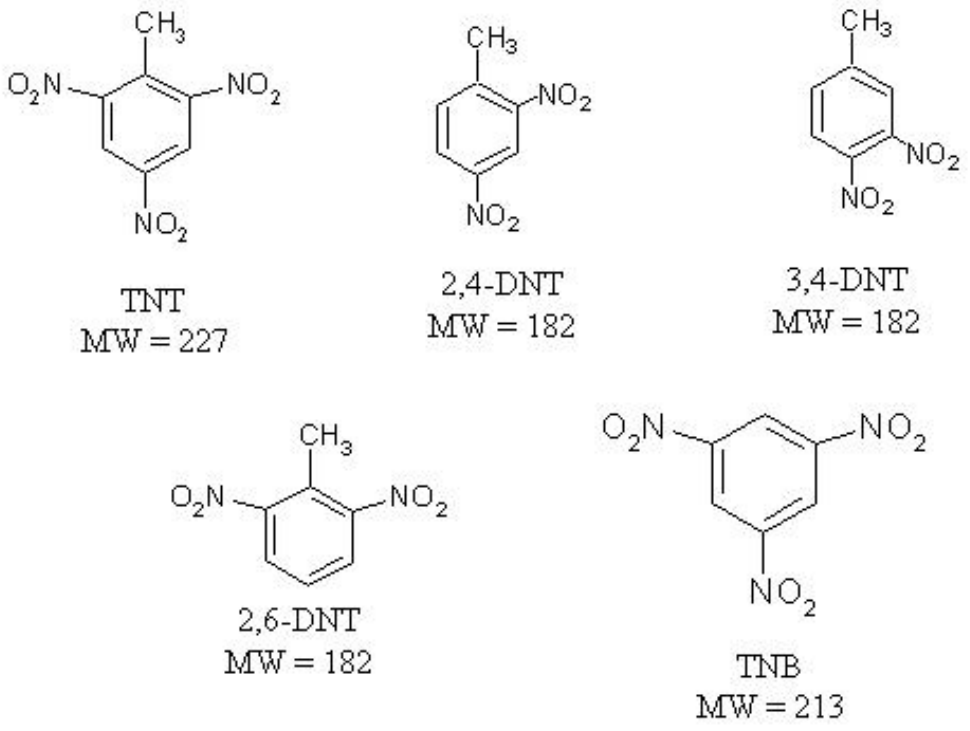

Figure 2-2. Nitroaromatics and molecular weights. [Adapted from Reich, Richard. 2001. (Figure 1-11). PhD dissertation. University of Florida.]

When TNT detonates it (ideally) decomposes according to the following equation:[28]

$$2C_7H_5N_3O_6 \rightarrow 7CO + 7C + 5H_2O + 3N_2$$

although complete decomposition is only reached after some oxygen from surrounding air is added as an ignition reactant.

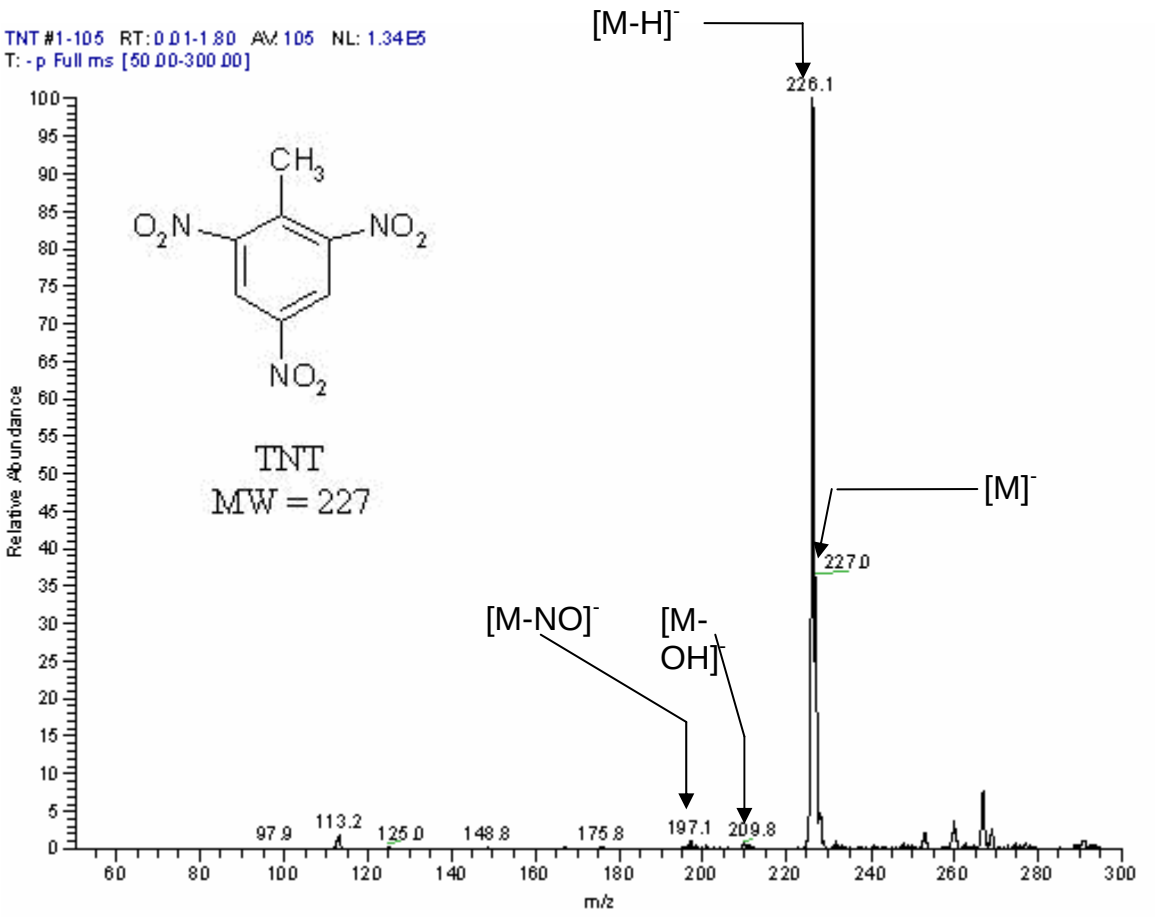

Figure 2-3. Negative ion APCI mass spectrum of TNT. The first spectrum (Figure 2-3) shows negative ion APCI of TNT without FAIMS separation. The $[M]^-$ ion at 227.0 and $[M-H]^-$ ion at 226.1 can be seen clearly, and a small amount of background noise (ions that correspond to minor fragment ions of TNT or impurities) is visible.

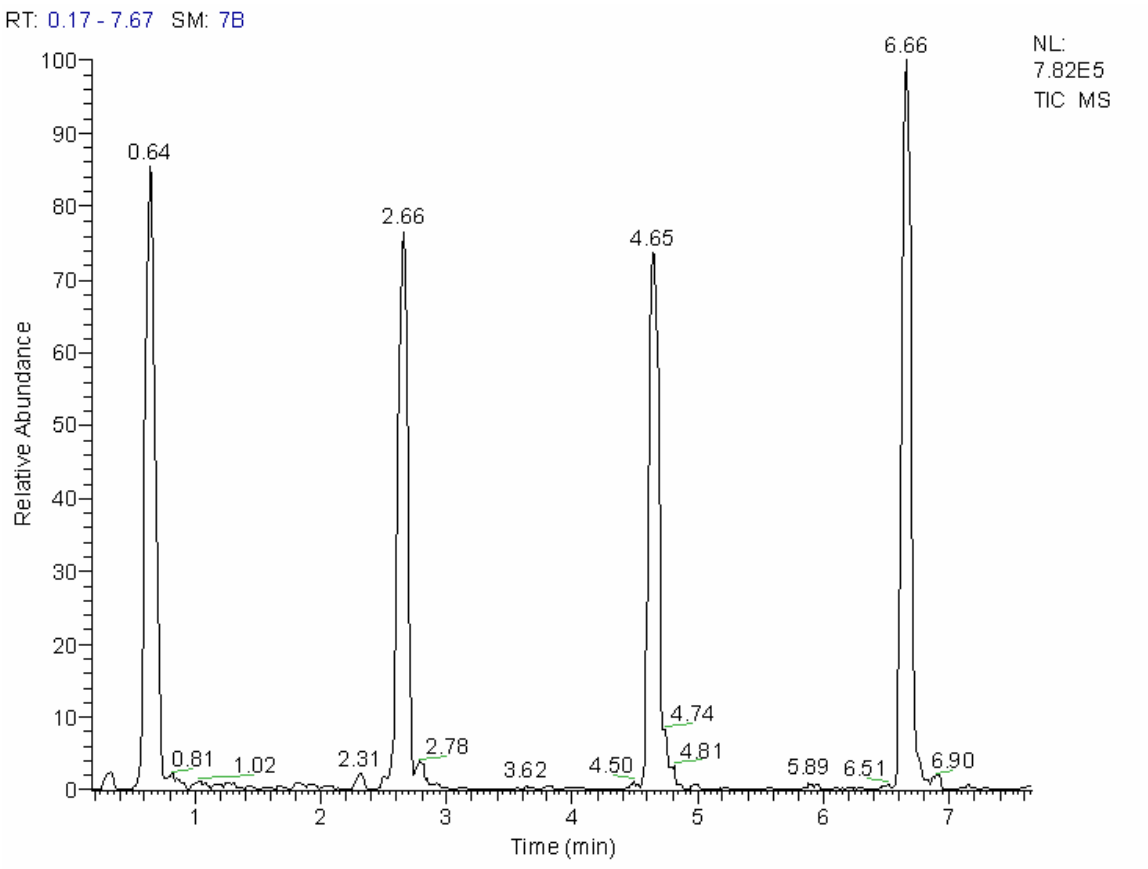

Figure 2-4. TNT total ion count over four 2 min CV scans. Figure 2-4 shows the CV spectrum (total ion count) for TNT. As mentioned earlier, the ion of interest will only pass through the FAIMS at its correct CV; therefore, there are ion peaks at these CV values. There were four CV scans from 0-20 V, each with a duration of 2 min, for a total of 8 min. It is from these spectra that the exact CV for each compound can be calculated. From this spectrum, the CV can be calculated. For instance, the peak at 0.64 min: (0.64 min/2.00 min) × 20.0V = 6.4V.

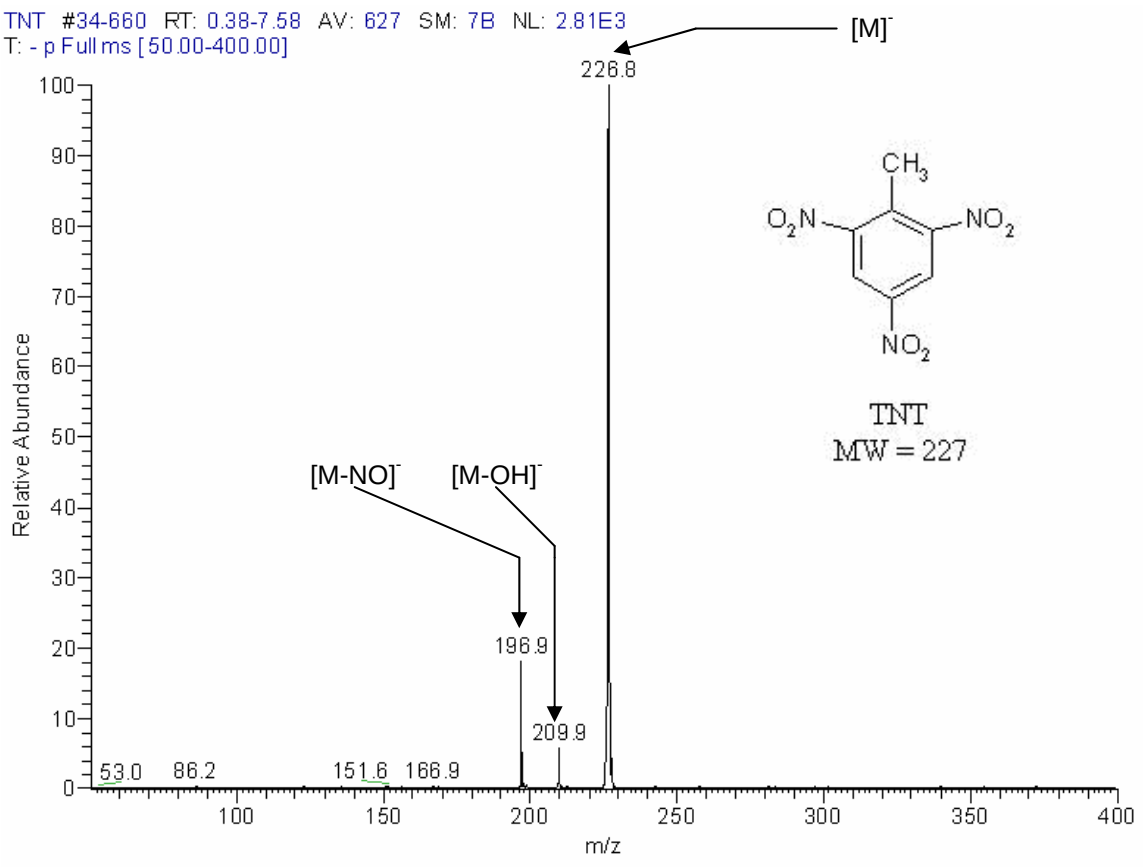

Figure 2-5. FAIMS/APCI mass spectrum of TNT. Figure 2-5 shows the FAIMS/MS spectrum for TNT. The background noise has been greatly reduced after the application of the FAIMS. (see figure 2-2) The evident tradeoff for the improved signal/noise ratio is the 50× reduction in signal strength. In addition, two fragments of TNT also pass through the FAIMS, as the fragment ion CVs are very close to the CV of the TNT $[M]^-$ ion. The fragments show that TNT is a delicate ion that readily loses NO and OH. The fragment peaks are in larger proportion to the molecular ion peak when FAIMS is applied, most likely because the total ion count is lower, and there are few to no impurities. Also, the $[M-H]^-$ no longer appears.

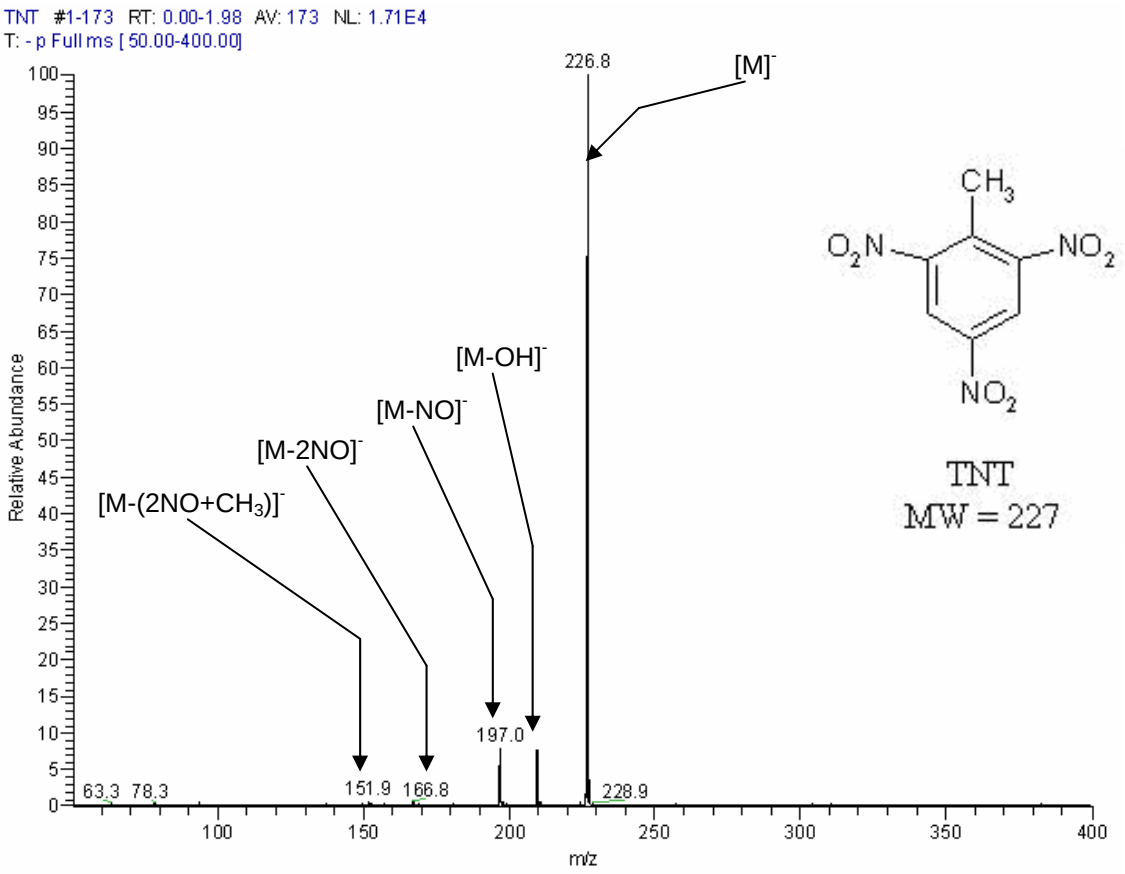

Figure 2-6. FAIMS/APCI mass spectrum of TNT: measured for 2 min at CV = 6.6V Figure 2-6 shows a 2 min spectrum taken at a CV of 6.6V, which is when the most TNT $[M]^-$ ion passes through the FAIMS. This spectrum is similar to that in the previous figure; the only difference is that instead of averaging one of the CV peaks, data points were taken for a stationary CV. As a result, this spectrum is improved further from that in figure 2-4.

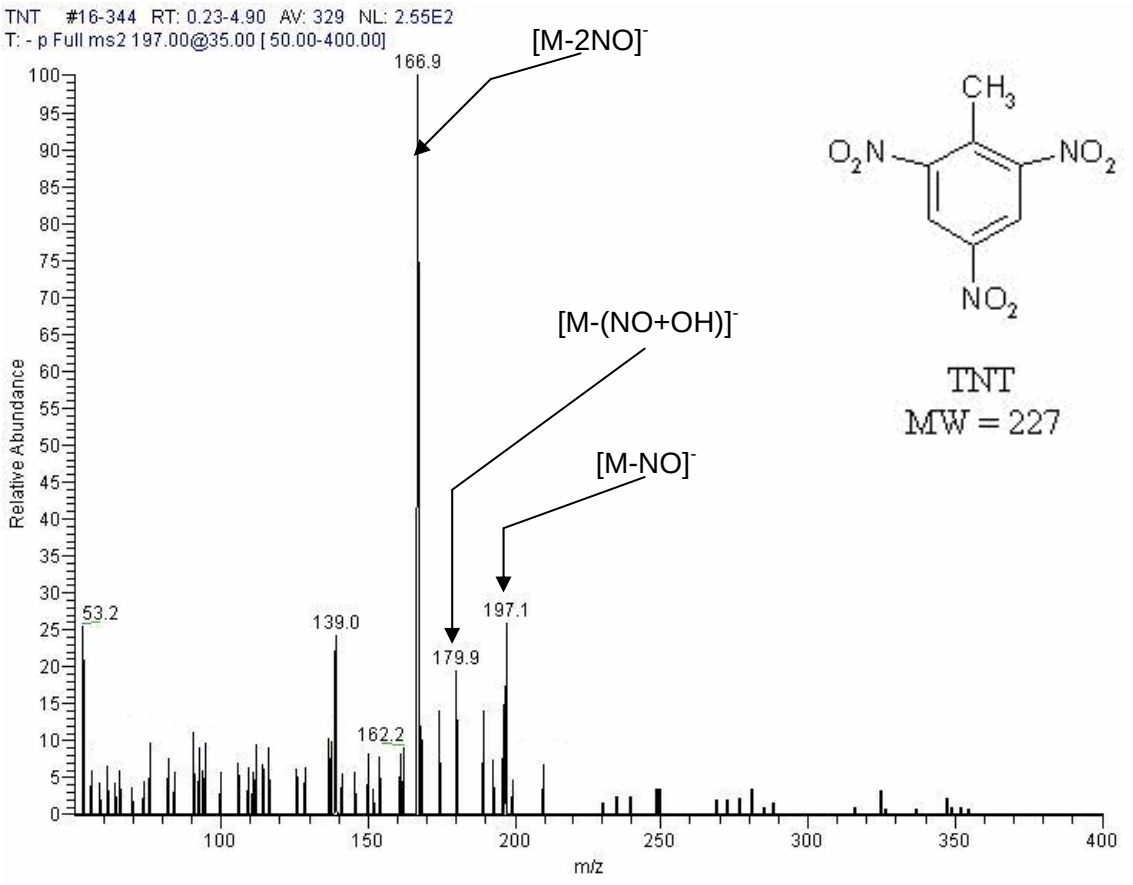

Figure 2-7. FAIMS/MS/MS of TNT m/z 197.1 peak at 35% collision energy. Figure 2-7 demonstrates that FAIMS/MS/MS of even weak ions from explosives is feasible. The FAIMS CV was set to 6.2V to allow the $[M\text{-}NO]^-$ fragment of TNT to pass through the cell. This ion was collided with 35% dissociation energy, causing the loss of a second nitro group. In other words, the predominant fragment ion peak shown here is the same elemental composition as the $[M]^-$ ion for mononitrotoluene.

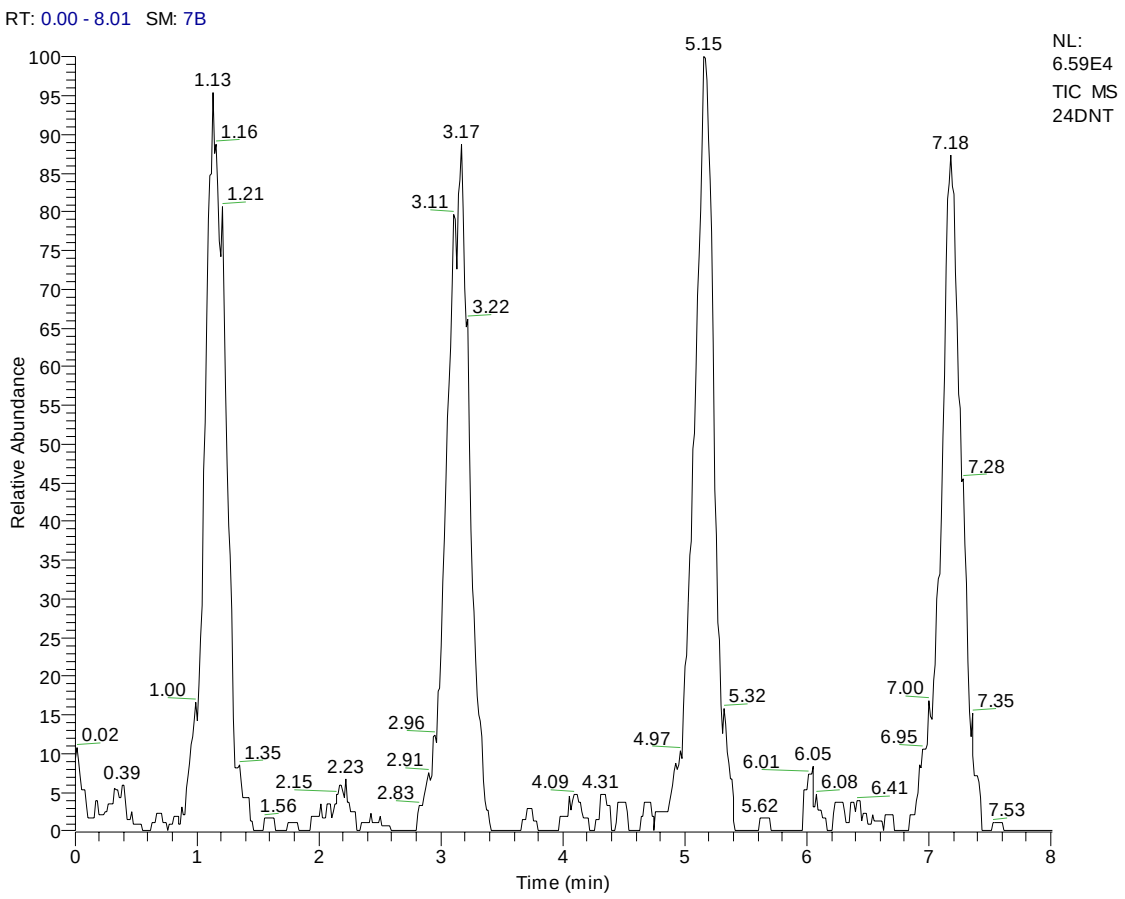

Figure 2-8. CV spectrum of 2,4-DNT. Figure 2-8 shows the CV spectrum for 2,4-dinitrotoluene (DNT), which is a precursor of TNT, and is often an impurity in explosives containing TNT. This CV spectrum is different from that of TNT (figure 2-4) in that the CV is 11.5V, compared to 6.6V. In addition, there is a small amount of solvent ions that transmitted at slightly lower CV than the major DNT ion through the FAIMS cell.

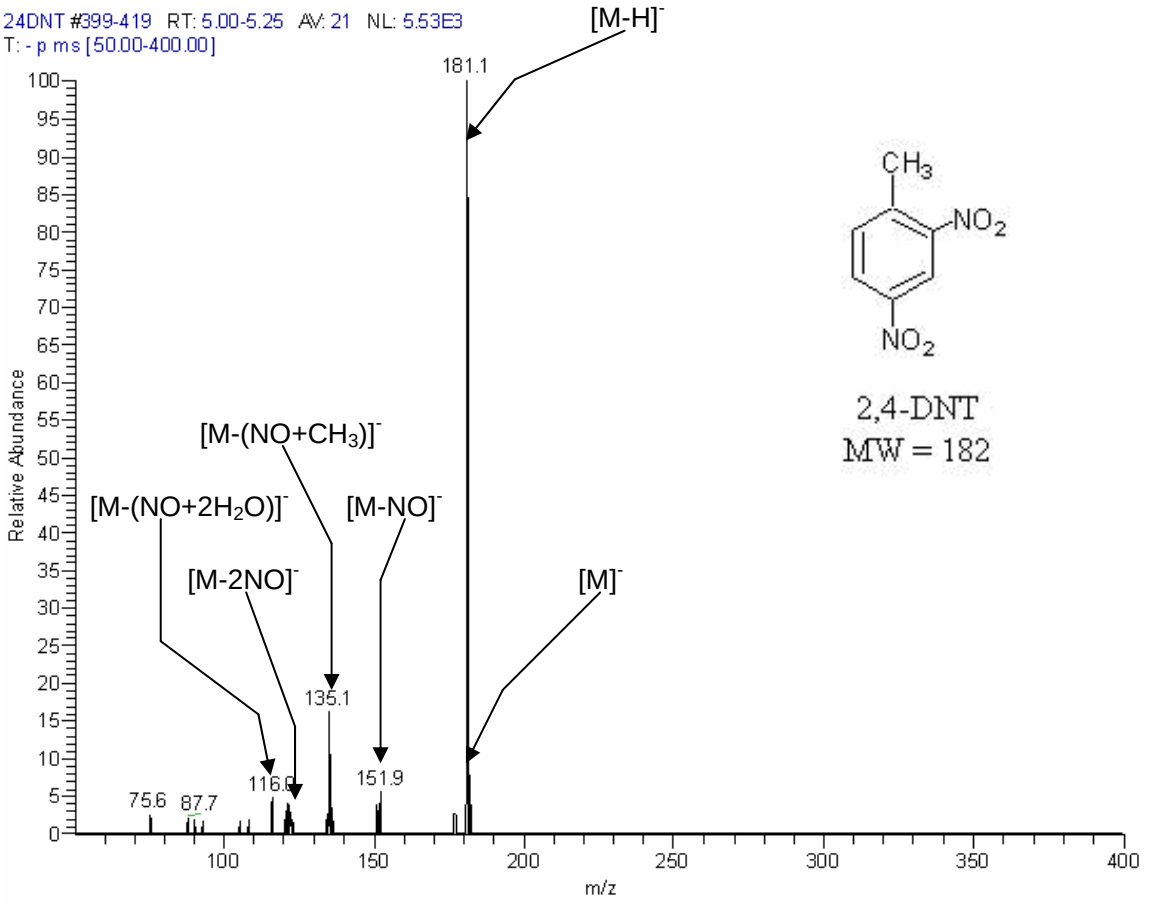

Figure 2-9. FAIMS/MS mass spectrum of 2,4-DNT. Figure 2-9 shows the mass spectrum of 2,4-DNT after FAIMS separation (averaged over the peak at 6.6 min in the CV spectrum in figure 2-8). As with TNT, this ion fragments readily, and experiments have shown that many of these fragments have CV's that are close to the primary ion.

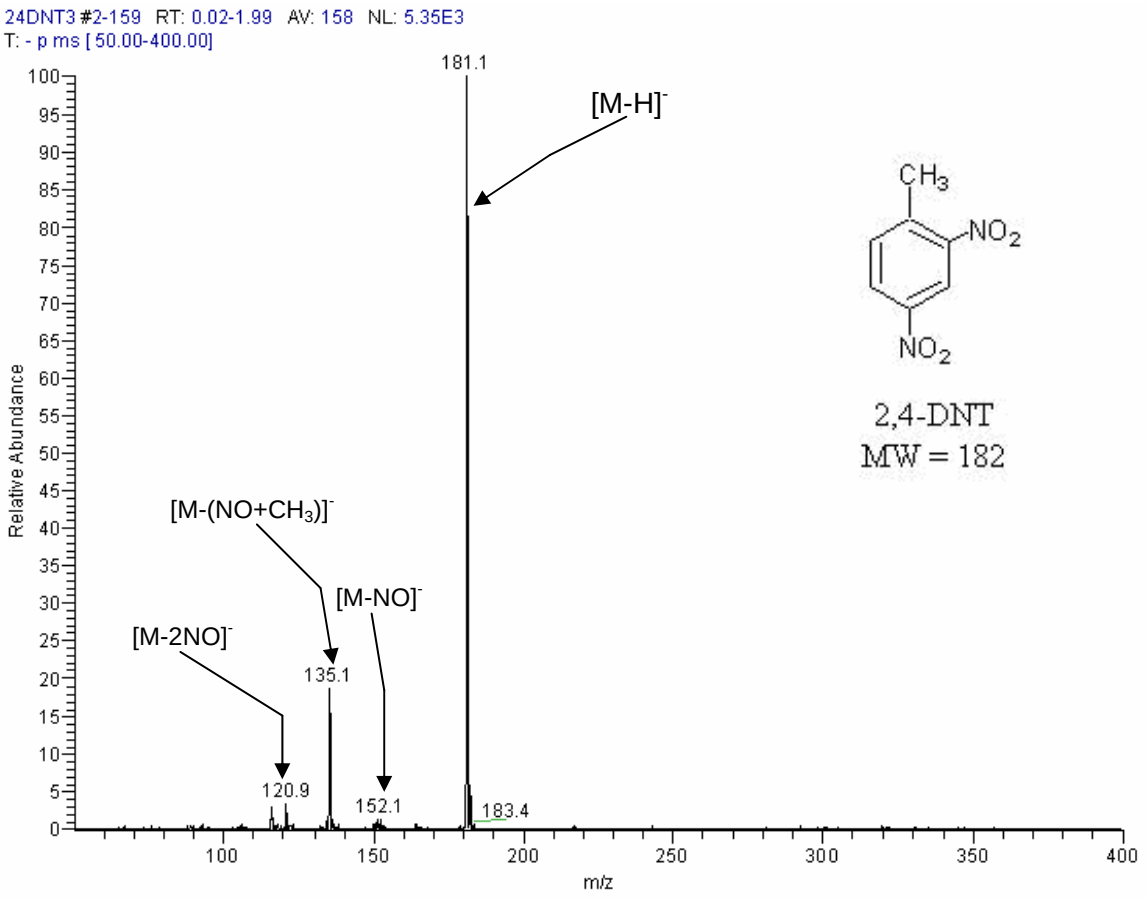

Figure 2-10. 2,4-DNT: 2 min at CV = 11.5V. A mass spectrum of 2,4-DNT at a fixed CV of 11.5V is displayed in figure 2-10. There is little to no noise.

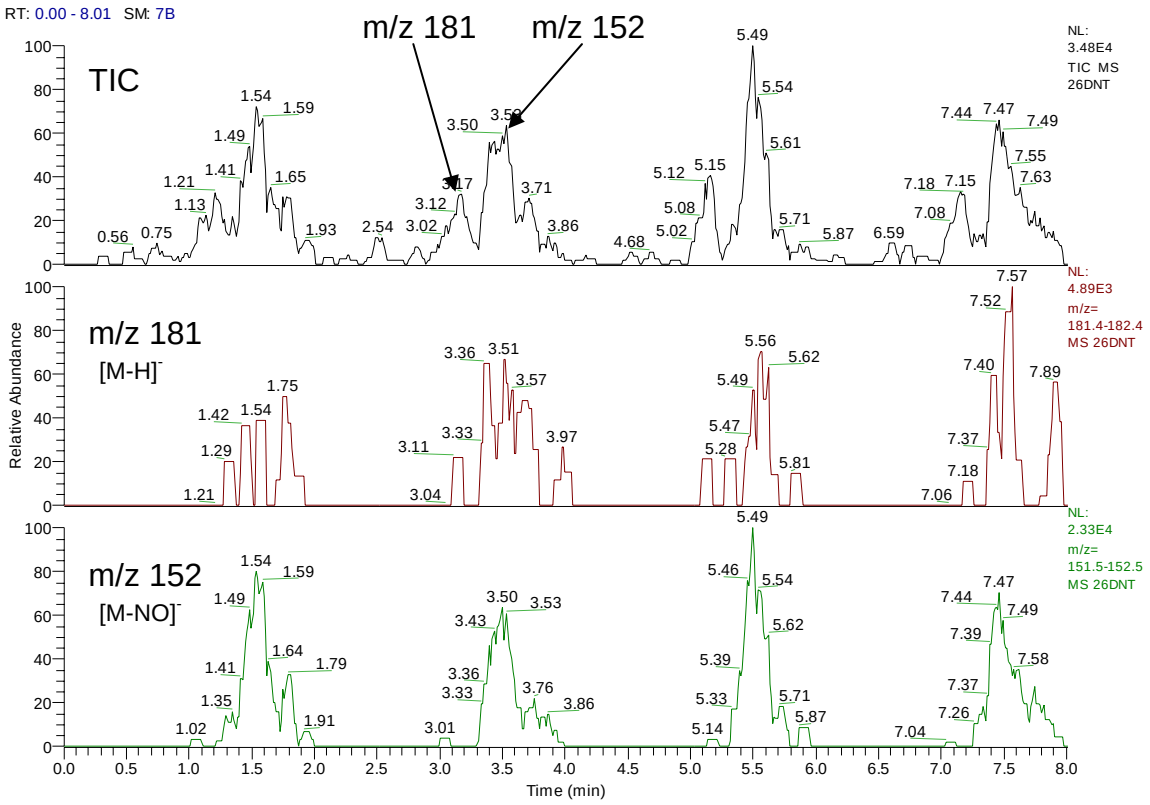

Figure 2-11. CV spectrum of 2,6-DNT. 2,6-dinitrotoluene is an isomer of 2,4-DNT and another precursor of TNT. Both nitro groups are in *ortho* positions to the toluene methyl group. 2,6-DNT is more likely than 2,4-DNT to lose an NO group, and as such, there are two predominant ions formed in APCI, causing the CV spectrum to display different behavior than 2,4-DNT. The two ion peaks have close CVs and are not completely resolved from each other. These can be seen in figure 2-11. Experimentation in improvement of FAIMS resolving power was conducted and will be discussed in chapter 3.

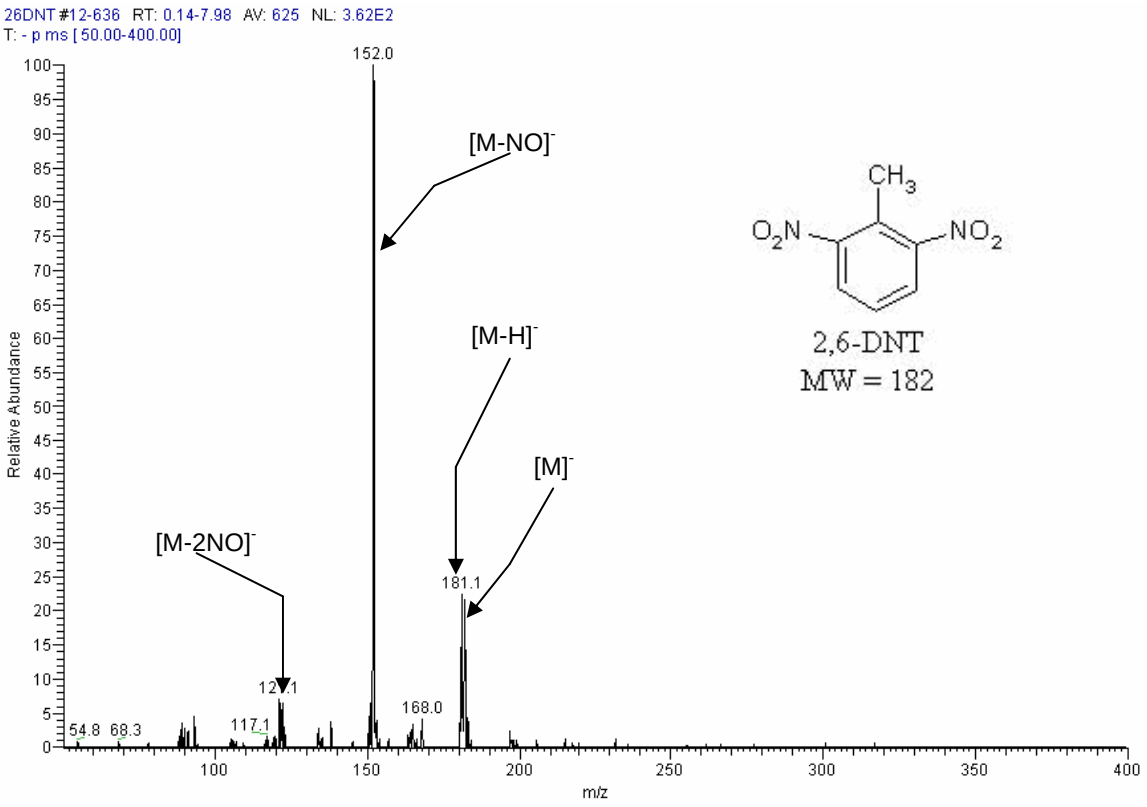

Figure 2-12. FAIMS/MS mass spectrum of 2,6-DNT. Figure 2-12 is a mass spectrum averaged over the entire 8 min run. The two predominant ions are visible at m/z 181 ($[M-H]^-$) and m/z 152 ($[M-NO]^-$), as described at figure 2-11.

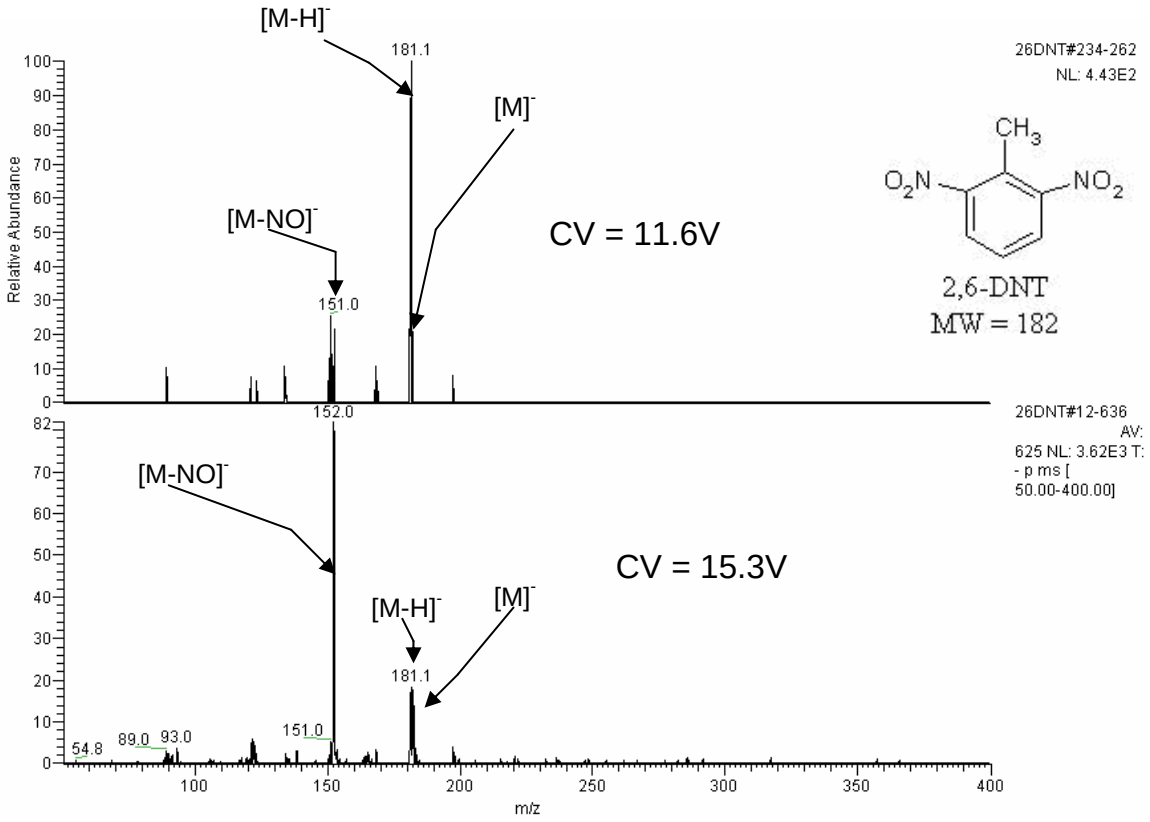

Figure 2-13. Mass spectra of 2,6-DNT: 2 min at CV = 11.6V and 15.3V. The fact that 2,6-DNT more readily fragments under APCI than its isomer does not affect the separation when the CV is fixed, as each ion is transmitted through the FAIMS cell at a separate CV. This behavior can be seen in figure 2-13. Note that the optimal CV values for the $[M-H]^-$ ions of the two isomers are too close (11.6V vs. 11.7V) for them to be separated. However, only 2,6-DNT produces a second FAIMS peak (at CV = 15.3V) for the $[M-NO]^-$ fragment ion.

2.6.2 Nitramines

2.6.2.1 Cyclotrimethylene trinitramine (RDX)

The nitroamine RDX (research department composition X) was developed as an explosive during the 1930s and was used widely during World War II. This explosive is found in many mixtures (such as Torpex, RDX mixed with TNT and aluminum powder), though it is usually encountered as the base for several types of plastic explosives, the most common of which is Composition C-4 (RDX with polyisobutylene and di(2-ethylhexyl)sebacate as the binder and plasticizer). RDX is stable at room temperature will not detonate without a detonator.[35] Another

type of plastique that contains RDX is Semtex, which is a commercial explosive that has been used by terrorists many times in the past (such as Pan Am Flight 103 in 1988). The other component in the Semtex mixture is PETN (pentaerythritol tetranitrate), which will be discussed in its own right.

RDX decomposes completely according to:

$$C_3H_6N_6O_6 \rightarrow 3CO + 3H_2O + 3N_2$$

and also reacts with oxygen in the air to complete the reaction.

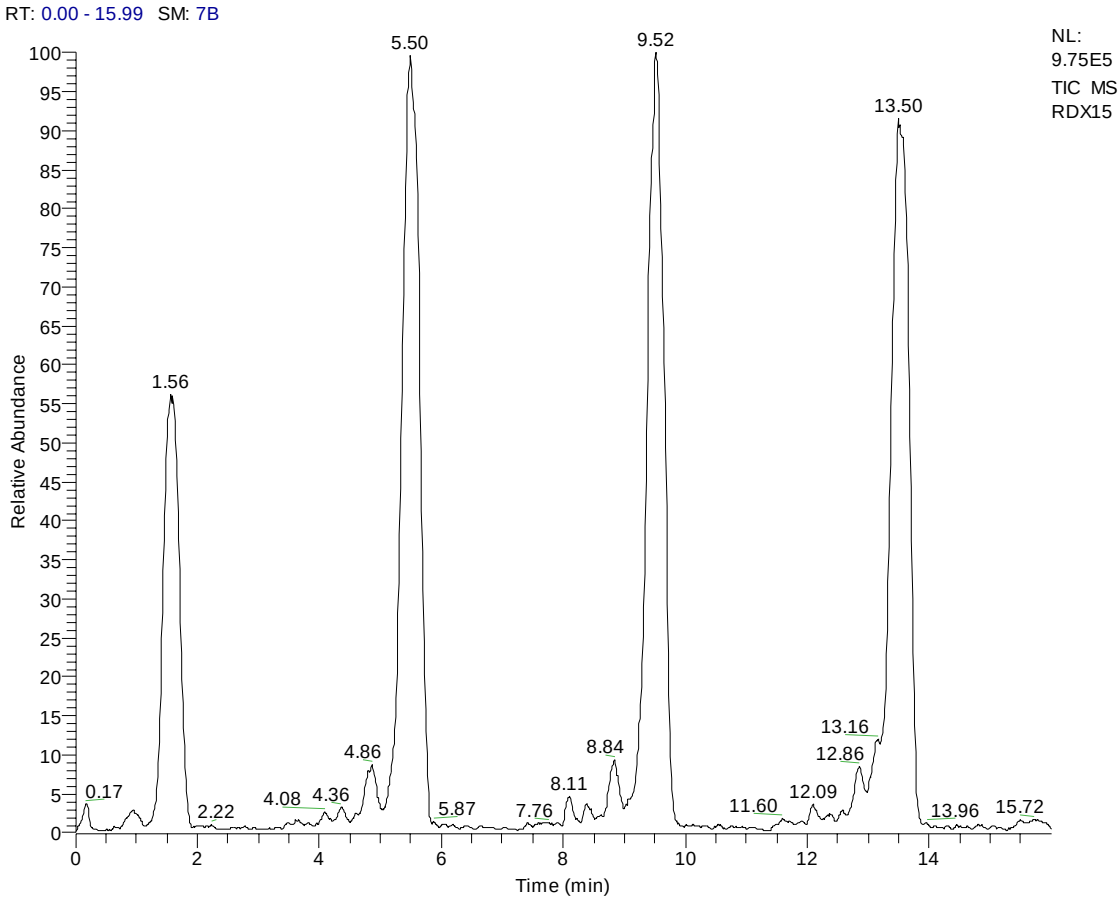

Figure 2-14. CV spectrum of RDX. Figure 2-14 shows the CV spectrum for RDX. The peaks are fairly well reproducible. There are two small peaks before the ion of interest in all four scans, which are identified in figure 2-15.

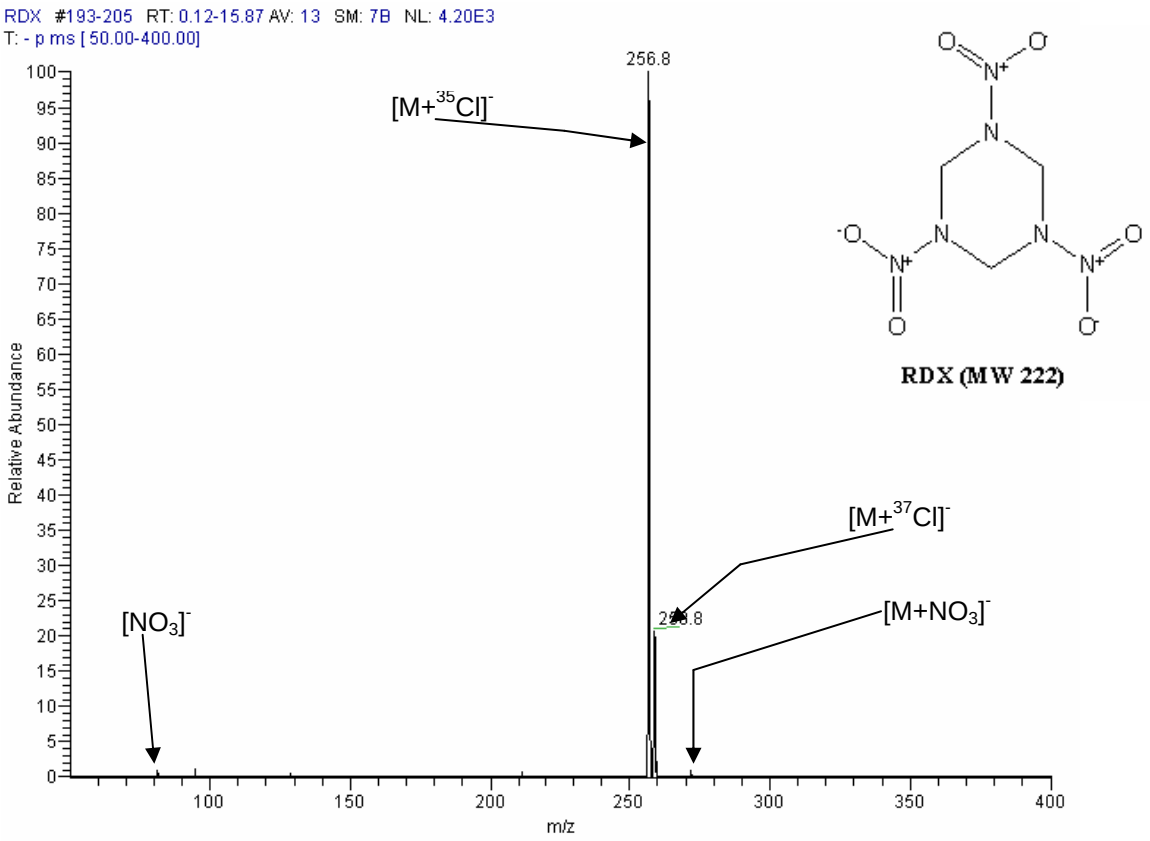

Figure 2-15. FAIMS/MS mass spectrum of RDX. The [M+Cl]- adduct is formed with the small amount of carbon tetrachloride in the solvent. (see Figure 2-15) One property of both RDX and HMX is the formation of little to no molecular ion. Interestingly, the adduct formed of RDX with the 37Cl isotope of chloride can also be seen in the mass spectrum. The first additional peak shown in the CV spectrum (figure 2-14) is m/z 62 which is an [NO3]- fragment peak; it is seen in many mass spectra of explosives, especially at higher temperatures. The second is a small amount of m/z 286, which is another adduct formed with RDX: $[M+NO_3]^-$.

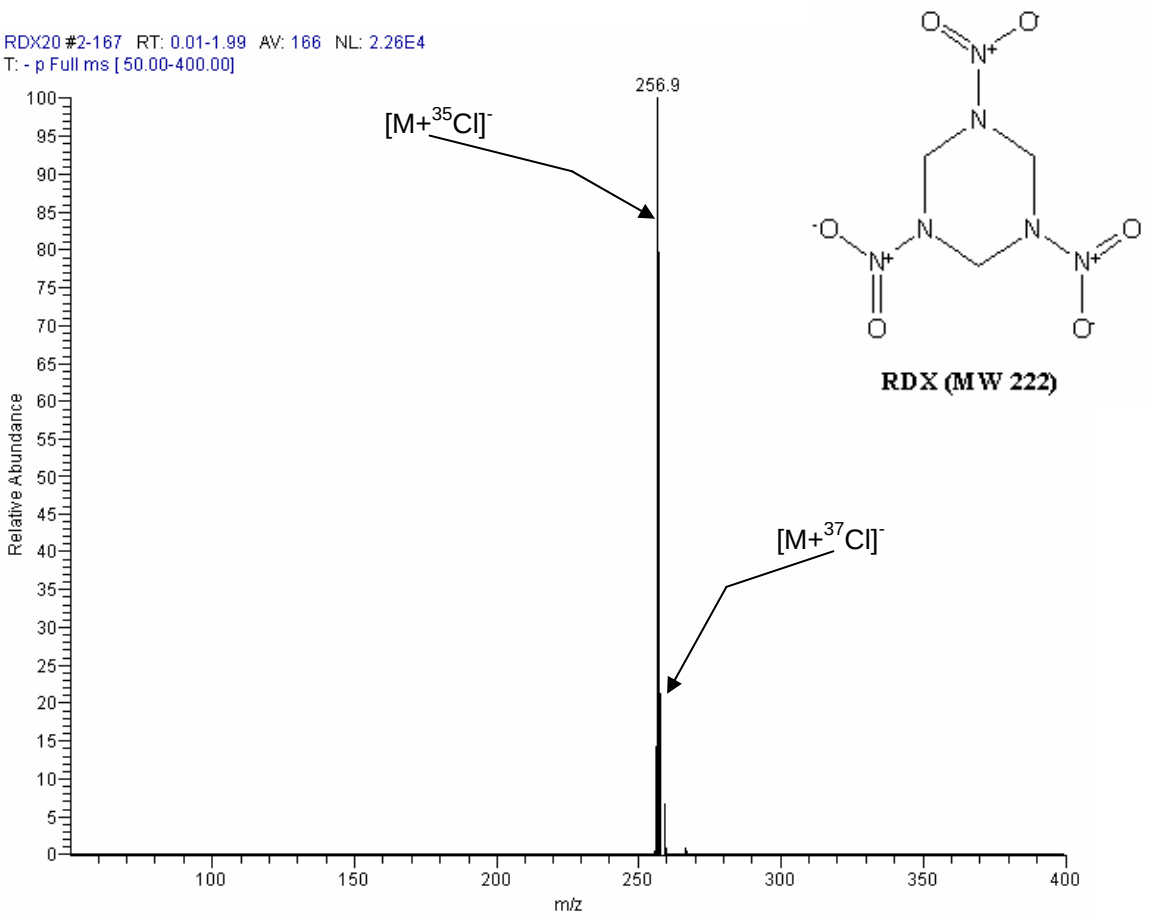

Figure 2-16. RDX: 2 min at CV = 5.1V. Figure 2-16 demonstrates that FAIMS/MS is an effective method of separating and detecting chloride adducts of RDX, as there are no interferences.

2.6.2.2 Cyclotetramethylene tetranitramine (HMX)

HMX, derived from High Molecular Weight RDX (sometimes known as High Melting Point Explosive), is a nitroamine discovered as a byproduct of RDX that consists of an eight-membered ring structure rather than a six-membered ring. It is slightly more powerful than RDX because molecules of greater mass generate greater energy when they decompose. Another difference between HMX and RDX is that HMX has a greater temperature at which the molecule begins to fragment (hence the name).[35] HMX is used exclusively for military applications, and is

most often included in a mixture, such as in some types of plastic bonded explosives, or octol, formed with TNT.

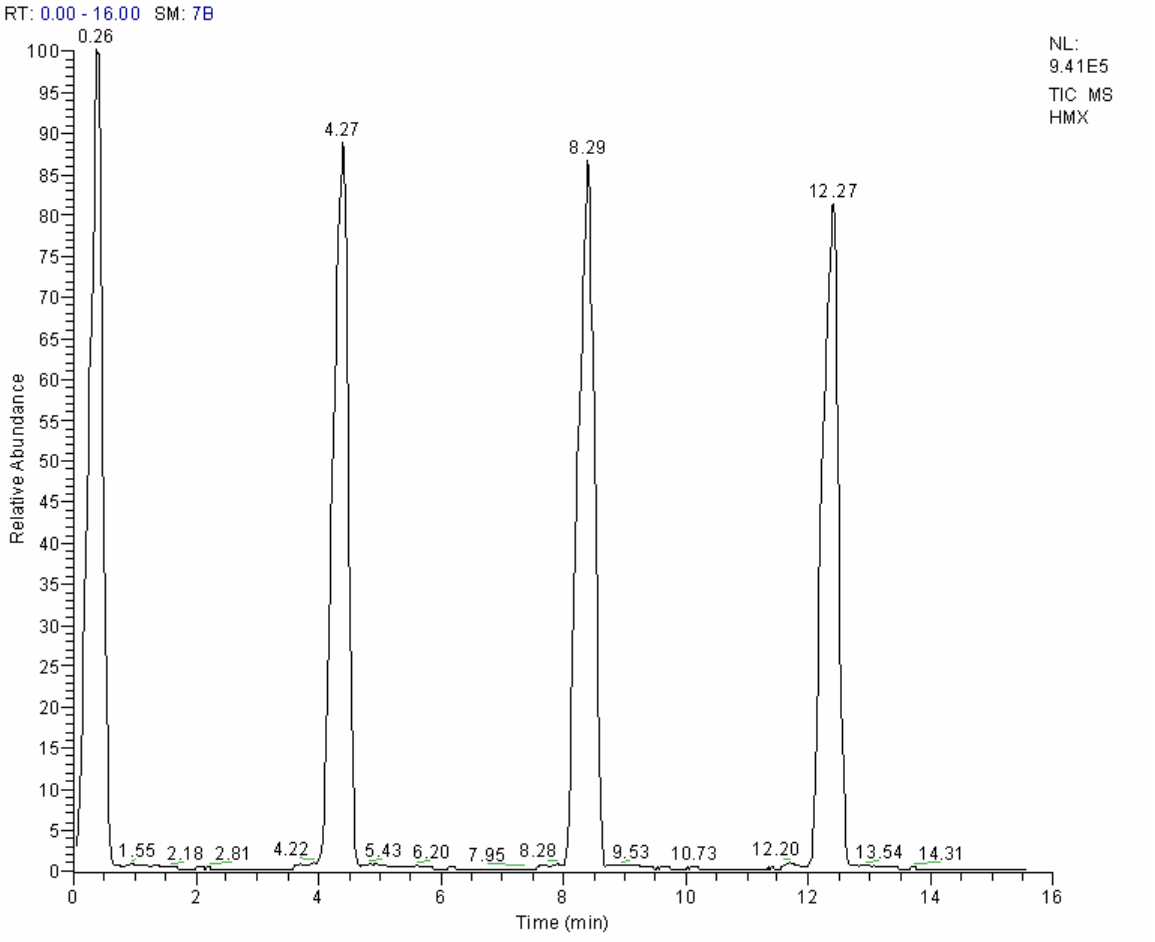

Figure 2-17. CV spectrum of HMX. HMX behaves similarly to its nitroamine counterpart RDX. The FAIMS CV spectrum shown in figure 2-17 reflects this. There are some differences between the two, though. HMX has a different CV (thus it can be resolved, as will be discussed in chapter 3), and there is no evidence of the $[NO_3]^-$ peak or formation of the $[M+NO_3]^-$ adduct.

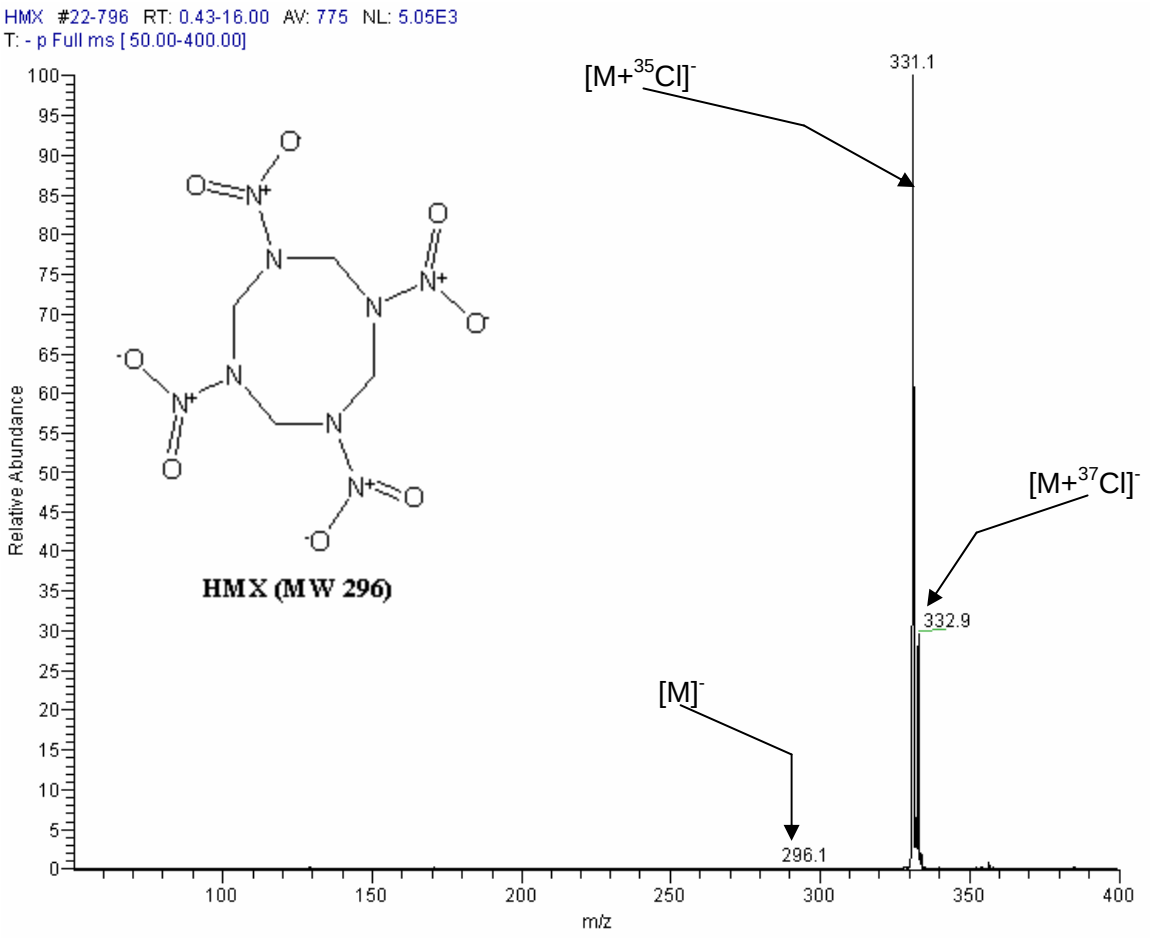

Figure 2-18. FAIMS/MS mass spectrum of HMX. Similar to RDX, the dominant ion for HMX was $[M+Cl]^-$. This can be seen in figure 2-18. Once again, adducts of HMX were formed with both dominant isotopes of chloride. There was also evidence of a small amount of $[M]^-$.

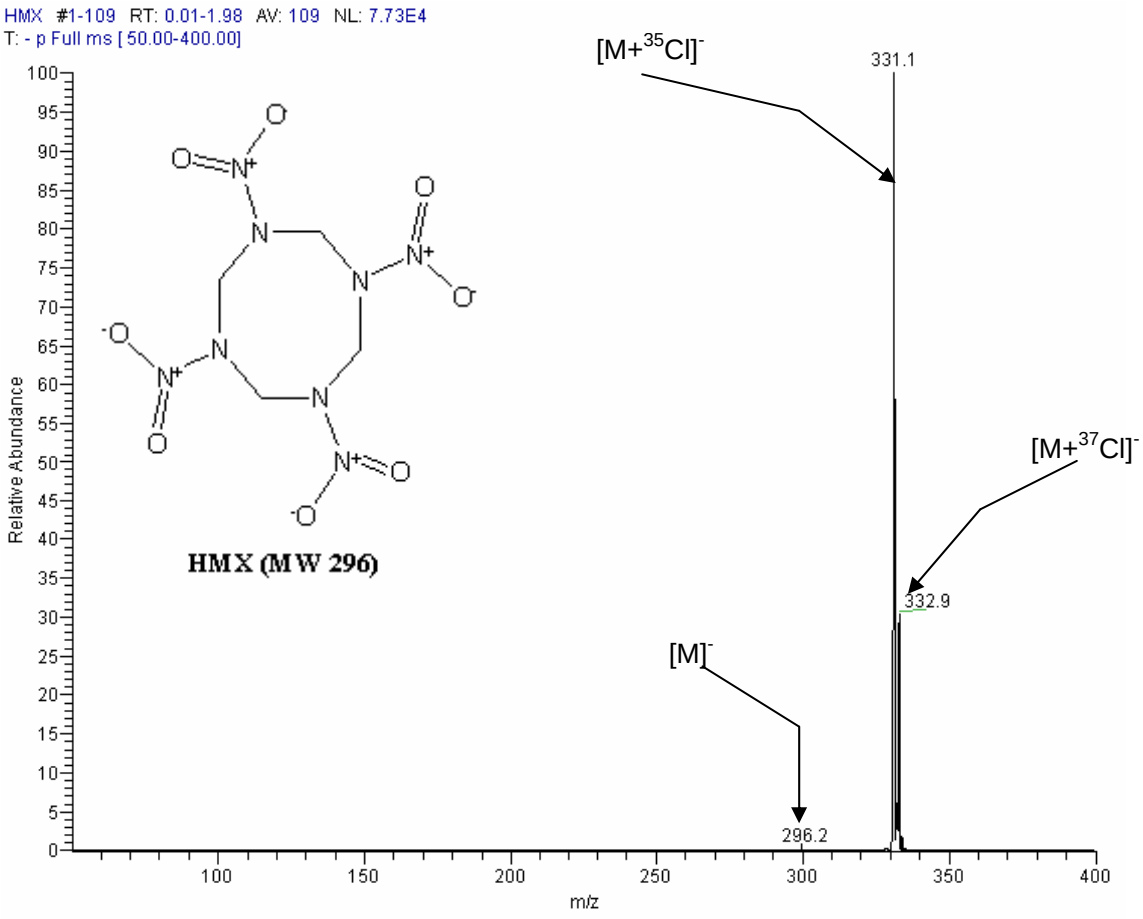

Figure 2-19. HMX: 2 min at CV = 1.2V. Figure 2-19 shows the HMX $[M+Cl]^-$ peak as the CV is fixed at 1.2V for a period of 2 minutes. The mass spectrum contains no interferences, and there is a small amount of the molecular ion peak, as there was during the CV scans (figure 2-18).

2.6.3 Nitrate Esters

2.6.3.1 Nitroglycerin (NG)

There were two nitrate esters that underwent characterization via FAIMS/MS. The first of these is nitroglycerin. Nitrate esters contain nitro groups like the previously mentioned explosives, though they are bonded to oxygen atoms, rather than nitrogen or carbon. There is also no ring structure, unlike the nitroaromatics and nitramines (Figure 2-20). Because of this structure, nitrate esters are extremely unstable, and fragment easily, requiring only a light shock to explode. Nitroglycerin is one of the oldest known explosives, discovered in the mid-nineteenth century.[28] It is mainly used in the manufacture of dynamite, gunpowder, and rocket propellants.

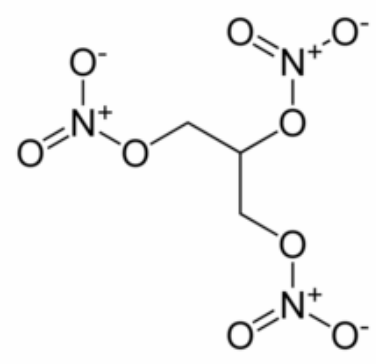

Figure 2-20. NG (MW 227) [Adapted from Paul W. 1996. Explosives Engineering, (Figure 3-3 p. 76), Wiley].

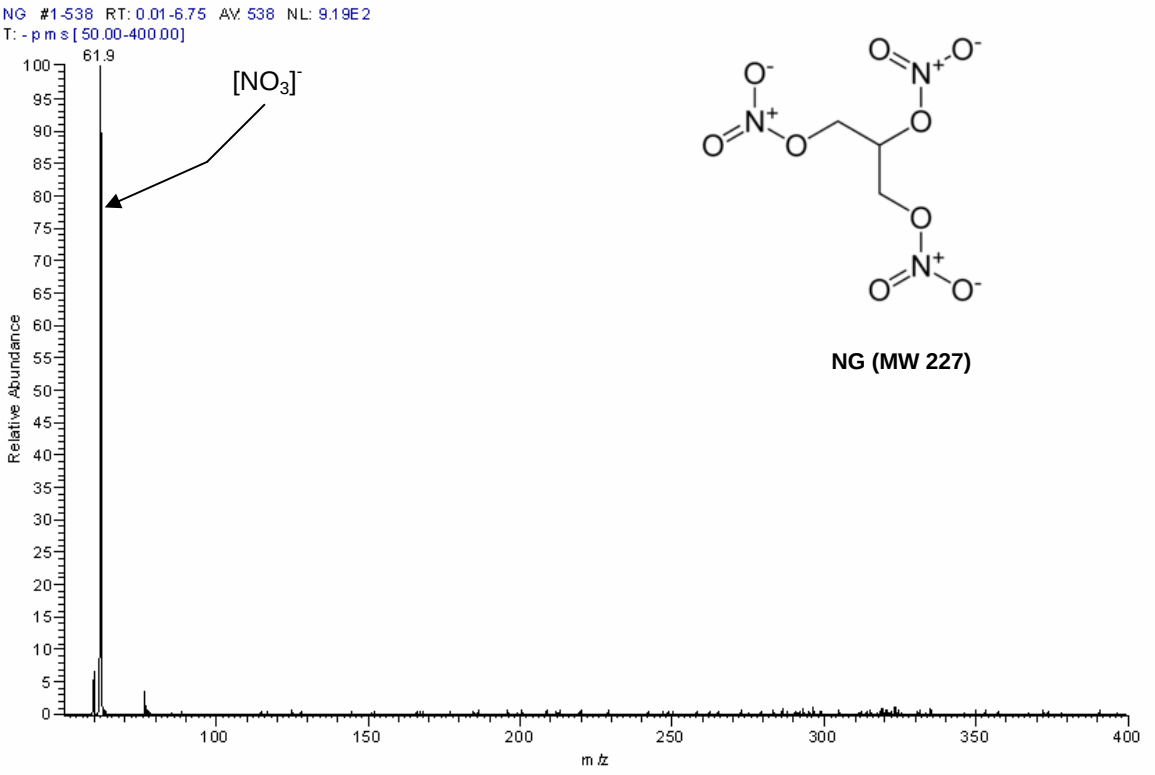

Figure 2-21. FAIMS/MS mass spectrum of NG. Similarly to the nitroamines, there is no molecular ion for NG. It also did not form adducts. Even though the heated capillary of the APCI source was decreased to the minimum of 100°C, all of the nitrate branches of NG were fragmented. These nitrate ions (m/z 62) were separated and detected with FAIMS/MS, as shown in Figure 2-21. Because the mass range will not extend below 50 amu for this instrument, it is not known how the carbon structure fragments. Ion count was about two orders of magnitude lower than most of the other explosives.

2.6.3.2 Pentaerythritol tetranitrate (PETN)

PETN is the second nitrate ester that was characterized. It is related in structure but is less stable than nitroglycerin and is more sensitive to shock or friction, and is one of the most powerful known explosives.[28] (see Figure 2-22) PETN was used in antitank weapons during WWII, and is today used in military demolition charges, in detonator charges for landmines and artillery, and in some types of small caliber ammunition. It is never employed alone due to its relative instability, and is always used in a mixture to enhance explosive capability and effectiveness.

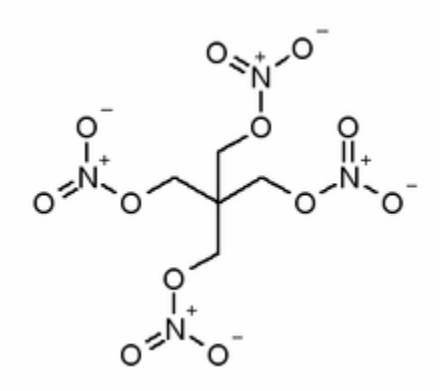

Figure 2-22. PETN (MW 316). [Adapted from Paul W. 1996. Explosives Engineering, (Figure 3-3 p. 76), Wiley].

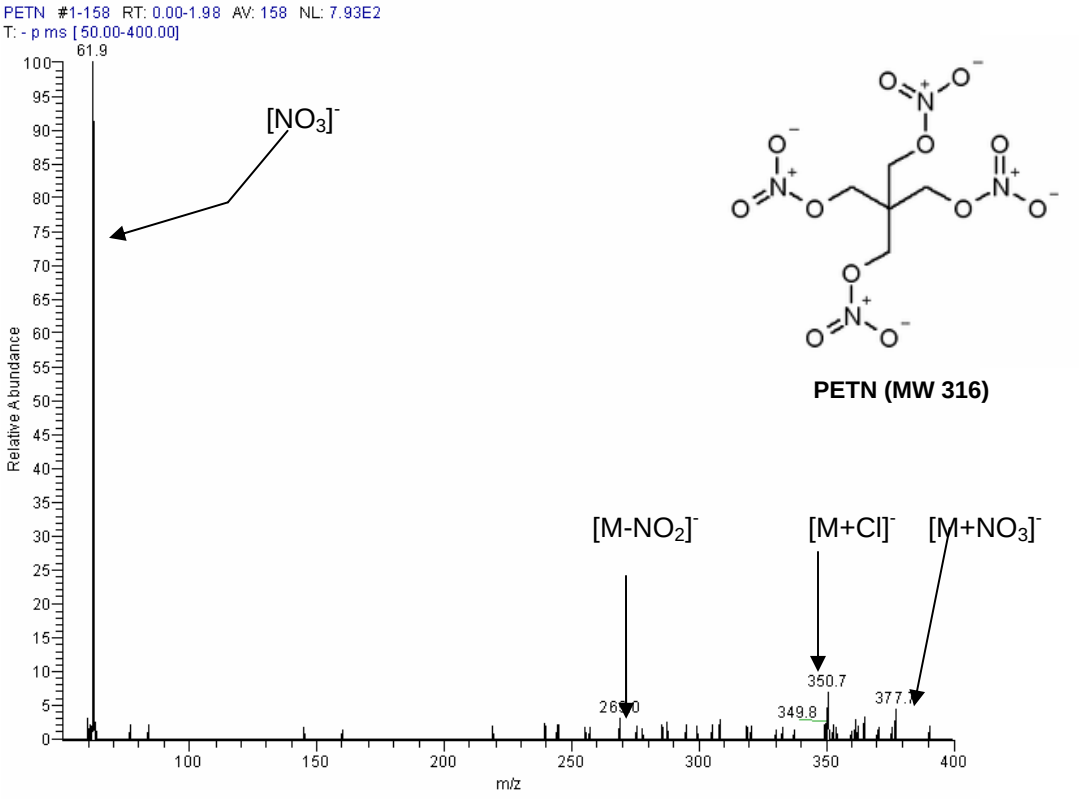

Figure 2-23. FAIMS/MS mass spectrum of PETN. Like the nitroamines and NG, PETN does not yield a detectable molecular ion. It did form both chloride and nitrate adducts; however, these were in extremely low intensity. As a result, PETN did not form any discernable peaks of high intensity during this experimentation. However, due to its extreme instability, (also like NG) PETN did fragment into nitrate ions which were separated and detected by FAIMS/MS (Figure 2-23). As this figure shows, the total ion count is relatively low.

2.6.3.3 Ammonium Nitrate Fuel Oil (ANFO)

ANFO is the most commonly encountered explosive today, used mostly for mining operations. It is simple and inexpensive to produce, and the components are not difficult to acquire. It is one of the most used explosives by terrorists, having been used by organizations such as: Fuerzas Armadas Revolucionarias de Colombia (FARC), Provisional Irish Republican Army (IRA), Palestinian extremists, and some American extremists. Ammonium nitrate (used in fertilizers) is an oxidizer and can explode inefficiently on its own if shocked. A hydrocarbon mixture provides fuel for the reaction. Usually kerosene or diesel fuels serve this purpose industrially; although, terrorists have used other fuels (such as nitromethane to make the "kinepak" mixture used for the Oklahoma City bombing). Since there are so many different production methods and types of fuels used in different proportions, no two batches are identical. This, coupled with the fact that ammonium nitrate and hydrocarbon fuels are present in background air, suggest that ANFO will be extremely difficult to detect. On the other hand, a destructive bombing requires large amounts of it (eg., over 5,000 pounds at Oklahoma City)

Ammonium nitrate decomposes according to: $2NH_4NO_3 \rightarrow 4H_2O + 2N_2 + O_2$
the most important product being oxygen. The hydrocarbon fuel added burns rapidly to include CO_2 as a product.[28]

ANFO is extremely stable, but is hygroscopic, which hinders long-term storage. ANFO will not explode without a secondary booster (blasting cap); the power of the explosion can be controlled by altering the mixture.

Five different types of ANFO were examined in this research. The hydrocarbon fuels used were: n-pentane, n-hexane, toluene, nitromethane, and diesel fuel. All were made using about 94% (by mass) ammonium nitrate and the remainder of fuel. The pentane and hexane were used to determine the effects of using a simple straight-chain hydrocarbon fuel to simplify (and thus

identify peaks in) the mass spectra. Nitromethane was used to produce the "kinepak" mixture that was discussed above; toluene was used to provide a large structure with a methyl group to compare and contrast results to kinepak ANFO. Characterization was done on the FAIMS/MS in both positive mode and negative mode. Dilute solutions (about 10-15 ppm) were heated slightly to instigate the oxidation reaction without causing detonation.

Characterization of ANFO using this method is difficult. There are no other mass spectra with which to compare the results of this effort. This is likely due to the fact that no two batches of ANFO are alike, and the mass spectra are difficult to reproduce. A limitation of the LCQ is that the mass range cannot be set below m/z 50; therefore, fragment ions from ammonium nitrate and the fuels cannot be seen.

Nearly all of the negative ion APCI data sets collected show an ion base peak in common: $[NO_3]^-$ (m/z 62). This may result from ammonium nitrate that has not yet reacted. For those fuels of m/z greater than 50; though, the fuel itself was not seen neither in positive mode MS, nor in negative mode MS (though straight chain hydrocarbons are almost never seen in negative mode MS), the exception to this being ANFO made with diesel. In every case for ANFO, a single 16 min scan was conducted comprising an area from CV -40V-40V. In each of the following figures (2-24 and 2-25), a single peak was detected.

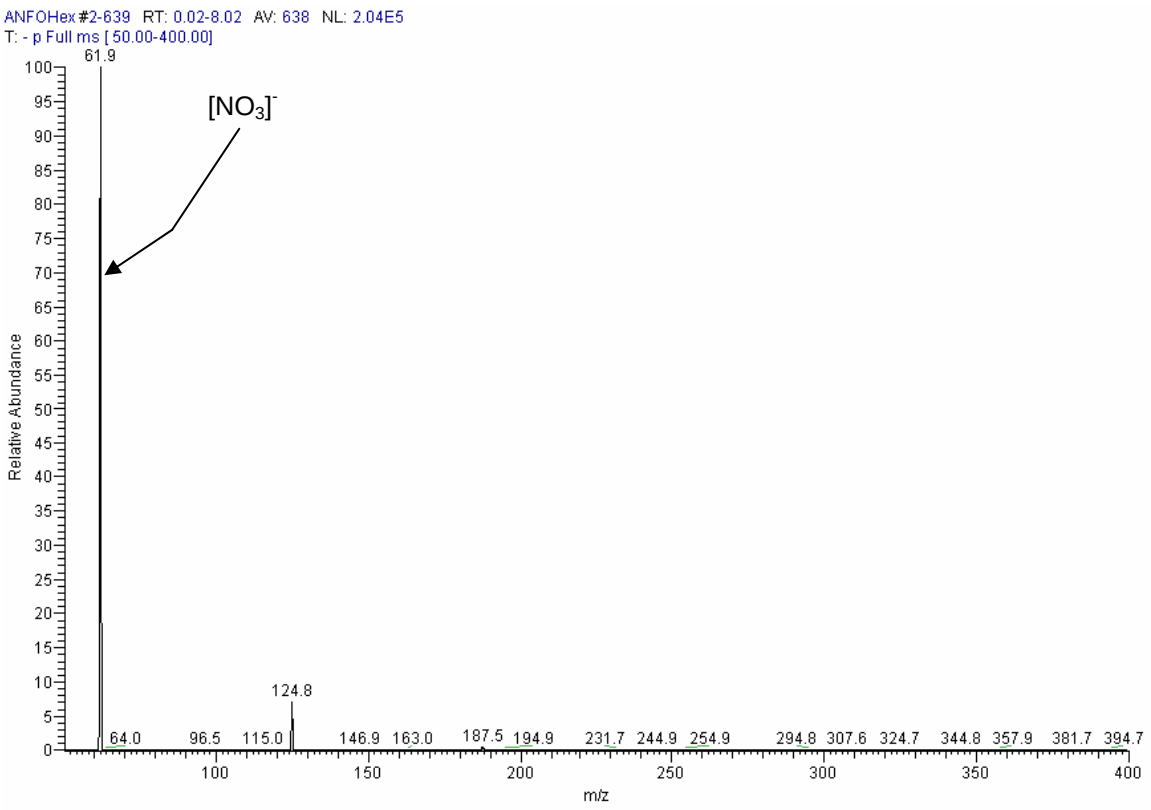

Figure 2-24. FAIMS/MS mass spectrum of ANFO made with hexane. Figure 2-24 shows a FAIMS/MS mass spectrum of ANFO made with hexane. The base peak is $[NO_3]^-$, which passed through the FAIMS cell at a CV of 9.7V. There is also a small peak at m/z 125.

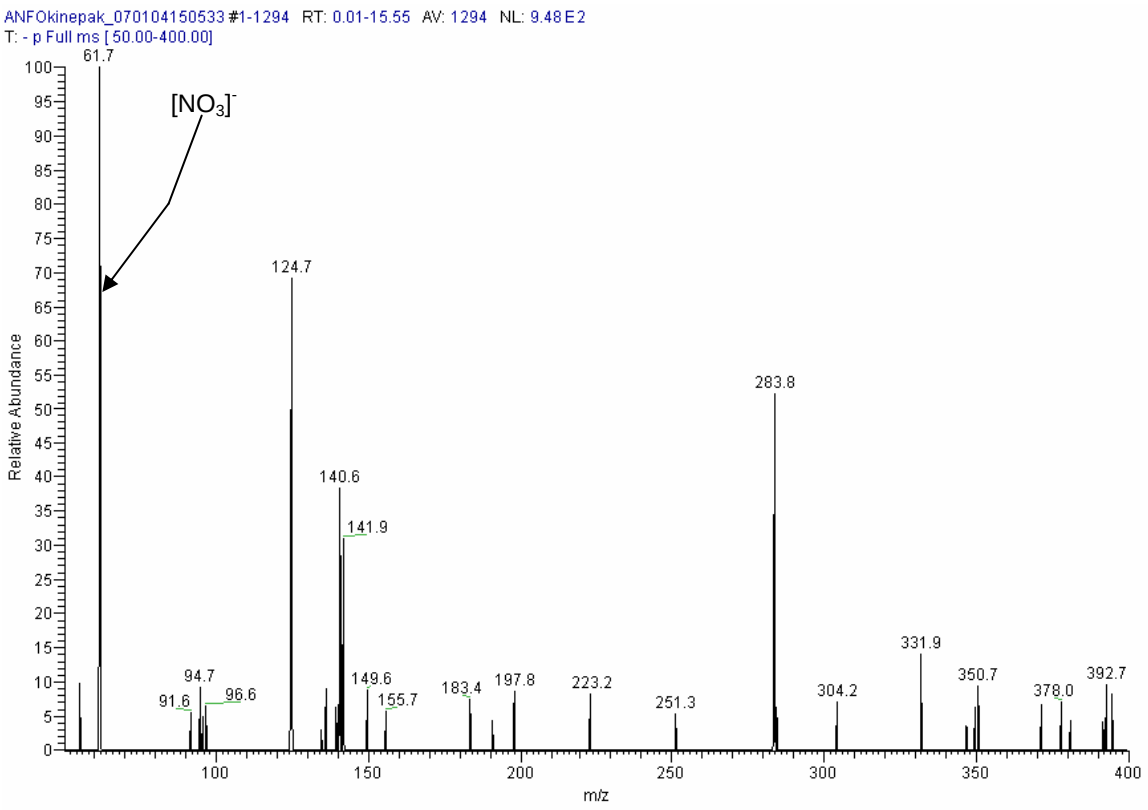

Figure 2-25. FAIMS/MS mass spectrum of ANFO made with nitromethane. ANFO made with nitromethane (figure 2-25) as the fuel has a much lower ion signal than that made with hexane; this behavior was also seen with ANFO made with toluene. It also has a $[NO_3]^-$ base peak, though there are some other ions as well. These ions were in common with some of the other runs as well: m/z 125, m/z 141, and m/z 284.

Detection of ANFO with a field instrument would prove to be difficult, as ammonium nitrate exists in the background (mostly in fertilizers) and the most common fuel, diesel, is used to power engines everywhere. The most likely type of ANFO to be detected would be "kinepak," for nitromethane is used for little other than as a fuel additive for race cars.

CHAPTER 3
FAIMS/MS AND IMS/FAIMS/MS OF EXPLOSIVES

3.1 Instrumentation

The experiments described in this chapter were conducted using a different instrument configuration than that in chapter 2. As in the other experiments, the mass spectrometer was a Finnigan LCQ.

3.1.1 Electrospray Ionization (ESI) Source

Electrospray ionization (ESI), employed in this study, is similar to APCI. Instead of relying on a corona discharge to ionize molecules in the gas phase, ESI uses electrical charge to ionize molecules in solution. A liquid solution containing the analyte of interest in solvent is passed through a capillary held at high potential. Droplets leaving the capillary become highly charged. As the solvent in the droplets evaporates, ionized molecules are ejected into the gas phase. [36]

The unique non-commercial ionization source used in the studies in this chapter was developed by the Herbert H. Hill laboratory at Washington State University (WSU). It is a fairly simple apparatus, consisting of a fused silica capillary held in place by a ferrule, and mounted in a nonconductive teflon casing. Sample is introduced via syringe pump into this capillary, to which approximately -13.5 kV of ionization potential is applied to a stainless steel ferrule through which the capillary is threaded. Due to the relatively small (about 0.5 mm) internal diameter of the capillary, the flow rate of the syringe pump can be low (as low as 1 mL/min).

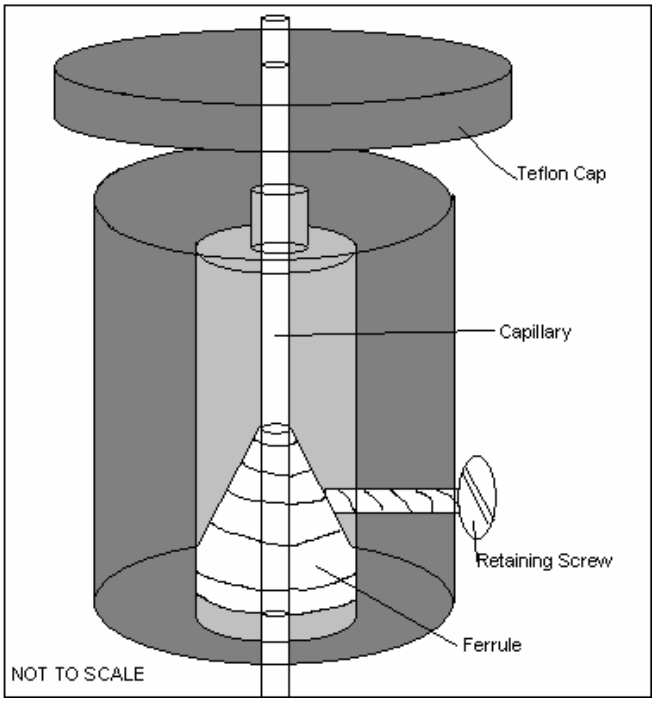

Figure 3-1. WSU electrospray ionization source. Figure 3-1 shows the WSU ESI source. The darkly shaded areas are constructed of Teflon, and the capillary is fused silica. The ferrule used is conductive stainless steel.

Figure 3-2. WSU electrospray ionization source photograph. Figure 3-2 is a photograph of the WSU ESI source. Note that the tip of the capillary extends through the screen of the IMS. This was done so that the ions would not be deflected backwards by the electric field.

3.1.2 Ion Mobility Spectrometer (IMS)

An ion mobility spectrometer (IMS), as briefly discussed in Chapter 1, is similar to FAIMS, in that it employs an electric field to separate ions based on mobility. An IMS drift tube was designed and patented[37] by the Hill laboratory at WSU. This tube has a total length of 34 cm, containing a series of flat ring-shaped electrodes composed of conductive stainless steel with dimensions of 50 mm outer diameter × 48 mm inner diameter × 3 mm, separated by ceramic rings. A voltage is applied to each of these ring electrodes that generates the electric field that propels ions through the drift tube. For negative ions, the first electrode carries a potential of about -10.5 kV, and this is incrementally decreased on successive electrodes such that the last electrode carries about -2 kV. The curtain plate of the FAIMS (set to -1 kV) acts as the final electrode of the IMS to attract negative ions into the FAIMS cell. This IMS operates at atmospheric pressure and employs heating to help desolvate the sample. The heater was adjusted to be as high as possible without fragmenting the sample ions (temperature ranging from about 150°C to 250°C). Countercurrent gas flow also aids in desolvation.

The IMS contains a Bradbury-Nielsen gate ring electrode[38] which divides the tube into a desolvation region and IMS drift region. A reference potential is used to "open" the gate, thus allowing ion transmission from the desolvation region into the drift region, or a different voltage can be applied to "close" the gate by creating an orthogonal electric field that prevents ion transmission. In these experiments, the IMS was first operated in total ion transmission mode, and then it was set to gate ions for separation.

3.1.3 Orthogonal Dome FAIMS Cell

This instrument configuration also utilized an Ionalytics Selectra beta prototype; however, the cell geometry was not the same as that used in the first series of experiments (chapter 2). The cell used in the characterization experiments consisted of a line-of-sight cylindrical geometry; in

contrast, the cell used in this chapter (figure 3.3) employs an orthogonal dome-shaped geometry. The waveform generator, application, and waveform shape are identical. Two major differences between the two configurations are that the dome-shaped cell permits the distance between the electrodes to be adjusted, and provides slightly higher resolution.[39]

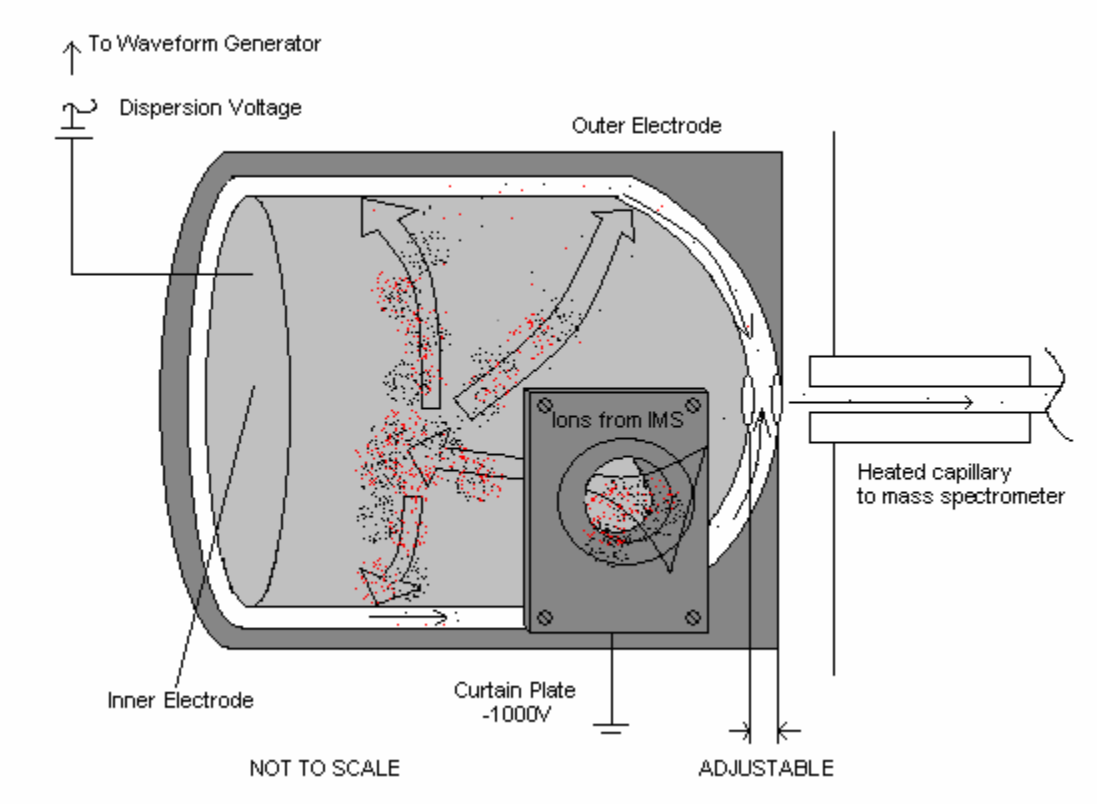

Figure 3-3. Drawing of Ionalytics orthogonal dome FAIMS cell. Figure 3-3 contains a drawing of the orthogonal dome FAIMS cell. The red and black dots describe a simple scenario in which the black dots represent the analyte of interest and the red dots are noise (interferent ions). Both types of ion enter the FAIMS cell through the curtain plate and are separated as the red ions collide with the walls of both electrodes when the proper CV is set. A percentage of the analyte ion is also lost, but this is the only ion type that enters the mass spectrometer.

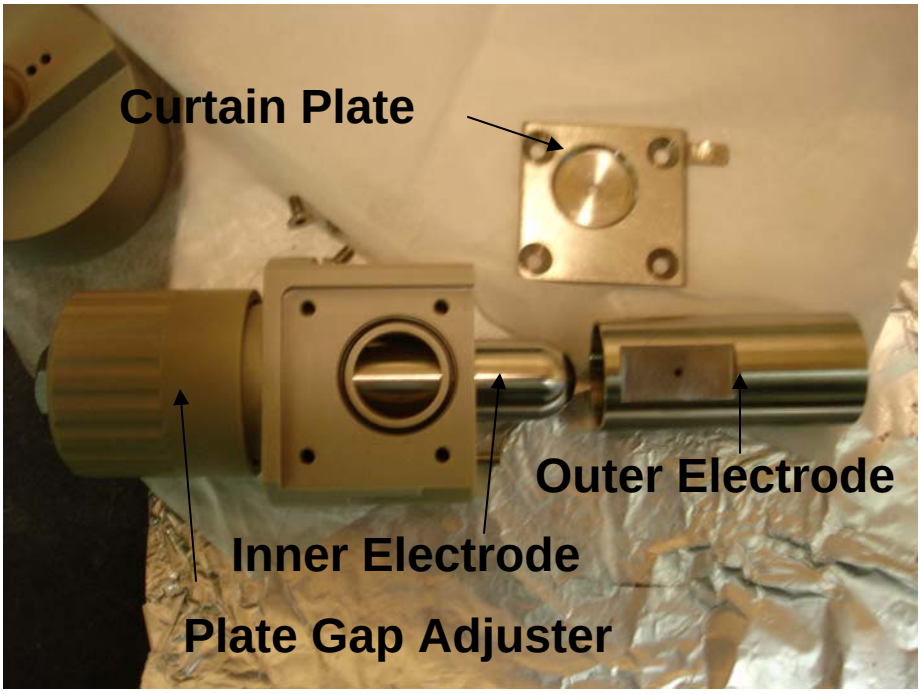

Figure 3-4. Photograph of Ionalytics orthogonal dome FAIMS cell. Figure 3-4 is a photograph of the disassembled orthogonal dome cell used for these experiments. The plate gap adjuster rotates to change the distance between the inner and outer electrodes.

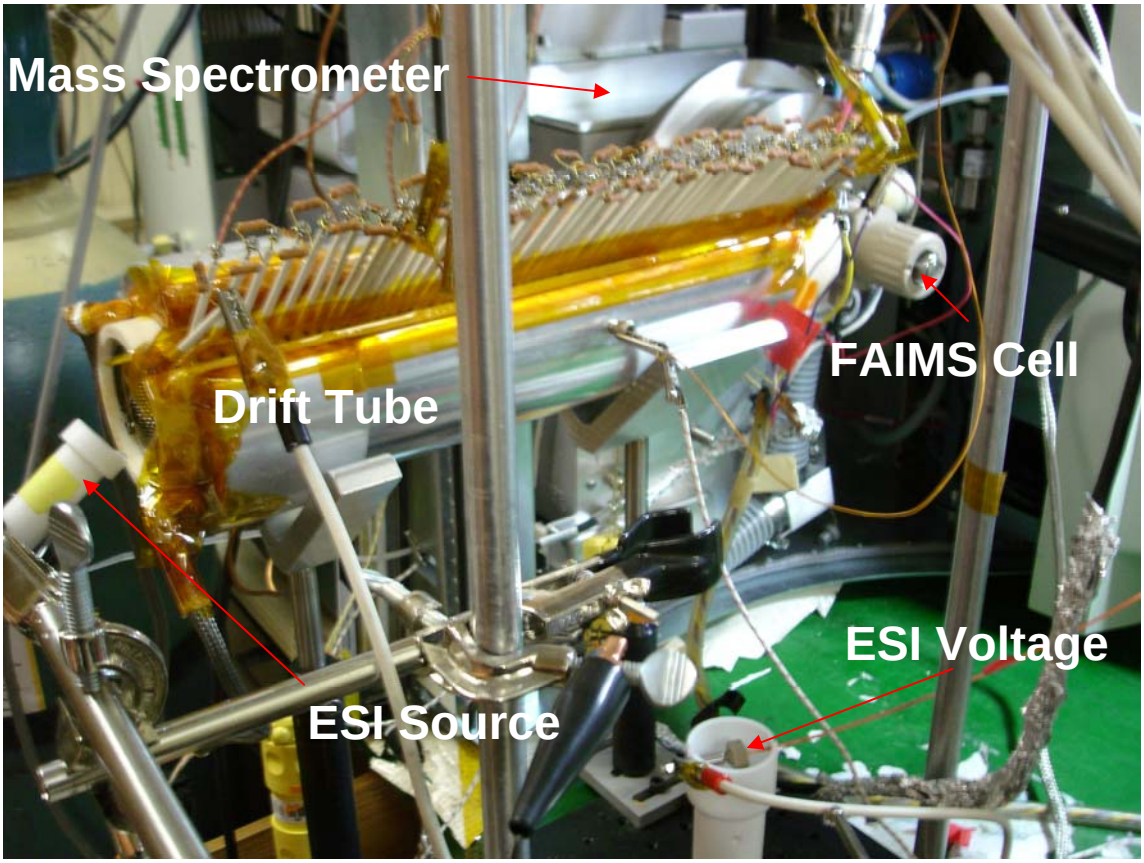

Figure 3-5. WSU apparatus. A photograph of the entire WSU apparatus including ESI source, IMS drift tube, and FAIMS cell can be seen in Figure 3-5. The waveform generator is not connected to the FAIMS cell so that it is easily visible.

3.2 FAIMS Limitations

As discussed briefly in Chapter 1, one of the primary limitations of FAIMS is fairly low resolution compared to chromatographic separation methods, hence its use here in conjunction with mass spectrometry as a separation device rather than a stand-alone instrument. There are several factors that can affect resolving power of a FAIMS cell.[40] The factors that have been addressed in the following experiments include dispersion voltage, distance between the inner and outer electrodes in the domed FAIMS cell, carrier gas consistency, and addition of a desolvation region prior to the FAIMS cell. In addition, another limitation is band broadening over time as buildup of solvent interferes with ion separation within the FAIMS cell.

3.3 Effects of Addition of Helium to the Carrier Gas

For the entire first set of experiments (chapter 2), the carrier gas in the FAIMS cell was 100% pure nitrogen. However, experimentation has shown that the addition of a percentage of helium can increase transmission and sensitivity. This effect slightly narrows CV peaks and therefore increases resolving power. The reason for this behavior is not clear; although, it is suspected that because helium increases mean free path within the cell, ion dispersion and desolvation are also increased. It is also possible that the high-field is effectively strengthened.

It is not desirable to use too high a percentage of helium carrier gas into the cell, as the high voltage can induce discharge. It should be noted that because the amount of helium in the atmosphere is trace, field instruments developed with FAIMS technology would most likely not employ helium in the carrier gas.

3.4 High-resolution FAIMS (HRFAIMS)

High-resolution FAIMS (HRFAIMS) experiments were conducted on the WSU apparatus described in this chapter. Three major differences between this instrument and that used for characterization in chapter 2 in terms of FAIMS resolution are: FAIMS cell geometry, addition of an IMS (set to total ion transmission mode) in front of the FAIMS cell, and use of a percentage of helium (25%) in the nitrogen carrier gas.

As discussed above, the FAIMS cell used for this set of experiments was an orthogonal dome cell, rather than a line-of-sight cylindrical cell. The dome cell can provide higher resolution, due in part to the longer path length through the cell, and due in part to the use of two field areas in series; there is a cylindrical area and a spherical area.

The IMS drift cell was set in full ion transmission mode (ie., there was no gating); although, the heater and electric field were still engaged. There is also gas flowing countercurrent through the IMS, which can dramatically reduce the amount of solvent reaching

the FAIMS cell. The temperature of the heater was set to be as high as possible without fragmenting the explosive molecules. The IMS had the most significant effect on overall resolution compared to the other factors. Transmission was increased, and CV peaks were narrower, demonstrating increased resolution. This is probably due to the fact that the heater desolvates the sample, and the electric field focuses ions into a tight beam for more efficient introduction into the FAIMS cell.

3.4.1 Separation of Mixtures of Explosives

Although use of FAIMS as a separation device may decrease total ion transmission, when the CV is set for a particular ion of interest, the signal-to-noise ratio of that ion can increase greatly.

The first mixture that was examined consisted of about 20 ppm of HMX and about 15 ppm of RDX. The DV was set to -2500V, which was the optimal setting when the IMS was installed. The carrier gas was made up of 75% nitrogen and 25% helium to improve ion count and resolution. Figure 3-6 is the CV spectrum for the HMX/RDX mixture. CV was scanned from 0-20V once over a period of 8 minutes. Each peak is distinct and fully resolved. The RDX peak is significantly smaller because there was not only a slightly smaller concentration in the sample, but also the boiling point is much less than HMX.

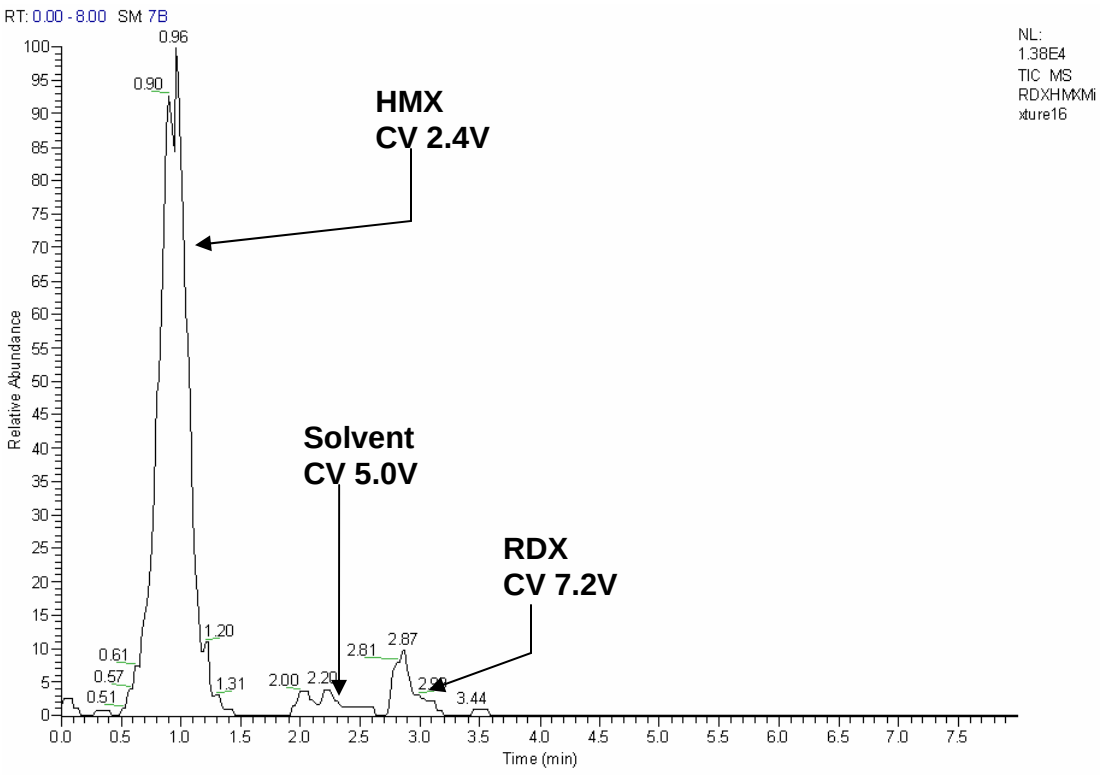

Figure 3-6. CV spectrum of HMX/RDX mixture.

.

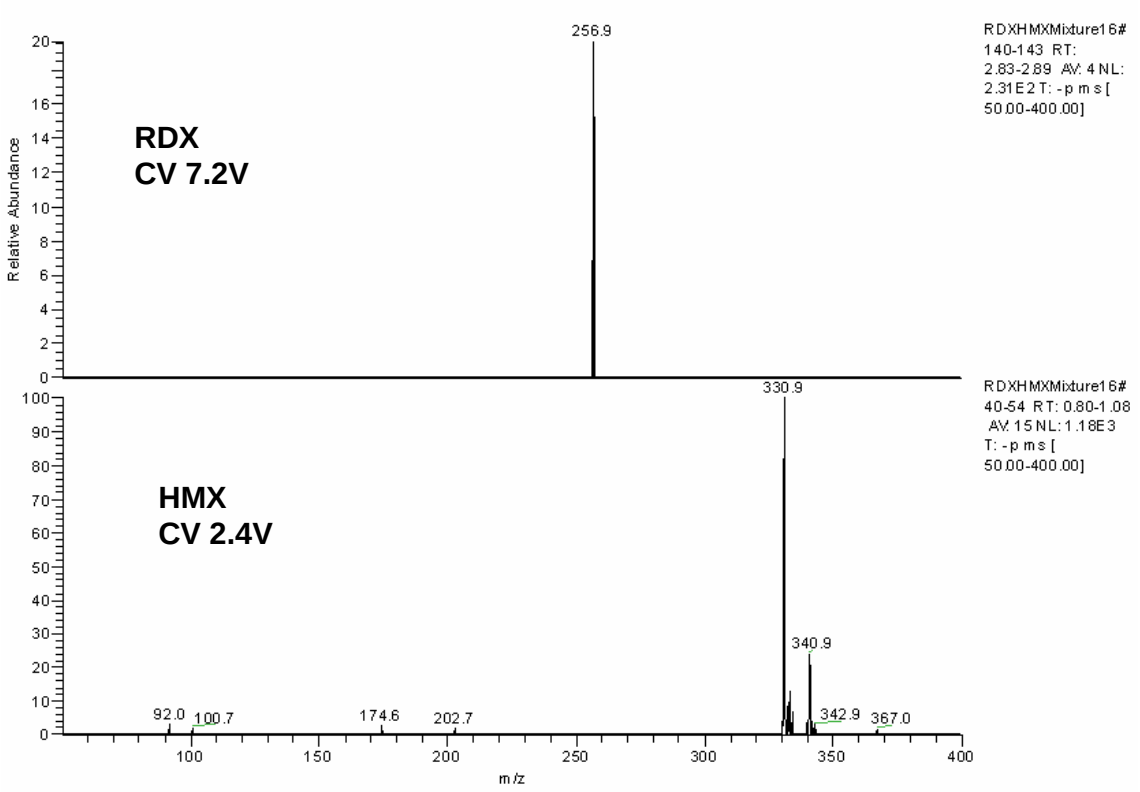

Figure 3-7. Mass spectrum of HMX/RDX mixture. Figure 3-7 contains the mass spectra of the RDX/HMX mixture, showing the $[M+Cl]^-$ adducts of both RDX (m/z 257) and HMX (m/z 331) taken from the relative CV peaks (which are seen in Figure 3-6). The HMX peak at m/z 341 is an $[M+NO_3]^-$ adduct

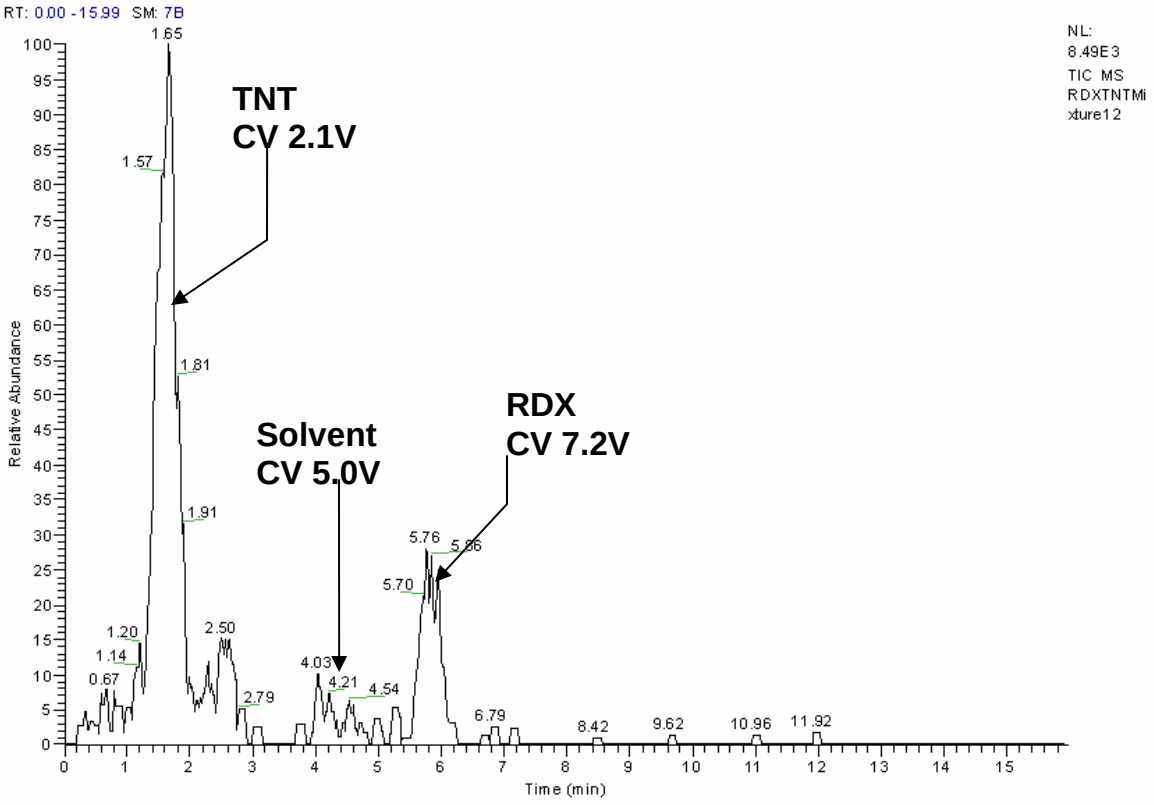

Figure 3-8. CV spectrum of TNT/RDX mixture. A second mixture examined was torpex, which consists of TNT and RDX in approximately equal portions. The only difference between the mixture that was examined here and the military explosive is that in this case there is no aluminum powder. In this case, one CV scan from 0-20V was done over 16 minutes. Once again, both components (see Figure 3-8) are fully resolved from each other and the solvent background in the CV spectrum.

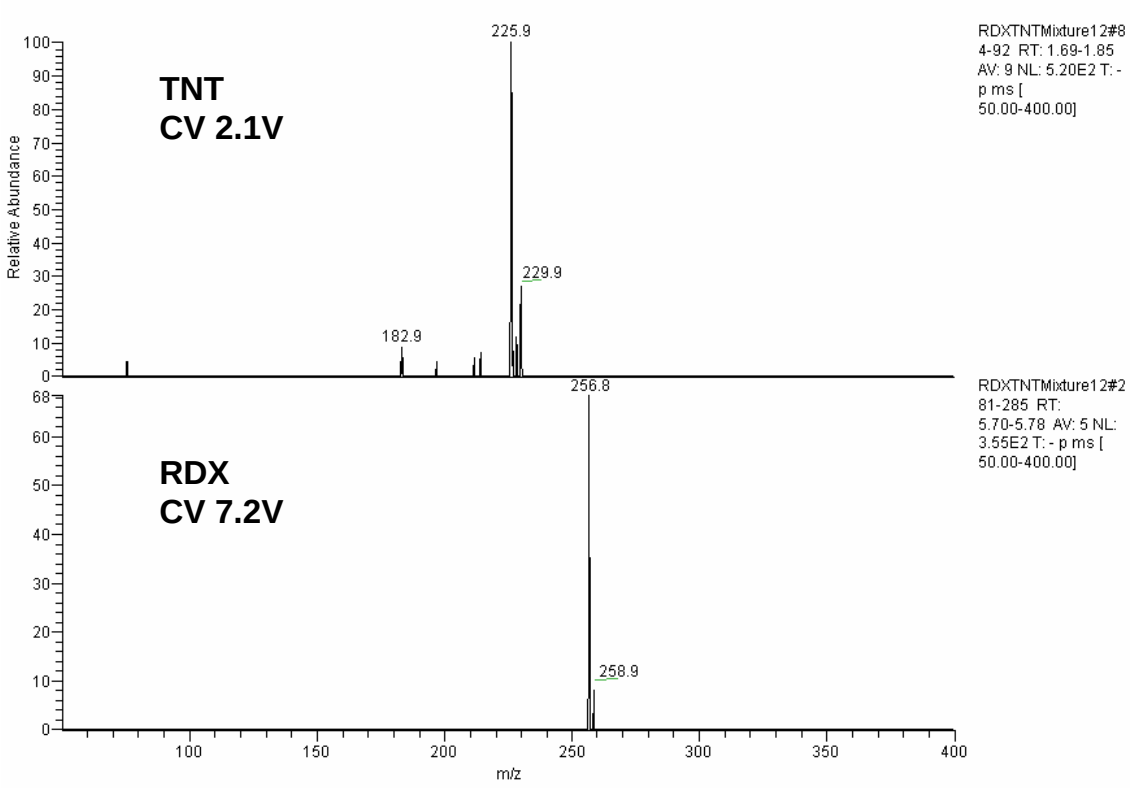

Figure 3-9. Mass spectrum of TNT/RDX mixture. Figure 3-9 shows the mass spectra of the respective CV peaks of TNT and RDX in the mixture (Figure 3-8). Both components (the TNT [M]- ion at m/z 226 and the RDX [M+Cl]- ion at m/z 257) are shown. It should be noted that because the same DV was used for both of these mixtures (-2500V), the CV values of RDX and the solvent is identical in the CV spectra of both mixtures. (Compare figs. 3-6 and 3-8)

3.4.2 Resolving Isomers

The next step in separation is the resolving of two isomers of the same explosive. The explosive chosen was dinitrotoluene (DNT), because it has two isomers that are precursors to TNT: 2,4-DNT and 2,6-DNT. The analysis of these isomers can potentially be important to explosives forensics. Few, if any, technologies deployed today can detect and resolve these isomers from each other. Because they are isomers, they have identical molecular weight. Both have similar mobility behavior, but due to the fact that the shapes of the molecules are slightly different, each behaves uniquely under high field.

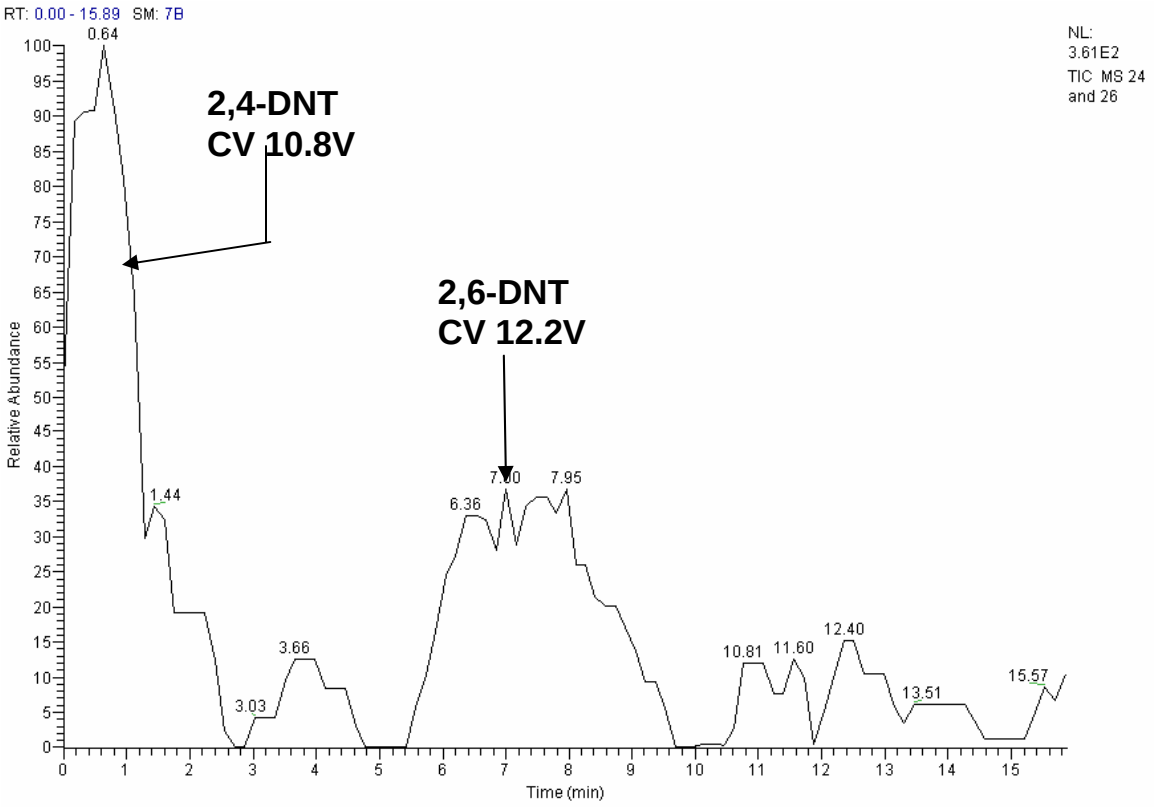

Figure 3-10. CV spectrum of both isomers of DNT. A mixture was created using about 20 ppm of both isomers in equal proportion. This is a relatively small amount, hence the low ion transmission. The CV scan was conducted slowly from only 10-15V over 16 minutes. Both isomers are clearly resolved from each other, as shown in Figure 3-10. It should be noted that there was a $[2,6\text{-DNT-NO}]^-$ fragment peak that appeared during the characterization (as discussed in Chapter 2, section 2.6). This fragment did not appear while using the high-resolution setup in the 10-15V CV range.

3.5 Dispersion Voltage

Another effect that the IMS added was that the optimal DV was no longer the highest possible (-4000V); the ion signal was nearly zero above a DV of -3000V. The FAIMS carrier gas flow rate also had to be reduced to about 0.5 L/min from 4.0 L/min for optimum performance. This is in contrast to the situation with FAIMS by itself (as in chapter 2), where optimum sensitivity is observed at maximum DV and high carrier gas flow rate. There are several possible reasons for this unusual behavior. For example, higher flow leaving the curtain plate may cause ion scattering at the IMS/FAIMS interface. This may be overcome by closing

the system with a nonconductive sleeve that encloses the space between the IMS and FAIMS. This might also make directing the ion beam into the FAIMS easier. Another possible explanation is that the small difference in potential between the last electrode of the IMS (-2kV) and the curtain plate (-1kV) required carrier gas flow to be decreased to allow the potential to transport ions efficiently into the FAIMS cell.

3.6 Effects of Adjustment of Plate Gap

As discussed above, the distance between the inner and outer electrodes of a FAIMS cell affects the electric field generated. Since the electrode gap of the dome cell can be adjusted (figure 3.3), data were collected to determine the optimal electrode gap for explosive detection.

The cylindrical cell electrode gap is fixed at 1 mm; whereas, the gap in the cylindrical portion of the dome cell is fixed, the gap in the dome portion is adjustable up to 2.4 mm in increments of 0.1 mm. Four data sets were taken with a fixed DV at -3000V, each consisting of two CV scans from 0-20V over a period of 8 min each. The sample selected was a solution of about 15 ppm RDX, which was chosen because it has a relatively low fragmentation temperature (about 170°C) compared to the other explosives. The FAIMS/MS behavior of both the $[M+Cl]^-$ ion and the fragment ions were analyzed.

The expected relationship between resolution and electrode gap is that the lowest gap should provide the highest resolution, as the field is stronger. As expected, the ion count was the lowest, as there is a lower mean free path; most ions collide with the electrodes.

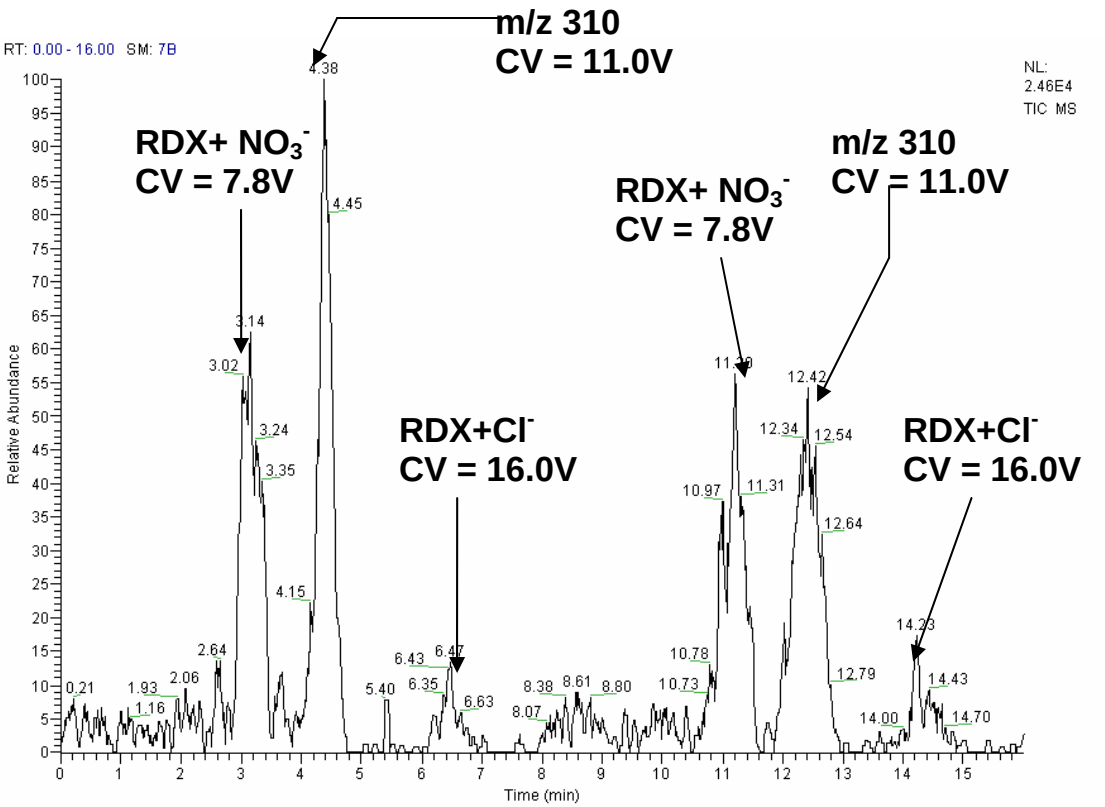

Figure 3-11. RDX CV spectrum at 0.5 mm. The first trial was at a relatively small gap of 0.5 mm (Figure 3-11). The CV was scanned from 0-20V over 8 minutes twice. On the figures, ion count is seen after "NL." This figure shows three peaks. One of these (m/z 310) is probably a solvent cluster. A second (m/z 283) is the nitrate adduct of RDX. The third (m/z 257) is the RDX chloride adduct. In this case, the RDX analyte of interest is the smallest peak compared to the solvent. Probability of transmission of RDX molecules relative to solvent indicates that when the electrode gap is smallest, most RDX molecules collide with the electrodes and are lost. The maximum ion signal is 2.46×10^4 counts.

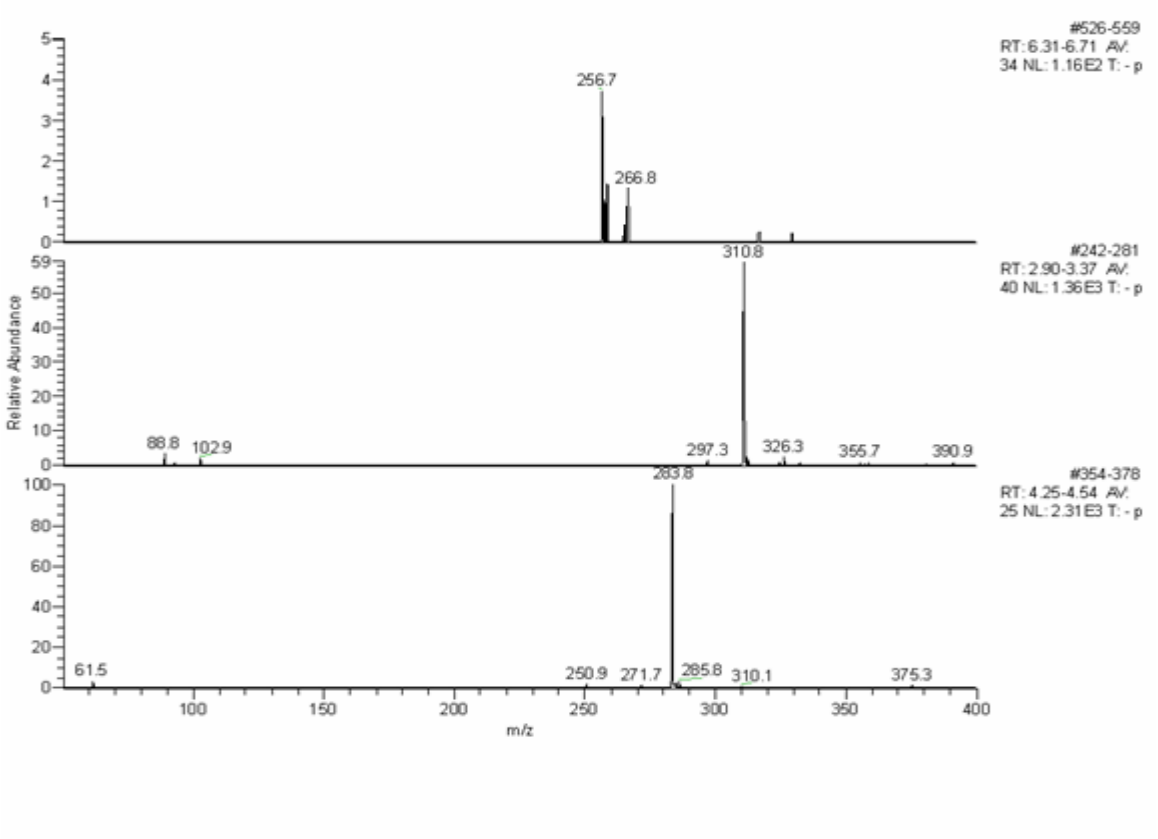

Figure 3-12. RDX mass spectra at 0.5 mm. Figure 3-12 shows the mass spectra for each of the three CV peaks at an electrode gap of 0.2 mm. Relative to the previous figure, the top mass spectrum is the right-most CV peak. The RDX mass spectrum has an additional peak at m/z 267, which is an adduct ion $[RDX+NO_2]^-$ that co-elutes through the FAIMS cell with the chloride adduct. This second adduct is not unusual, though it is usually found in extremely low intensity compared to the chloride adduct.

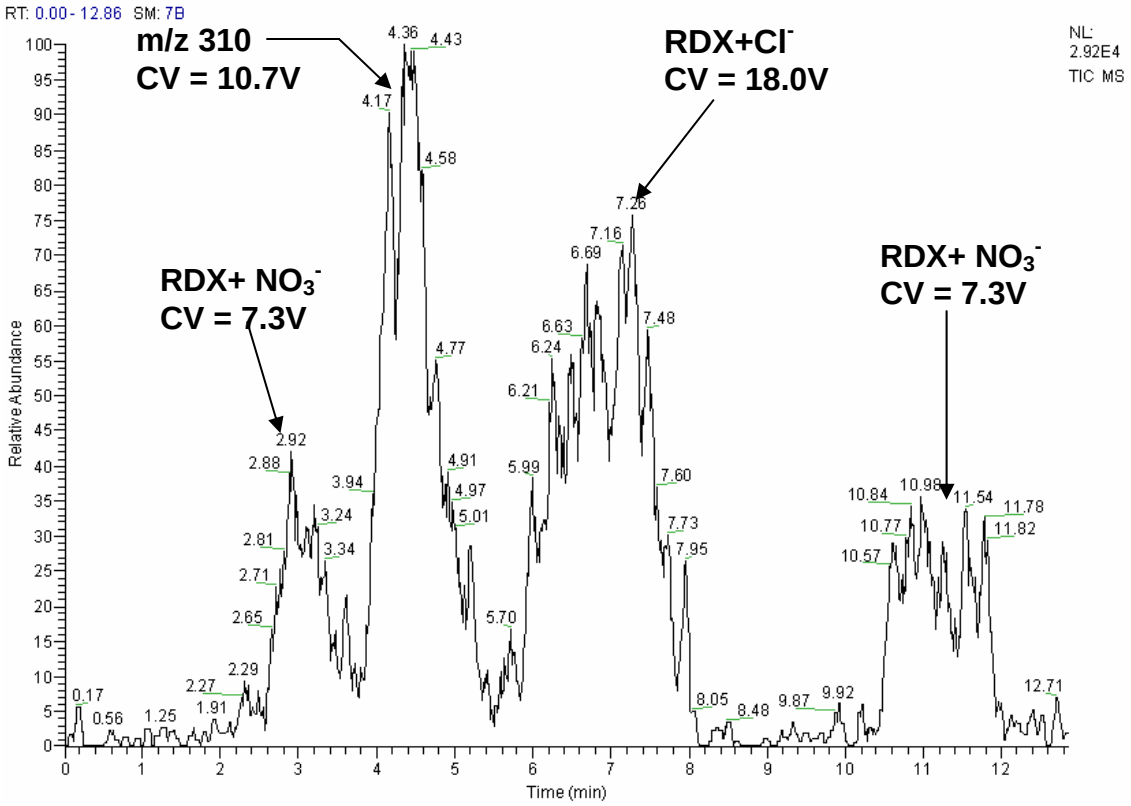

Figure 3-13. RDX CV spectrum at 0.75 mm. The second trial done was at a gap of 0.75 mm, which is 1.5 times larger. Again, the CV was scanned twice from 0V to 20V over a total period of 16 minutes. As expected the ion count is slightly higher. With this larger gap, the resolution is lower (CV peaks are wider); furthermore, the relative intensities of the different ions appear different (in particular, the RDX $[M+Cl]^-$ ion is significantly more abundant). The maximum ion count is 2.92×10^4 counts. Due to an error, only the first 12 minutes are shown.

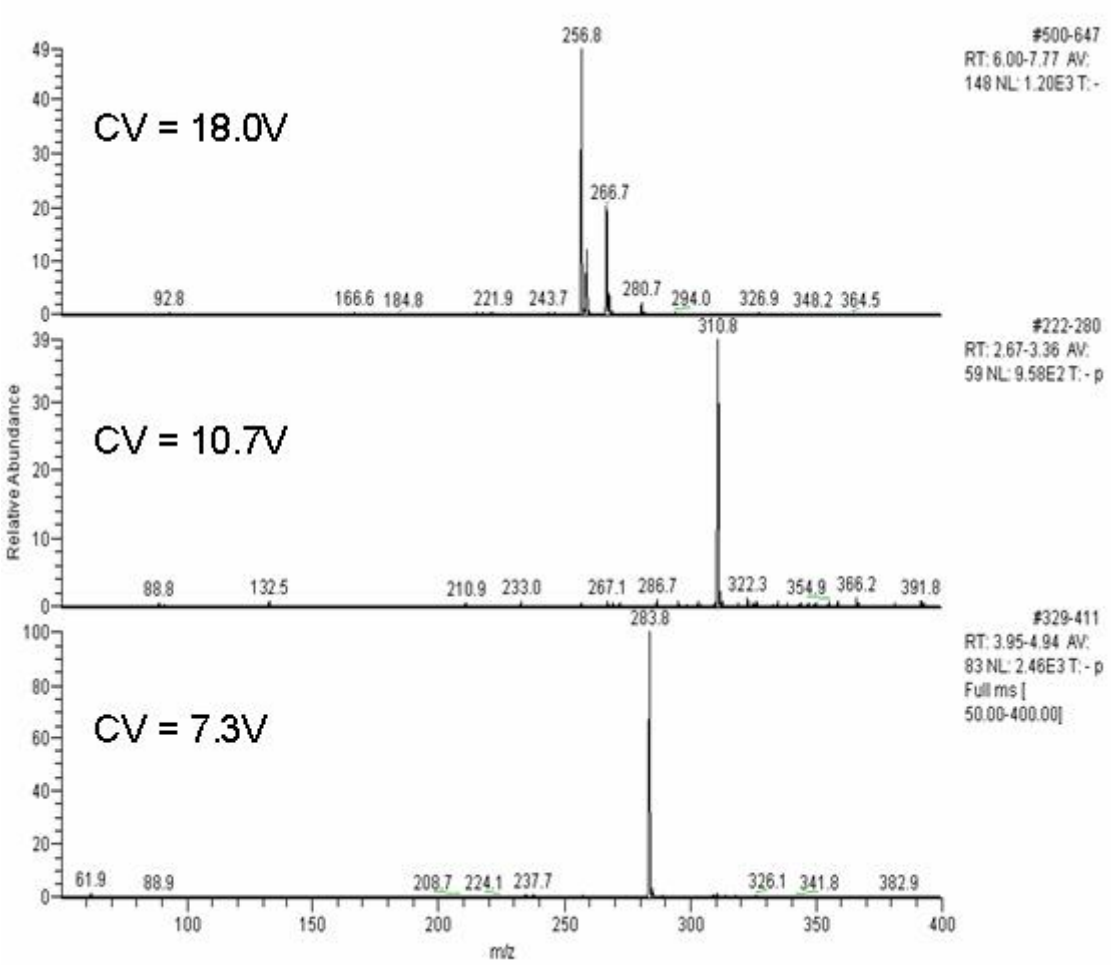

Figure 3-14. RDX mass spectra at 0.5 mm. Figure 3-14 displays the mass spectra corresponding to the three CV peaks in the previous figure. These are similar to those with the smaller electrode distance, as each ion is well resolved.

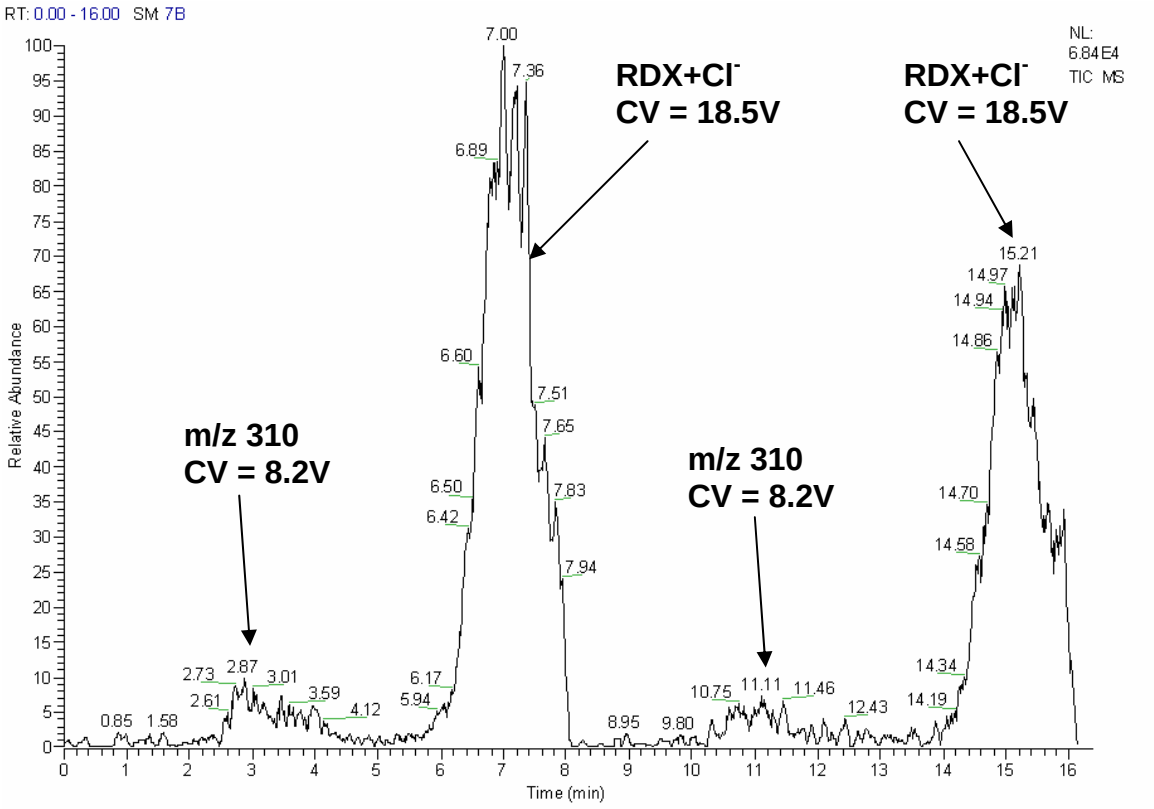

Figure 3-15. RDX CV spectrum at 1.0 mm. Next, the electrode gap was increased by a factor of 1.3, to 1.0 mm (Figure 3-15). The ion count was higher, yet the transmission behavior is completely different from the smaller gaps. This CV spectrum appears much like those in previous chapters, with a well-resolved peak for the analyte ion and only small background. The RDX $[M+Cl]^-$ ion is much more intense, the peak at m/z 310 is much less intense, and the peak at m/z 283 is hardly visible. The maximum ion intensity has increased to 6.84×10^4 counts.

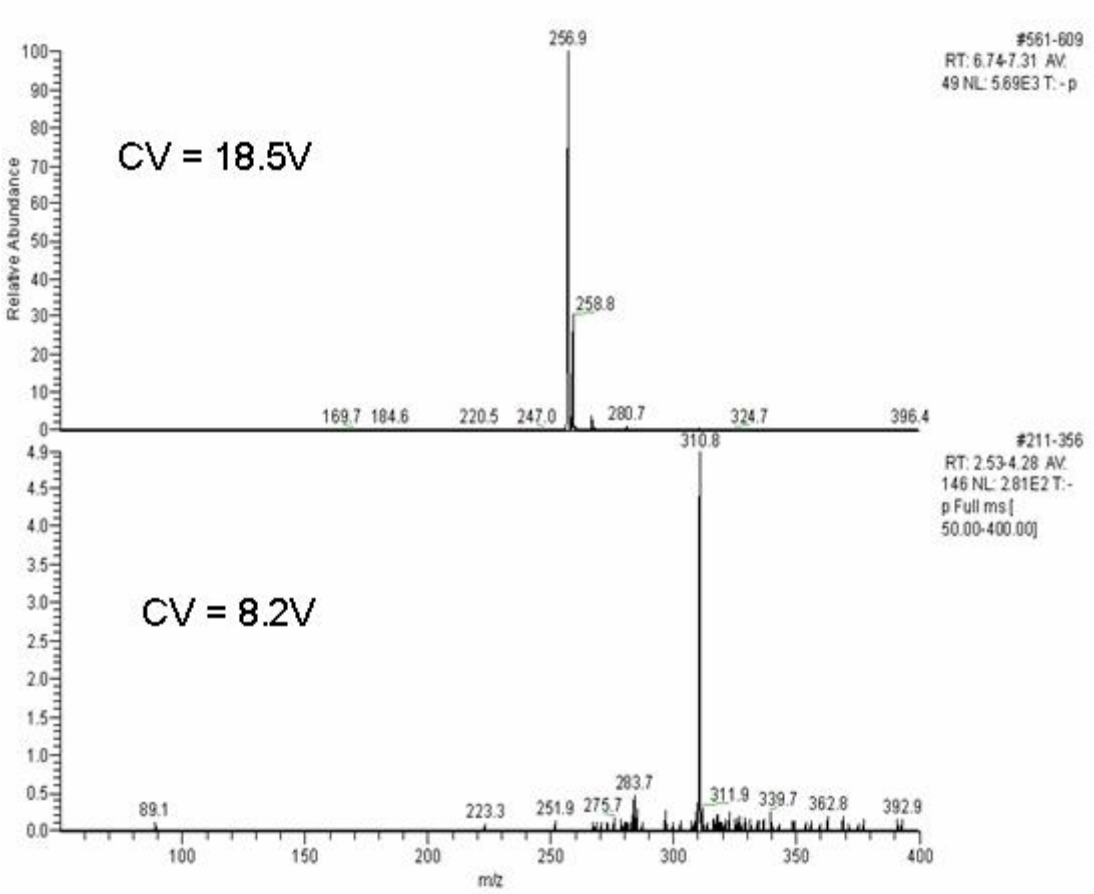

Figure 3-16. RDX mass spectra at 1.0 mm. The mass spectra for RDX taken at a FAIMS electrode gap of 1.0 mm can be seen in Figure 3-16. Thus far, both ion count and resolution are superior to those at smaller electrode gaps. At this gap, resolution and ion count are well-balanced. Likely, the electric field is at a strength optimal for ion focusing. Note that the peak at m/z 267 is barely visible.

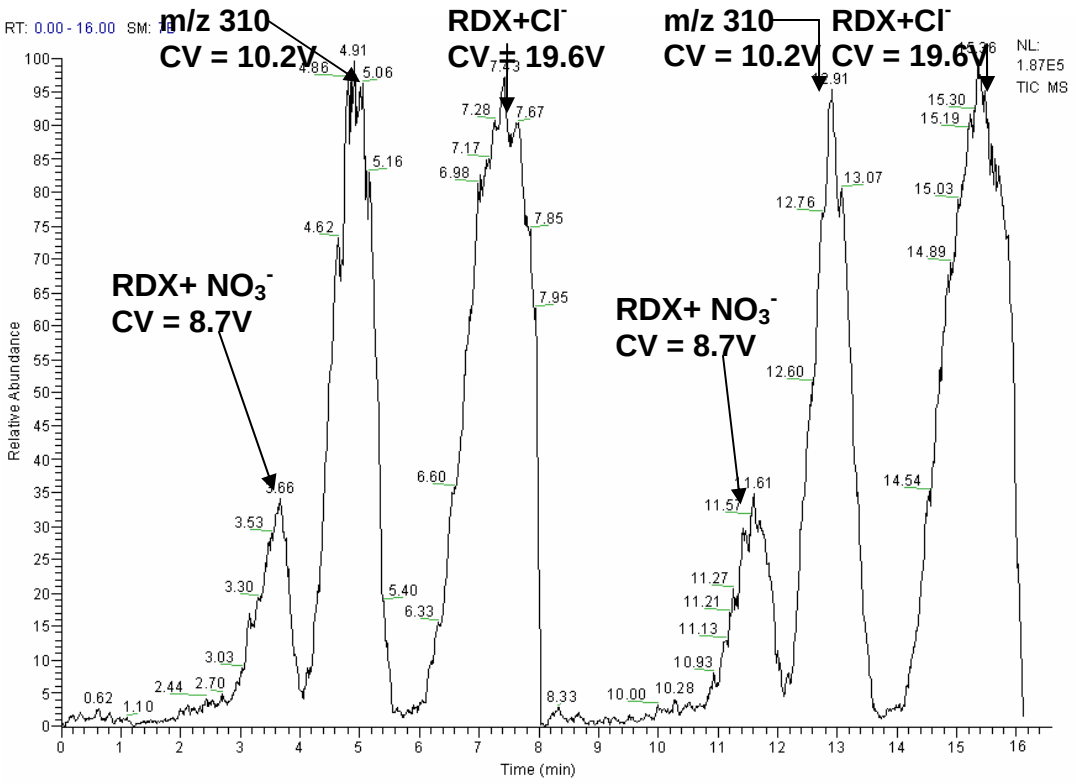

Figure 3-17. RDX CV spectrum at 2.0 mm. The last trial was done with an electrode gap of 2.0 mm (Figure 3-17). If the distance is set too high, as in this case, then the electrodes can no longer carry a waveform. This ion count was the highest of all these trials, presenting three orders of magnitude greater transmission than the smallest setting at 0.5 mm. The RDX peak was robust and well-resolved; however, the peaks at m/z 283 and m/z 310 were again visible.

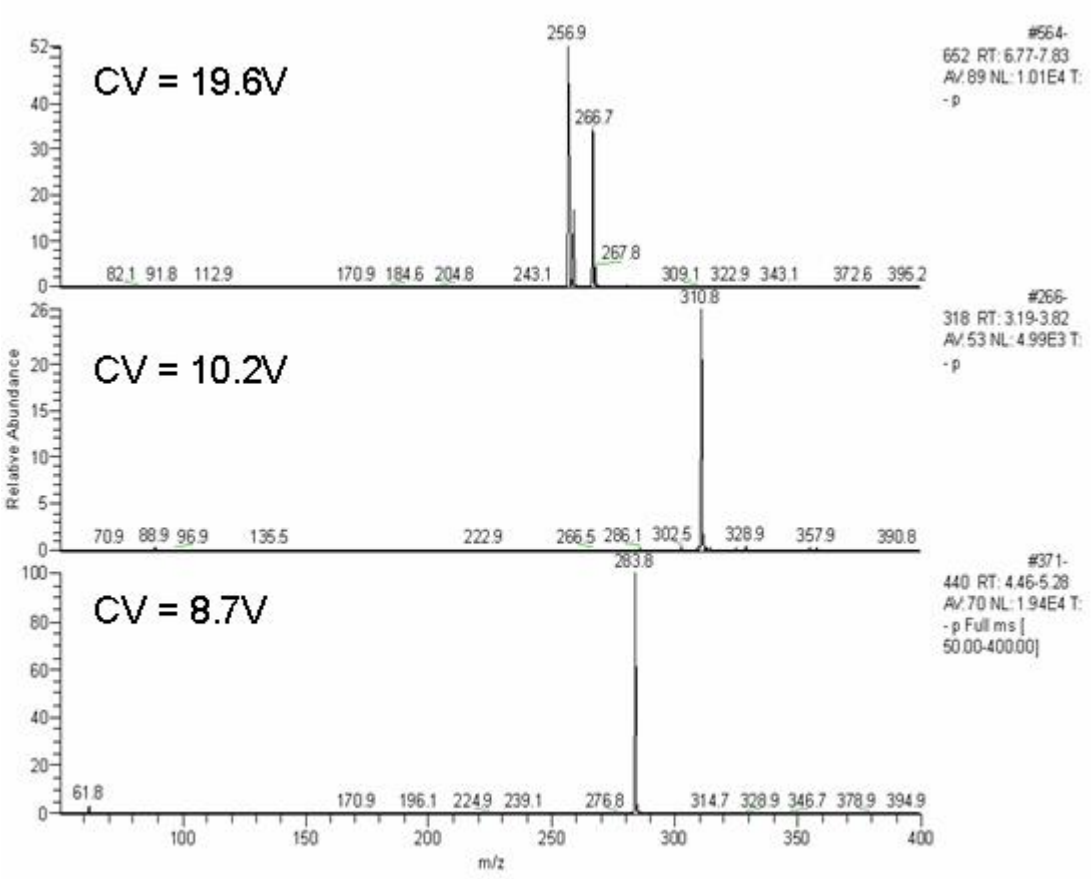

Figure 3-18. RDX mass spectra at 2.0 mm. The mass spectra in Figure 3-18 show that the ion counts are the highest compared to the spectra taken at other electrode distances. These four trials confirmed that a distance between the inner and outer FAIMS electrodes in the dome region set at about 1.0 mm yields the optimal transmission and resolution for explosives. It was observed that the CV for the chloride adduct of RDX increased as the electrode gap was increased, while the other peak CVs decreased (allowing the peaks to be resolved), but when the gap was at 2.0mm, the m/z 283 and m/z 310 peak CVs increased.

Table 3-1 shows the intensities of each of the major ions discussed above. As the electrode gap was increased, the intensity of the chloride adduct of RDX increased by almost two orders of magnitude, while the m/z 310 and m/z 283 ion counts decreased until the electrode gap was set to 2.0 mm, where the trend reverses.

Table 3-1. Relative Ion Intensities.

Electrode gap (mm)	$[RDX+ NO_3]^-$ (counts)	m/z 310 (counts)	$[RDX+Cl]^-$ (counts)
0.5	1.5×10^4	2.5×10^4	2.5×10^3
0.75	1.2×10^3	2.9×10^3	2.5×10^4
1.0	5.7×10	6.0×10^3	6.8×10^4
2.0	6.0×10^4	2.0×10^4	2.0×10^5

Table 3-2 lists the CV values for the same ions. The behavior mentioned above occurs for the CV values as well as the ion intensities. The chloride adduct of RDX increases slightly as the electrode gap increases, and the other ions decrease until the electrode gap is set to 2.0 mm, where the CVs increase.

Table 3-2. Relative CV Values.

Electrode gap (mm)	$[RDX+ NO_3]^-$ (V)	m/z 310 (V)	$[RDX+Cl]^-$ (V)
0.5	7.8	11.0	16.0
0.75	7.3	10.7	18.0
1.0	5.9	8.2	18.5
2.0	8.7	10.2	19.6

To examine the ultimate resolution of the FAIMS system, an attempt was made to resolve $[M]^-$ from $[M-H]^-$ ions for individual explosive compounds. Unfortunately, none of the explosives have both of these ions in approximately equal proportion; this makes it more difficult to allow for the separation of the ions. Nevertheless, for other types of ions, resolution is certainly feasible. To maximize resolution, the CV scan would have to be extremely slow or

over a narrow CV range, and the gas (and thus ions) entering the FAIMS cell would need to be completely desolvated. Different adducts of the same explosive, however, have been separated, for instance, the $[M+Cl]^-$ and $[M+NO_3]^-$ ions of RDX (see section 3.5).

3.7 Relationship of DV to CV

As discussed earlier, there is no single set of conditions that optimizes separation of every mixture for every FAIMS-based instrument. In order to characterize a FAIMS-based separation instrument, CVs must be found based on field strength, which is mainly a function of DV and cell geometry. There is, however, the same relationship between DV and CV for all FAIMS instruments, as this relationship is based on the change in mobility for an ion between low and high field.[12]

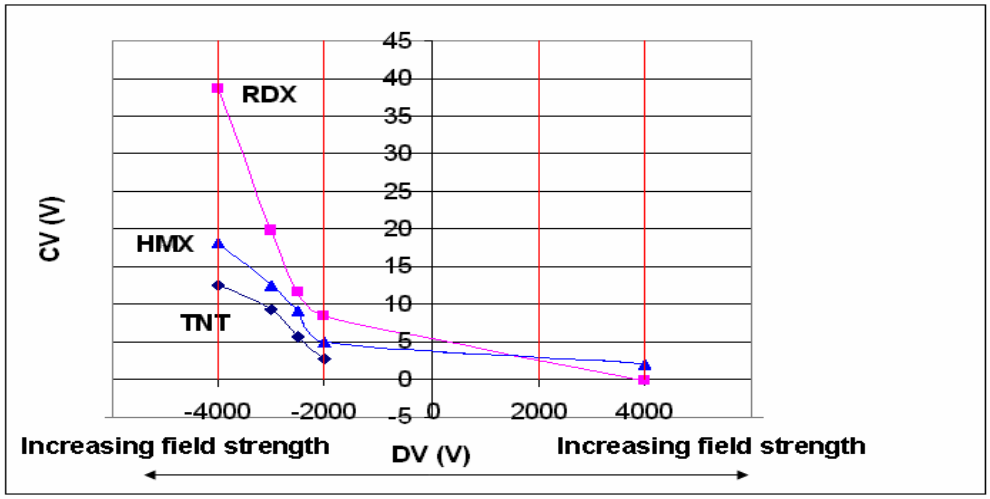

Figure 3-19. Relationship between CV and DV. Figure 3-19 is a plot of the relationship between CV and DV created using data sets taken using the FAIMS/MS setup described in chapter 2. The curves indicate that the CV of each ion increases at more negative DV (hence greater field strength). TNT and other nitroaromatics do not produce ions that are transmitted at a positive DV, although the chloride adduct ions of RDX and HMX respond to both positive and negative DVs. The Ionalytics instrument will not allow the DV to be set less than ± 2000V or greater than ± 4000V; this is indicated by the vertical red lines. Because of this DV/CV relationship, most of the explosives appear to exhibit "B" type behavior when high field is applied.

3.8 Sensitivity

Data sets collected on the FAIMS instrument used for characterization (as described in chapter 2) show that the DV for the optimal separation (highest resolution with lowest background) for the nitroaromatic explosives is -4000V, and +4000V for the nitramines. The IMS/FAIMS instrument (as described in this chapter) did not display the same behavior. The peak DV was at about -2500V, and at any DV set higher than -3000V the ion signal decreased rapidly to zero. In addition, the flow rate of the FAIMS carrier gas for this instrument could not be set higher than 1 L/min, or ions were lost. There are several possibilities for this behavior; the desolvation and focusing attributes of the IMS most likely require that a lower amount of carrier gas and voltage are needed to achieve the same separation results.

One method to measure sensitivity and resolving power of a FAIMS instrument is to examine the CV spectrum for both peak width and ion intensity. As discussed earlier, there is a degree of ion loss through a FAIMS (data gathered during this research shows about two orders of magnitude compared to no FAIMS cell in the system). Most FAIMS instruments (including the instrument used for chapter 2) demonstrate an average CV peak width of about 2-3V;[40] in contrast, the best HRFAIMS system CV peaks were as narrow as about 0.75V (for examples, see figs. 3-6 and 3-8). This has both benefits and disadvantages; narrower peaks require slower scan speed to define the peak, and necessitate precise CV values when fixed, but the narrower peaks are better resolved from each other and from background ions.

3.9 IMS/FAIMS of Explosives

In another set of experiments, the IMS was operated in gating mode in order to attempt to add an additional dimension of separation. This involved manually setting the times at which the gate would pulse open with a delay to allow ions of a fixed drift time (and, thus, ion mobility) to pass through the drift tube.

All other ions would be excluded from transmission. Hence, a percentage of all ions were discarded by the IMS, in addition to those discarded by the FAIMS portion of the instrument. An attempt was made to separate explosive mixtures by gating the IMS; however, ion counts were not high enough to discern individual components of the mixture. This is largely due to the loss in sensitivity due to the low duty cycle of the IMS/FAIMS system. For instance, if a 500 ms gate width is used, and the gate is only open for 25 ms, then the duty cycle is only 5%, which results in a significant loss of signal. Furthermore, the lack of synchronization between the IMS gate pulses and the fill times of the LCQ quadrupole ion trap may result in even greater loss in sensitivity.

Gating the IMS was not critical in these studies, as data have indicated that individual explosive peaks as part of a mixture are fully resolved while the IMS is functioning simply as a desolvation and focusing apparatus for the FAIMS. Any future experiments should include efforts to increase ion signal when the IMS is gating. (For full discussion see Chapter 4)

CHAPTER 4
CONCLUSIONS AND FUTURE WORK

4.1 Conclusions

The United States is under constant threat from the use of explosives by her enemies. There is a great need for the development of technologies that can eventually be applied in instruments that will be used to detect improvised explosive devices. These analytical instruments mainly will consist of laboratory and intermediate-sized instruments or man-portable field instruments, and all will be utilized both overseas and domestically.

Instruments designed for the detection of explosive compounds can fall into two categories, depending on function and/or mission. These are either qualitative threat detectors, or quantitative threat characterizers.[41] Factors that affect instrument use are portability, resolving power, sensitivity, and selectivity.

Mass spectrometry is a widely used analytical methodology. When a separation device is coupled to a mass spectrometer, all of the analytical figures of merit are drastically improved.

FAIMS is a promising technology that functions well as a separation device and is compatible with a mass spectrometer. There are many advantages to employing FAIMS as such. Even though the use of FAIMS may lower overall ion transmission, the signal-to-noise ratio of the overall instrument may be much higher than a lone mass spectrometer. This can be extremely important when an instrument is used in a field environment, away from the laboratory, when there is a great deal of background matrix with which to contend.

The goal of this research was to determine the degree to which a FAIMS/MS device can be employed to detect explosive compounds that are most likely to demonstrate a threat, and to attempt to ascertain methodologies to eventually do so in a field environment. The experiments discussed herein consisted primarily of three parts. The first characterized explosive compounds

using a FAIMS/MS, while the second included additional FAIMS/MS experiments conducted to analyze and improve the analytical factors of the instrument. The third section described a novel high-resolution FAIMS/MS method, employing an IMS drift tube to desolvate and focus ions into the FAIMS cell. The HRFAIMS method is sensitive, and the resolution is high enough that valuable forensic data can be collected.

4.1.1 Characterization of Explosive Compounds

A list of explosive compounds was compiled based on both the frequency of encounter during terrorist events and the presence in common military explosives. The feasibility of detection of these compounds was first evaluated; once accomplished, the characteristics of each compound were analyzed and noted. All of the explosives in this study contained nitro leaving groups. This list includes three nitroaromatics: TNT, which is one of the oldest known and commonly encountered explosives, and two isomers of DNT that are precursors to the manufacture of TNT, and, therefore, are forensically important. TNT is also found in many military explosive mixtures. All of the nitroaromatics were easily detectable and were readily characterized using the FAIMS/MS instrument.

There were two nitramines evaluated, RDX and HMX, which are encountered along with TNT in military explosives and plastic explosives mixtures. The most common explosives include mixtures of TNT and RDX. Both RDX and HMX are similar molecules that have similar characteristics. The formation of a molecular-type ion requires adduct formation to be well detected. The best adduct for this purpose is formed with the addition of a chloride (Cl^-) ion (improved by doping the solvent with a small amount of a source of chloride, such as CCl_4), though all will form adducts with nitrate (NO_3^-) as well.

There were two nitrate esters evaluated, NG and PETN. Both are extremely unstable. The molecular ion cannot be detected by MS; PETN will only form adducts in low concentrations.

NG will not form adducts at all. Because of this instability, though, NG and PETN are rarely, if ever, used without another explosive in a mixture.

The last explosive evaluated in this study was ANFO, a mixture of ammonium nitrate and a fuel, which is a commonly used commercial explosive. It is also favored by terrorists due to the ease of its manufacture and acquisition of its components. The nature of these components creates difficulties for detection, as ammonium nitrate and many of the fuels used (usually diesel) may be found in high levels in the background. Because there is no single structure, ANFO has not been well characterized for detection by MS.

4.1.2 FAIMS Characteristics

FAIMS separates ions using a high electric field to affect the change in ion mobility. One of most important FAIMS characteristics that affect the strength of this field is the dispersion voltage. Once the optimum DV was determined, then other analytical parameters could be ascertained for each explosive compound. No two types of FAIMS instruments can be characterized identically, though there is a basic relationship that applies in all cases between DV and CV.

Other FAIMS factors that were examined were the addition of a small amount of helium to the carrier gas, which improves resolution and ion transmission, and the distance between inner and outer electrodes of a FAIMS cell. The optimal electrode gap for the detection of explosives on the instrument used corresponds to other FAIMS studies that have been done (a distance of 1mm).

4.1.3 IMS/FAIMS/MS

During these experiments, an IMS was added to the instrument to add another dimension of separation. When the IMS was gated, only ions with a specific ion mobility were transmitted on to the FAIMS cell; therefore, only a fraction of the ions were transmitted. The ion counts

during this experiment were not high enough to distinguish individual components of a mixture. Changes could be made to the instrument to attempt to improve transmission and sensitivity. This is discussed further in the "recommendations" section of this chapter.

4.1.4 High-resolution FAIMS

The addition of the IMS drift cell was proven to be beneficial to the instrument, however. When the IMS was in total ion mode, there was no ion gating, and all ions passed through the drift tube. Because the tube is heated and carries an electric field, the analyte was desolvated, and the ion beam was focused into the FAIMS. When this method was used along with the optimal FAIMS parameters, resolving power of the FAIMS, and ion transmission increased drastically. At certain junctures, the CV peaks were so narrow that the CV scan speed had to be slowed to allow the entire peak to pass through before the CV changed.

4.1.5 Mixture Separations with FAIMS/MS

Once characterization was completed, then the value of the FAIMS to separate mixtures was analyzed. If an analytical instrument is unable to resolve mixtures, then its value as a field instrument is limited. This phase of experiments was greatly enhanced using the HRFAIMS method. First, two mixtures containing different explosives were separated successfully and the components were well-resolved. Resolution was high enough that mixtures containing two isomers of the same compound (DNT) were also successfully separated from each other. This ability can be valuable for forensics analysis of either post-blast or manufacturing of TNT.

4.1.6 Disadvantages of FAIMS

FAIMS instruments still have limitations, especially pertaining to field use. The resolution and transmission of the FAIMS cell are strongly affected by water and other solvent, and the cell must be as dry as possible. After continued use, if the FAIMS cell is not periodically dried out, the sensitivity and resolving power drop as either the electrodes are hindered from carrying a

high electric field, or the saturation of solvent causes ion-molecule reactions. As such, the carrier gas must not contain impurities; furthermore, carrier gas is required in large volumes (between 3-5 L/min). This can provide issues in terms of instrument period of use, maintenance, and design, for it is undesirable to add large cylinders of gases to an apparatus if the objective is portability.

The Ionalytics prototype instruments are extremely delicate, and are not compatible with field use. For instance, the DV is transported from the waveform generator to the FAIMS cell via an insulated cable. Any environmental changes in the area around the cable can significantly affect the waveform and field generated.

4.2 Recommendations

Analysis of data sets collected during this series of experiments has determined that FAIMS/MS is a feasible method to use for the detection of explosive compounds. A high-resolution methodology for the detection of explosives with FAIMS/MS has been identified during this research study, and should be further explored.

4.2.1 Further HRFAIMS Improvements

The use of the IMS as an ion focusing/desolvation device could be further improved, because its use during this study was not intended to be so. The interface between the IMS and FAIMS consisted of an empty space between the two components. The IMS drift tube must be lined up with the FAIMS cell manually, and both the electric fields as well as carrier gas may cause ions to leave the system. A nonconductive sleeve could be used to enclose the system, and may decrease ion loss, and may improve transfer into the FAIMS cell.

4.2.2 FAIMS Carrier Gas Experiments

Further, experimentation could be conducted into the composition of the FAIMS carrier gas. Future field instruments will probably not include carrier gas cylinders. Other gas mixtures

could be tested, and the effects determined. A desirable approach would be, first, to use laboratory-provided pure, dry "zero air," and if this is effective as a FAIMS carrier gas, then to use ambient air run through a scrubber/dessicant just prior to introduction to the FAIMS cell.

4.2.3 Practical Separations and Analysis

Because the separation of mixtures was done successfully, the next logical step is to separate unknown mixtures by, for example, having another individual prepare the samples. Also, efforts should be made to separate explosive compounds from various background matrices, thus determining the lowest possible concentrations at which explosives can be detected. After this is done, then a study should be done to identify matrices (if any) that strongly interfere with detection, and attempt to ameliorate them.

4.2.4 IMS Gating

The IMS/FAIMS/MS method requires more efforts to be made in terms of synchronizing times when the gates open to the FAIMS CV scanning, and the injection times of the quadrupole ion trap. This will further ensure that the lowest number of ions possible is lost.

4.2.5 CV Scanning

A practical instrument would require scan speeds that are as fast as possible, so that possible threats can be detected and warnings can be administered. CV scan speed can be adjusted to any length of time, though the higher resolution the instrument, the slower the scan speed that is necessary. For practical use, an optimal length of time should be set such that mixtures are fully resolved, but the instrument can scan as quickly as possible. The CV scan range can also be adjusted so that all of the explosives of interest are covered, yet it is set to the minimum amount of time needed. If a qualitative threat warning is all that is required, then the scan time can be minimized to allow just enough of the analyte ions to pass through the system to be detectable above the noise level, thus further reducing the time required for a scan.

4.2.6 Instrument Maintenance

Both IMS/FAIMS instruments used in this research introduced samples into the system as liquids. As such, the sensitivity and resolution of the FAIMS degraded over time, and regular cleaning of the cell with a volatile solvent that did not leave a residue, such as methanol, followed by drying of the cell were needed. Sampling explosives in a vapor or particulate sample, rather than in liquid solution, may reduce this problem. Practical instruments should include a small amount of solvent for regular cleaning; and note that carrier gas should always be run through the system when in standby.

4.3 Future Work

Now that feasibility has been established, and the first step toward method development for explosives detection via FAIMS/MS has been taken, the next step includes working toward developing an instrument employing this method. A great deal of effort is required, however, to design and create an apparatus that can be employed for use in a field environment. The best way to approach this would be to first design and test an intermediate instrument that would be used specifically for explosives and other related compounds. This work would likely include further research in interfaces between each component of the instrument, FAIMS cell geometries, and other ways to allow the instrument to serve its purpose. Also, a method of practical sample introduction to the system is needed, as explosives have low vapor pressures and are not conducive to collection via gas collection.

4.3.1 Ionization Sources

One possible way to move toward development of a field instrument was actually attempted during this research study: the use of a more portable ionization source. ESI is designed for ionizing liquid solutions, and APCI requires a heater and corona discharge; both of these limit the capabilities of an instrument.

A novel type of ionization source was evaluated during this research for use with an IMS/MS for the detection of explosives. Developed by Blanchard & Co., the distributed plasma ion source (DPIS) is designed to provide ionization at atmospheric pressure using a simple, portable, low-power device. The DPIS is constructed with two overlapping electrodes of different sizes that are separated with a dielectric. A potential applied across the electrodes creates a distributed plasma around the edge of the small electrode, which ionizes the surrounding air and sample vapor. This type of source can be useful because sample can be introduced as a vapor. In this case, liquid sample was kept in a bottle, across which a nitrogen carrier gas was blown, and the headspace was directed over the DPIS source, into one of WSU's homebuilt IMS tubes.

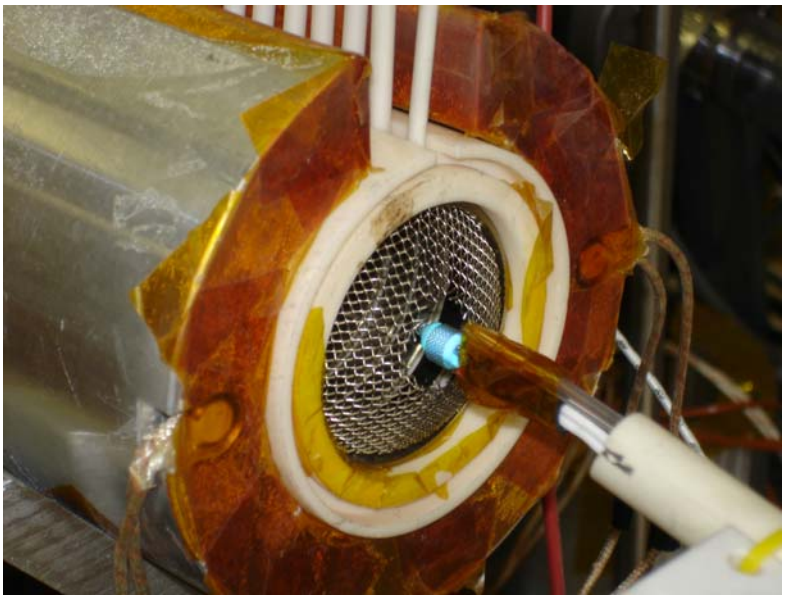

Figure 4-1. Distributed plasma ionization source. Figure 4-1 is a photograph of the DPIS extended through the ion screen of the IMS drift tube. The plasma discharge is a distinct blue color. The sample line is taped to the insulated wire that powers the source.

The DPIS circuit has limitations, however. There is no diode to prevent overload of the circuit, and the maximum potential cannot exceed -1kV. Data were collected with several explosives. The DPIS source did ionize the samples, but the signal-to-noise ratio was extremely

low. There may be many reasons for this. First, the source voltage is low compared to the high voltage of the IMS, which may limit transmission of ions into the IMS drift tube. Also, the only sample directed into the instrument is headspace, which contains significantly less analyte than a liquid which is vaporized.

This source is not compatible with laboratory-scale IMS/MS instruments, as the ionization voltage is not scaled with the other voltages of the system. Nevertheless, the DPIS did ionize the explosive samples, and can potentially be used with low-power, portable field instruments.

4.3.2 Development of Field Instruments

The first step in this research has been to determine the feasibility of the IMS/FAIMS/MS method for detecting explosives. Now that this has been accomplished, improvements can be made to the overall method (as discussed above). Once this is done, then work can proceed to reduce size and power consumption of each component, and then durable packaging can be developed for a fieldable instrument.

REFERENCES

1. *Country Reports on Terrorism*, US State Department, 2005.

2. *Opportunities to Improve Airport Passenger Screening with Mass Spectrometry*, Committee on Assessment of Security Technologies for Transportation, National Materials Advisory Board, 2004.

3. Shea, Dana A.; Morgan, Daniel, *Detection of Explosives on Airline Passengers: Recommendation of the 9/11 Commission and Related Issues*, Congressional Research Service, Library of Congress, 2006.

4. Eiceman G. A.; Borsdorf H., *Ion Mobility Spectrometry: Principles and Applications*, Applied Spectrometry Reviews, 2006, vol. 41, no. 5, pp. 323-375.

5. Hill, Herbert H.; Simpson, Greg. Ca*pabilities and Limitations of Ion Mobility Spectrometry for Field Screening Applications*, Field Analytical Chemistry, 1997, vol.1, no. 3, pp. 119-134.

6. Lee, Harold G.; Lee, Edgar D.; Lee, Milton L., *Atmospheric Pressure Ionization Time-of-flight Mass Spectrometer for Real-time Explosives Vapor Detection*, Proceedings of the First International Symposium on Explosive Detection Technology, pp. 619-633, 1992.

7. Osorio, Celia; Gomez, Lewis M.; Hernandez, Samuel P.; Castro, Miguel E., *Time-of-flight Mass Spectroscopy Measurements of TNT and RDX on Soil Surfaces*, Detection and Remediation Technologies for Mines and Minelike Targets, 2005, v ol. 5794, pp. 803-811.

8. Bottrill, A.R., *High-energy Collision-induced Dissociation of Macromolecules using Tandem Double-focusing/Time-of-flight Mass Spectrometry*, PhD thesis, University of Warwick, Coventry, UK., 2000.

9. Gruber, Ludwig. *Characteristics of Different Mass Analyzers,* Fraunhofer-Institute for Process Engineering and Packaging**,** http://www.ivv.fraunhofer.de/ms/ms-analyzers.html, 2000.

10. Purves, Randy W.; Guevremont, Roger; Day, Stephen; Pipich, Charles W.; Matyjaszczyk, Matthew S., *Mass Spectrometric Characterization of a High-field Asymmetric Waveform Ion Mobility Spectrometer*, Review of Scientific Instruments, 1998, v ol. 69, no. 12, pp. 4094-4106.

11. Kolakowski, Beata M.; McCooeye, Margaret A.; Mester, Zoltan; D'Agostino, Paul A., *Rapid Separation and Identification of Chemical and Biological Warfare Agents in Food and Consumer Matrices Using FAIMS-MS Technology*, National Research Council of Canada, 2006.

12. Guevremont, Roger, *High-Field Asymmetric Waveform Ion Mobility Spectrometry (FAIMS),* Ionalytics Corp., Ottawa Canada, 2004.

13. Reich, Richard, *Fundamentals and Applications of Atmospheric Pressure Chemical Ionization Quadrupole Ion Trap Mass Spectrometry for the Analysis of Explosives,* MS thesis, University of Florida, 2001.

14. *Finnigan LCQ Series APPI/APCI Combination Probe Operator's Manual*, Rev. A, Thermo-Electron Corp., 2004.

15. Buryakov, I.; Krylov, E.; Nazarov, E.; Rasulev, U., *A New Method of Separation of Multi-atomic Ions by Mobility at Atmospheric Pressure Using a High-Frequency Amplitude-asymmetric Strong Electric Field*, International Journal of Mass Spectrometry, 1993, vol. 128, pp. 143-148.

16. Kanu, Abu B.; Hill, Herbert H., *Ion Mobility Spectrometry: Recent Developments and Novel Applications*, Washington State University, LabPlus International, 2004.

17. Atkins, Peter; dePaula, Julio, *Physical Chemistry, 7th Ed*., Chap. 24, Oxford Univ. Press, Oxford, UK, 2001.

18. Welling, M.; Schuessler, H.A.; Thompson, R.I.; Walther, H.; *Ion/Molecule Reactions, Mass Spectrometry and Optical Spectroscopy in a Linear Ion Trap,* International Journal of Mass Spectrometry and Ion Processes, 1998, vol. 172, no. 1, pp. 95-114.

19. De Hoffman, Edmond and Stroobant, Vincent, *Mass Spectrometry Principles and Applications*, 2nd Ed., 2005

20. Paul, W., *Electromagnetic Traps for Charged and Neutral Particles*, Modern Physics, 1992, vol. 62, no. 3, pp. 531-540.

21. *Finnigan LCQ Series Hardware Manual*, Rev. A, Thermo-Electron Corp., 2003.

22. Mathieu, E., *Mémoire sur Le Mouvement Vibratoire d'une Membrane de forme Elliptique*, Journal of Pure Mathematics, 1868, vol. 13, pp. 137-203.

23. McLachlan, N. W., *Theory and Application of Mathieu Functions*, Dover, 1947.

24. March, Raymond E.; Todd, John F. J., *Quadrupole Ion Trap Mass Spectrometry*, Wiley, 2005.

25. Murray, K. K.; Boyd, Robert K.; et. al., *Standard Definitions of Terms Related to Mass Spectrometry*, IUPAC, 2006.

26 Sparkman, O. D.; Klink, F. E., *LC/MS: Fundamentals and Applications*, ACS, 2001.

27. *Annual Threat Assessment of the Director of National Intelligence for the Senate Armed Services Committee*, Statement by the Director of National Intelligence, John D. Negroponte to the Senate Armed Services Committee, transcript available on www.globalsecurity.org, Feb. 2006.

28. Davis, Tenney L., *The Chemistry of Powder and Explosives*, Ch. 1, Angriff Press, Hollywood, CA, 1972.

29. Wade, L. G., *Organic Chemistry, 6th Ed*., Ch. 15-16, Prentice Hall, 2005.

30. Hannum, David; et. al., *Miniaturized Explosives Preconcentrators for Use in Man-portable Explosives Detection Systems*, Sandia National Laboratory, 1999.

31. Committee on the Review of Existing and Potential Standoff Explosives Detection Techniques, *Existing and Potential Standoff Explosives Detection Techniques*, National Research Council, National Academies Press, 2004.

32. Yinon, Jehuda, *Toxicity and Metabolism of Explosives*, CRC Press, Boca Raton, FL, 1990.

33. Cooks, R. Graham; et. al., *Direct, Trace Level Detection of Explosives on Ambient Surfaces by Desorption Electrospray Ionization Mass Spectrometry*, Royal Society of Chemistry, 2005, vol. 15, pp. 1950-1952.

34. Federal Facilities Assessment Branch, *Public Health Assessment, US Army Umatilla Depot Activity*, Centers for Disease Control and Prevention, 1997.

35. Cooper, Paul W., *Explosives Engineering*, Ch. 3, Wiley, New York, NY, 1996.

36. Fenn, John B., *Electrospray Ionization, Principles and Practices*, Mass Spectrometry Reviews, 1990, vol. 9, no. 1, pp. 37-70.

37. United States patent 7071465: Ion mobility spectrometry method and apparatus, inventors: Hill, Herbert H. et. al., Washington State University research foundation, 2006.

38. Bradbury, Norris E., and Nielsen, Russell A., *Absolute Values of the Electron Mobility in Hydrogen*, Physical Review, 1935, vol. 49, no. 5, pp. 388-393.

39. Guevremont, R.; Thekkadath, G.; Hilton C. K., *Compensation Voltage (CV) Peak Shapes Using a Domed FAIMS with the Inner Electrode Translated to Various Longitudinal Positions*, Journal of the American Society of Mass Spectrometry, 2005, vol. 16, no. 6, pp. 948-956.

40. Schvartsburg, A.; et. al., *High-Resolution FAIMS Using New Planar Geometry Analyzers*, Analytical Chemistry, 2006, vol. 78, no. 11, pp. 3706-3714.

41. *Transportation Security: Systematic Planning Needed to Optimize Resources*, statement of Cathleen A. Berrick to the US Senate Committee on Commerce, Science, and Transportation, USGAO, 2005.

BIOGRAPHICAL SKETCH

Jared J. Boock was born in Hazleton, PA, in 1980. He grew up in Torrington, CT, and Panama City, FL. He completed his B.S. in chemistry from Florida State University in 2002 and received a commission in the US Air Force.

His first duty station was the Molecular Sciences Division, Materials Technology Directorate, Air Force Technical Applications Center, Patrick AFB, FL, where he served as the division Test Director. His primary duty was to plan and execute field tests, and evaluate data for the test and evaluation of chemical weapons detection equipment. He wrote several classified test and technical reports.

In 2005, he was selected for the Air Force Institute of Technology Civilian Institutions program, to study for his M.S. degree. He chose to pursue his M.S. degree in analytical chemistry at the University of Florida. Upon completion of his M.S. degree he will be stationed at the High Explosives Research and Development Facility at Eglin AFB, FL.